Transport and aviation hazard from the Eyjafjallajökull volcanic ash, determined from satellites and dispersion modelling

Fred Prata[1]

Andreas Stohl[1], Cirilo Bernardo[1], Lieven Clarisse[2], Ian Davies[3], Adam Durant[1,4], Sabine Eckhardt[1], Nina Kristiansen[1,5], Andrew Prata[6], Petra Seibert[7], Kerstin Stebel[1]

Affiliations

[1]Norwegian Institute for Air Research, Kjeller, Norway

[2]Free University of Brussels, Belgium

[3]easyJet, Luton, England

[4]University of Cambridge, England

[5]UK Meteorological Office, England

[6]University of California Los Angeles, USA

[7]University of Vienna, Austria

Outline

- Geological setting
- Satellite detection of volcanic ash
- Dispersion modelling
- Aircraft and Ash don’t mix
- What the future holds

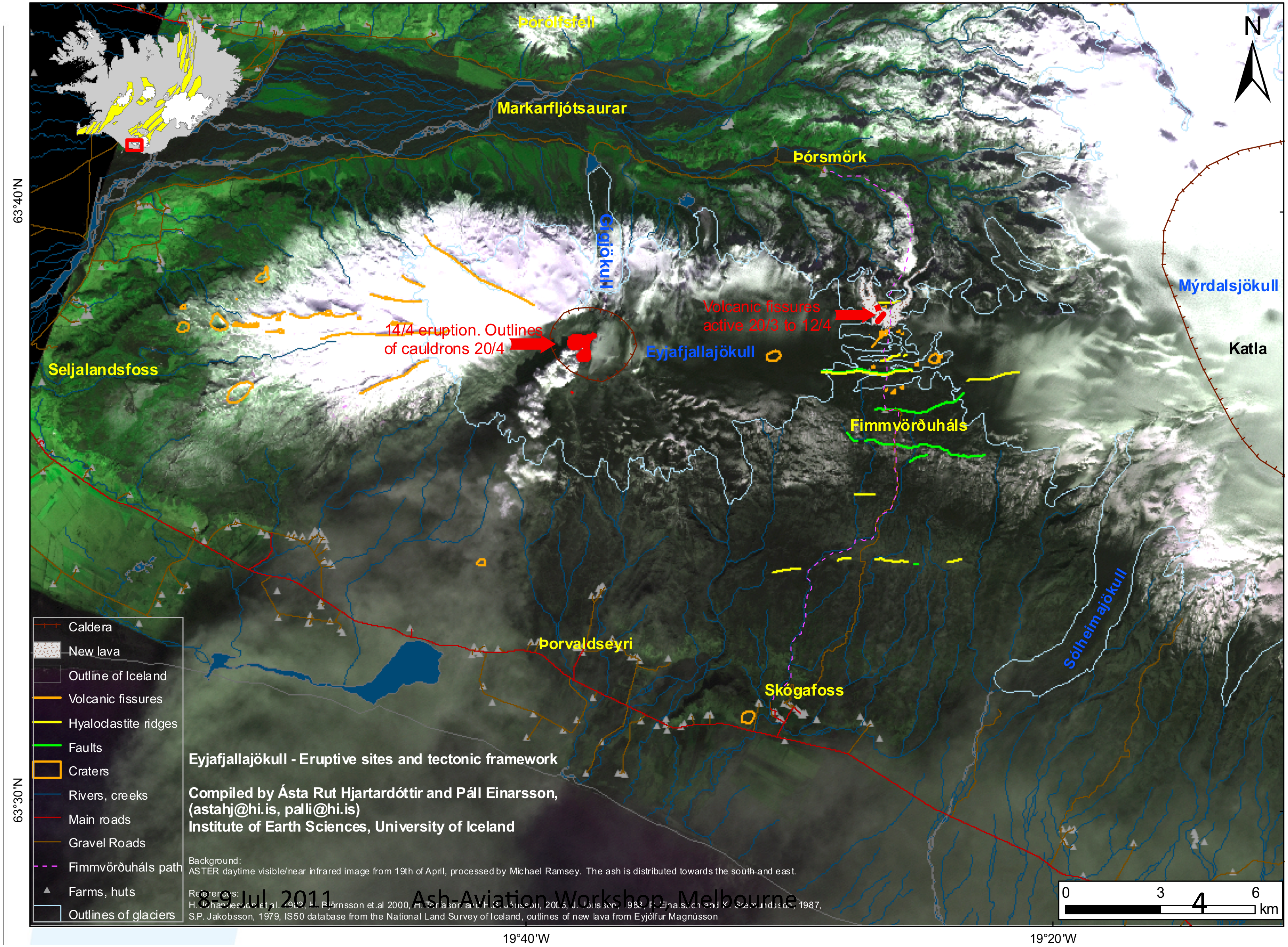
Þórólfsfell
Markarfljótsaurar
Þórsmörk
Gígjökull
Mýrdalsjökull
Volcanic fissures
active 20/3 to 12/4
14/4 eruption. Outlines
of cauldrons 20/4
Eyjafjallajökull
Katla
Seljalandsfoss
Fimmvörðuháls
Sólheimajökull
Þorvaldseyri
Skógafoss
N
63°40'N
63°30'N
19°40'W
19°20'W
0
3
6
km
Caldera
New lava
Outline of Iceland
Volcanic fissures
Hyaloclastite ridges
Faults
Craters
Rivers, creeks
Main roads
Gravel Roads
Fimmvörðuháls path
Farms, huts
Outlines of glaciers
Eyjafjallajökull - Eruptive sites and tectonic framework
Compiled by Ásta Rut Hjartardóttir and Páll Einarsson,
(astahj@hi.is, palli@hi.is)
Institute of Earth Sciences, University of Iceland
Background:
ASTER daytime visible/near infrared image from 19th of April, processed by Michael Ramsey. The ash is distributed towards the south and east.
References:
S.P. Jakobsson, 1979, IS50 database from the National Land Survey of Iceland, outlines of new lava from Eyjólfur Magnússon

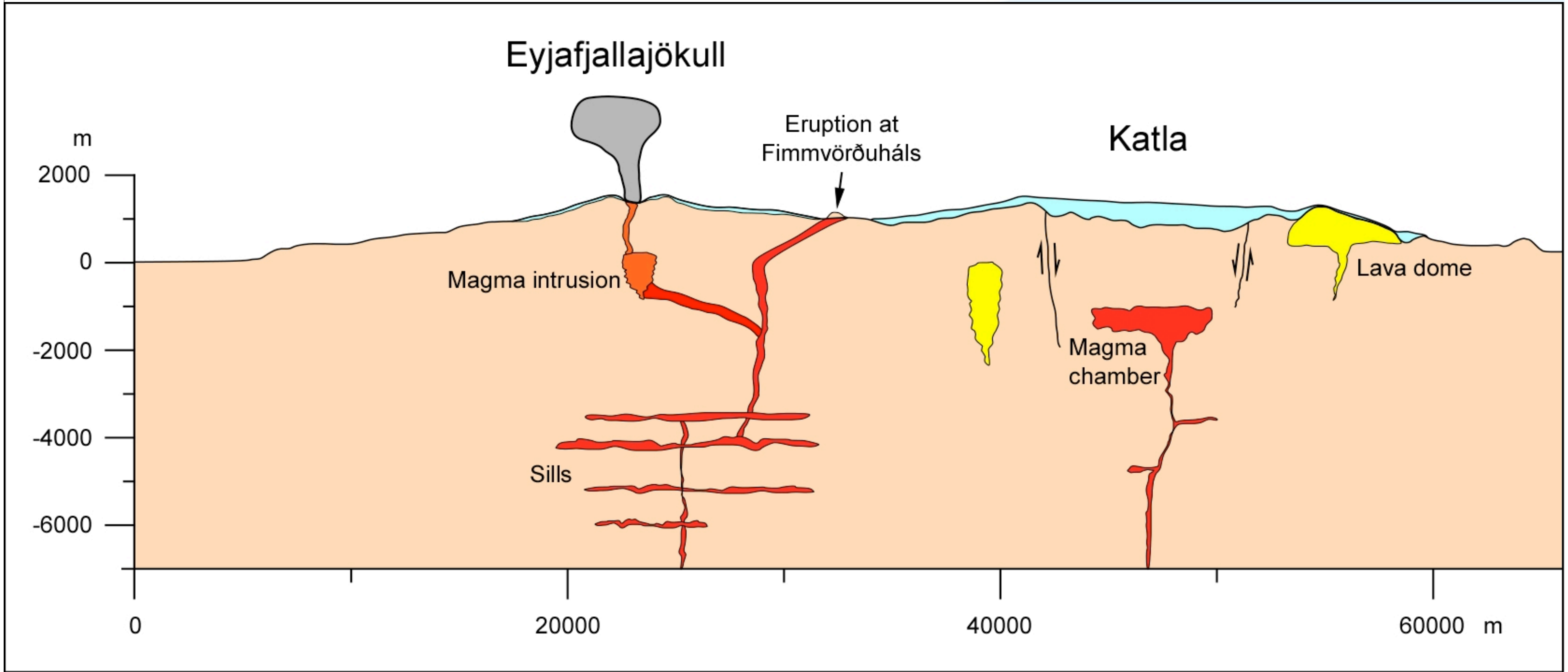

Credit: University of Iceland
Páll Einarsson (palli@raunvis.hi.is)


mila

Field work on 18 Sept 2010

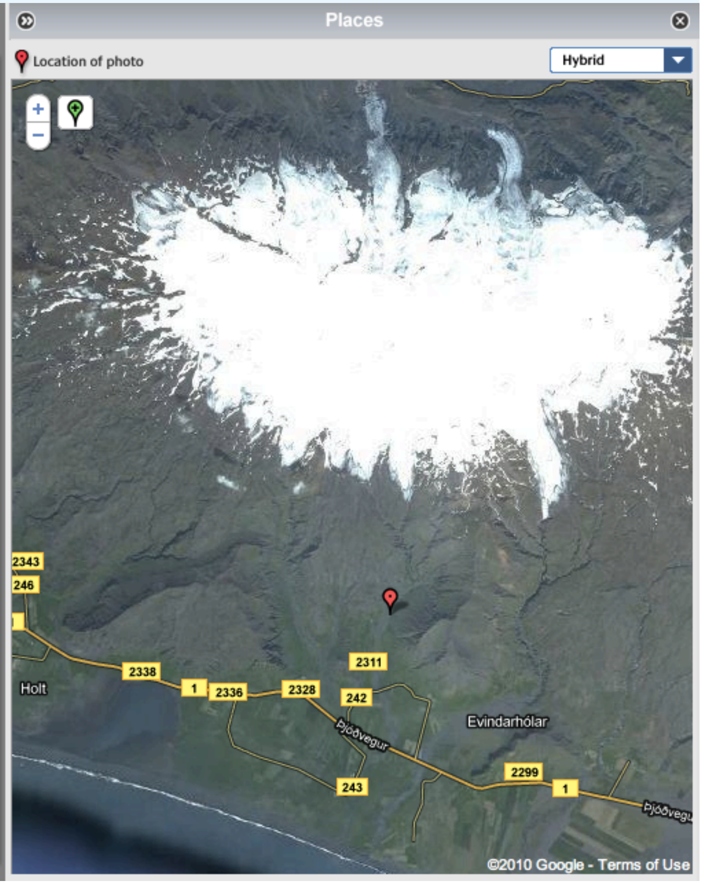

What's this?


NÆLAND GRIMSSON


Location of photo
Hybrid
261
248
Stóridalur
1
Þjóðvegur
246
Ásólfsskáli
245
Holt
242
Evindarhólar
243
2313
221
©2010 Google - Terms of Use

Gigjokull glacier

SEVIRI

IR channels

- 6.3 µm
- 7.4 µm
- 8.6 µm
- 9.7 µm
- 10.8 µm
- 12.0 µm
- 13.2 µm

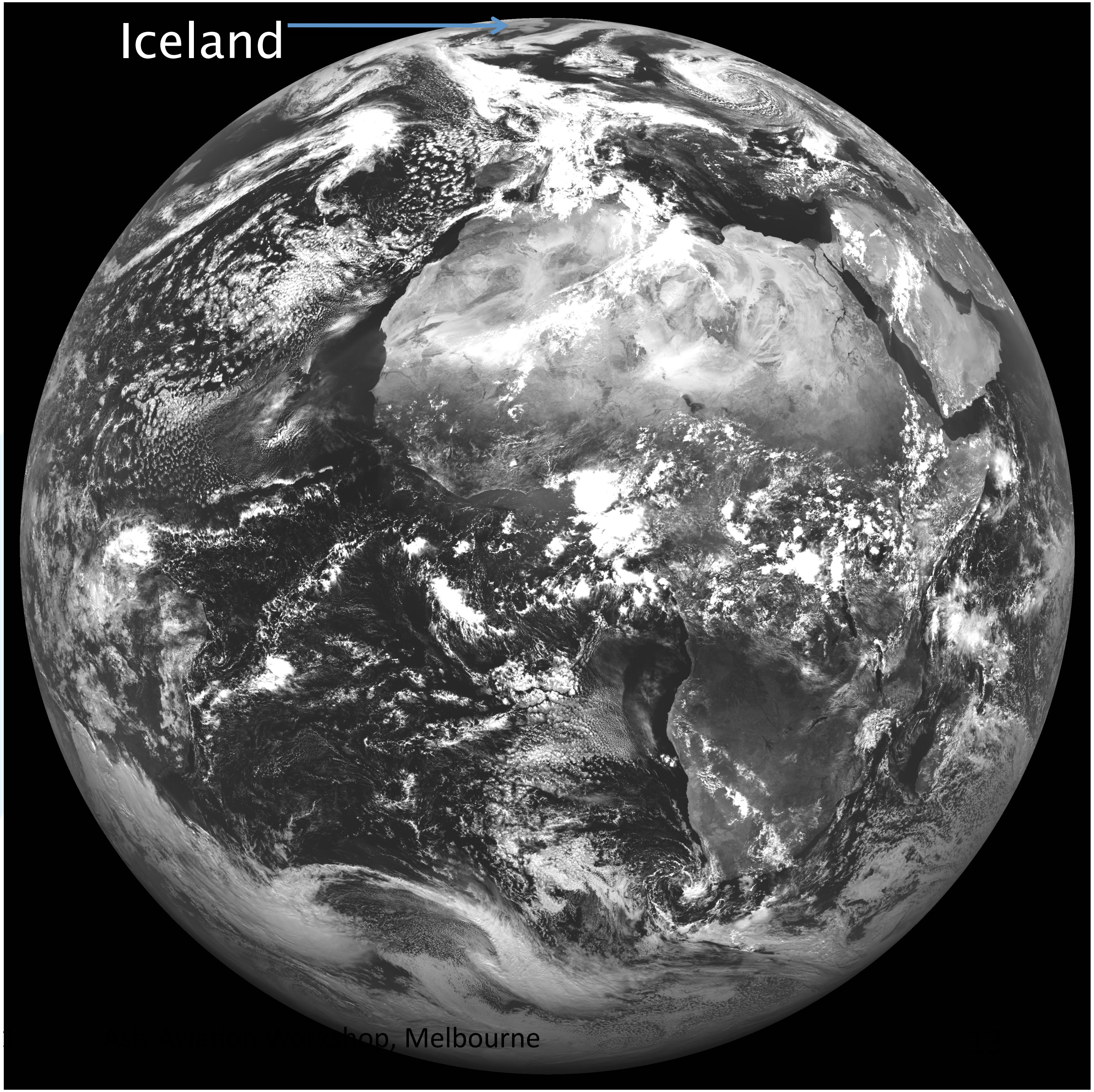

(a) Ash column from Ruang volcano, Indonesia

(b) Drifting ash and gas from Karthala volcano, Comoros

(c) Low-level diffusive gas plume - Vanuatu

(d) Kluichevskoi - winter

(e) Kluichevskoi - summer

(f) Noxious cloud from industrial fire in southern England

(g) Saharan dust outbreak – Canary islands

(h) Re-suspended ash - Iceland

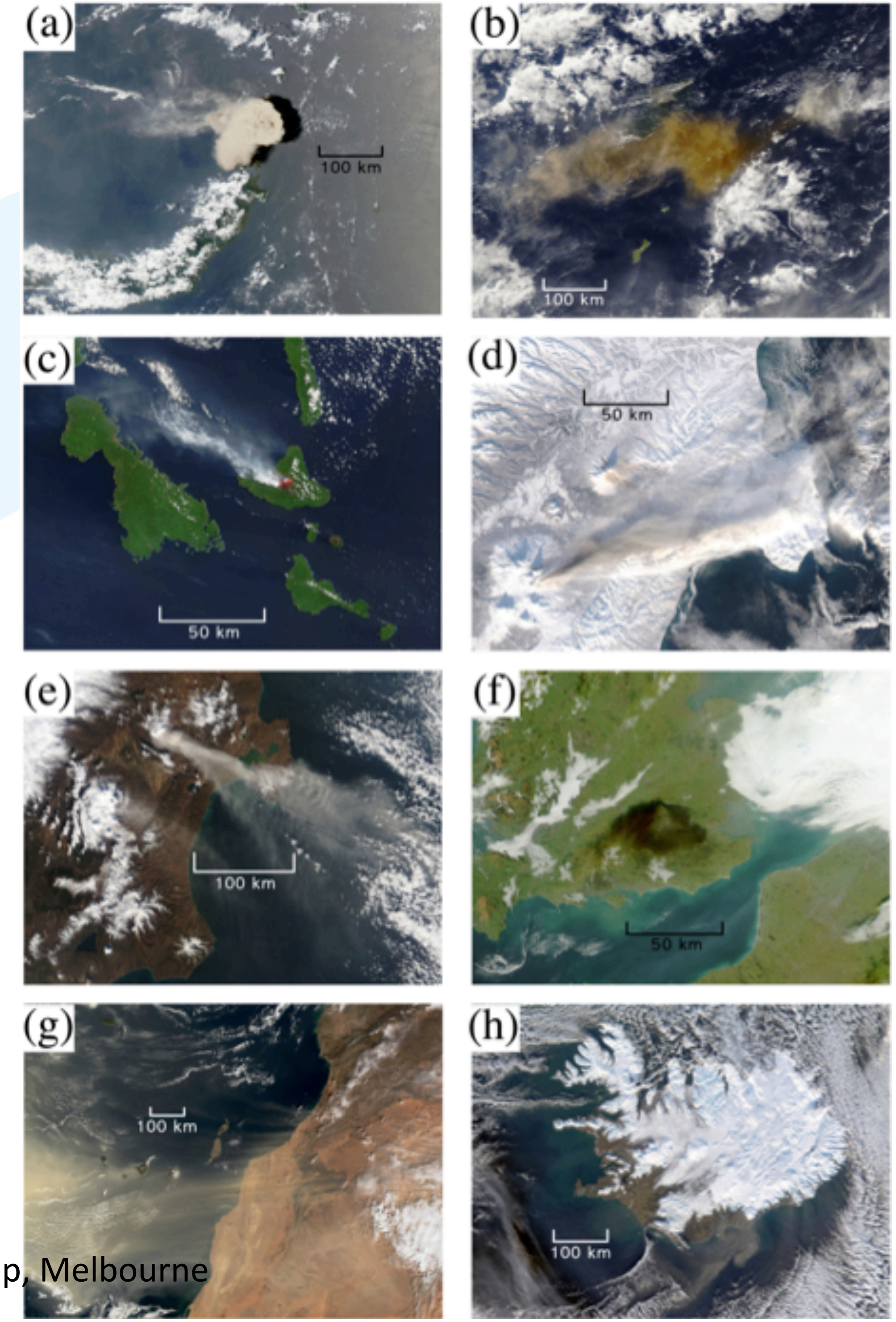

Prata, A. J. (2008): *Satellite detection of hazardous volcanic clouds and the risk to global air traffic*, **Nat. Hazards**, DOI 10.1007/s11069-008-9273-z.

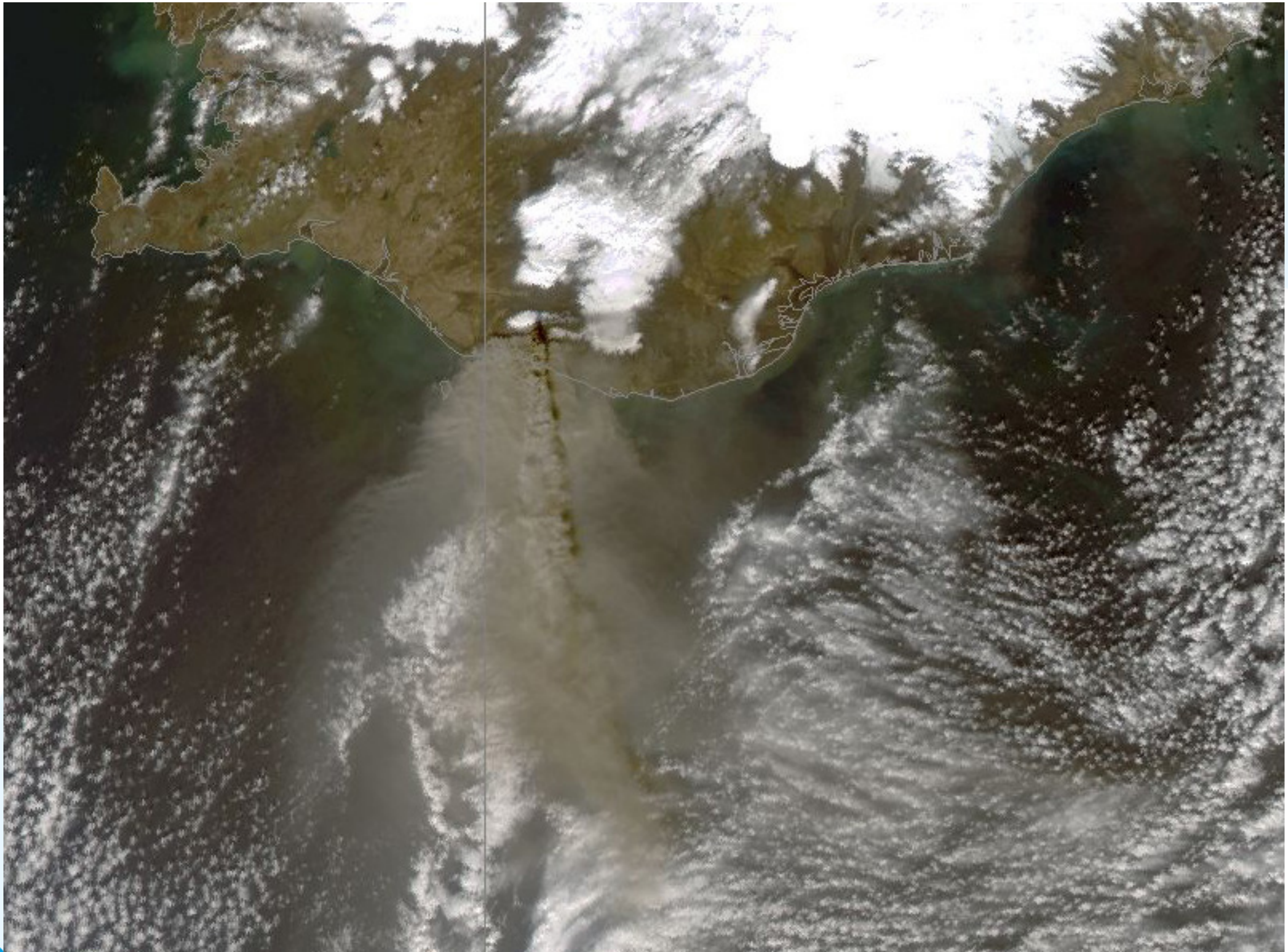

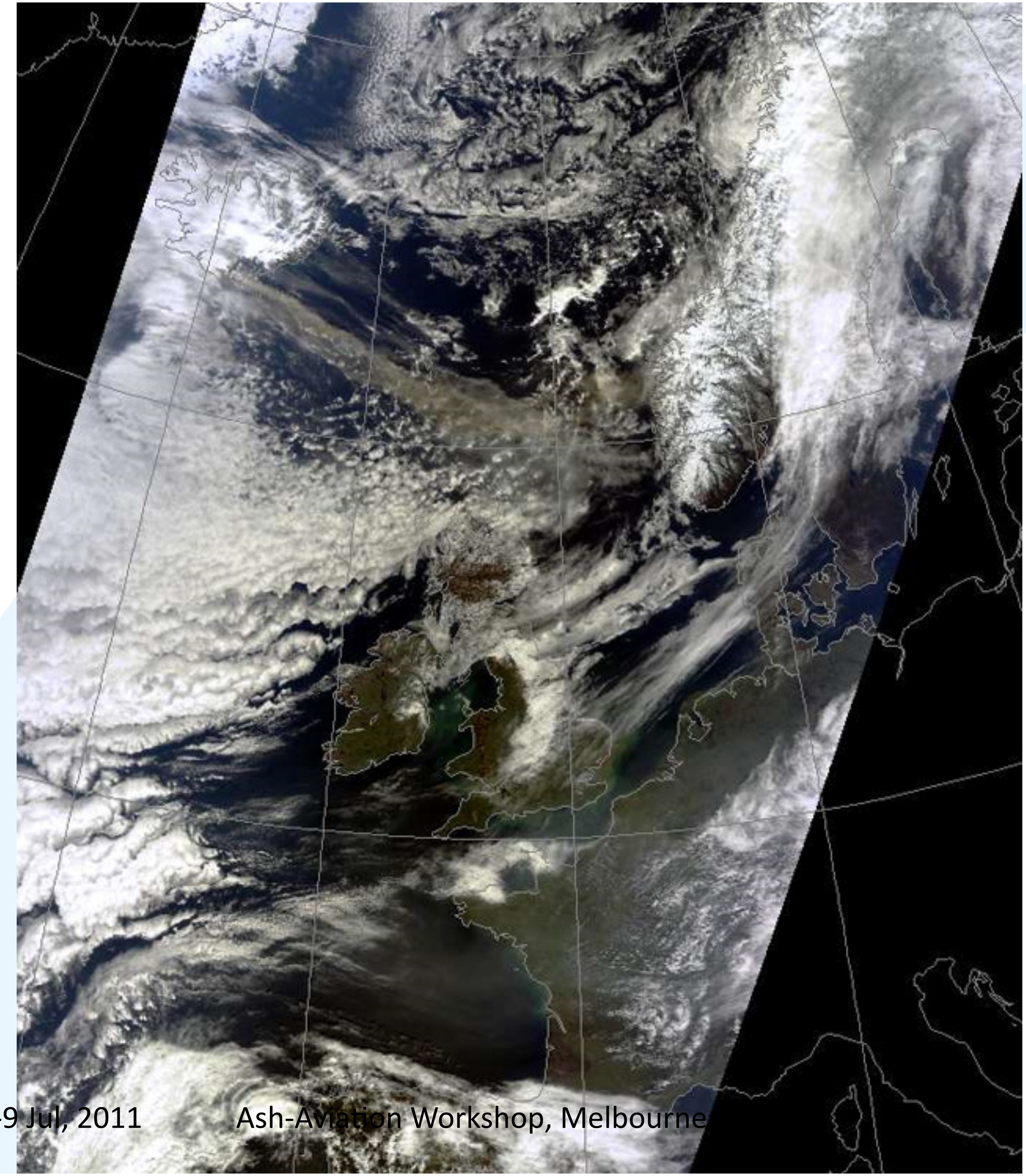

Eruption of Soufriere Hills, Montserrat, 11 Feb 2010

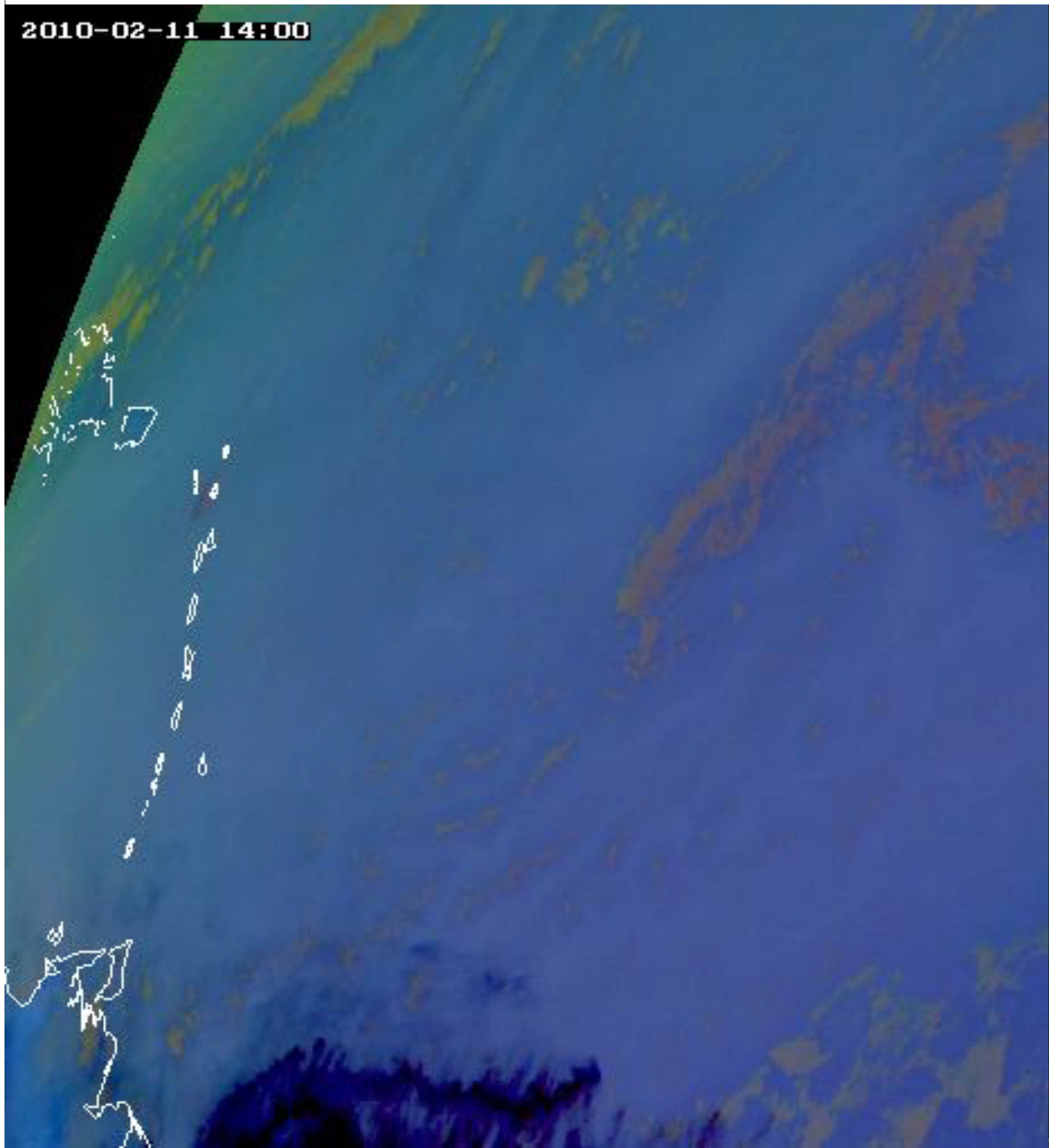

SEVIRI – triple detection

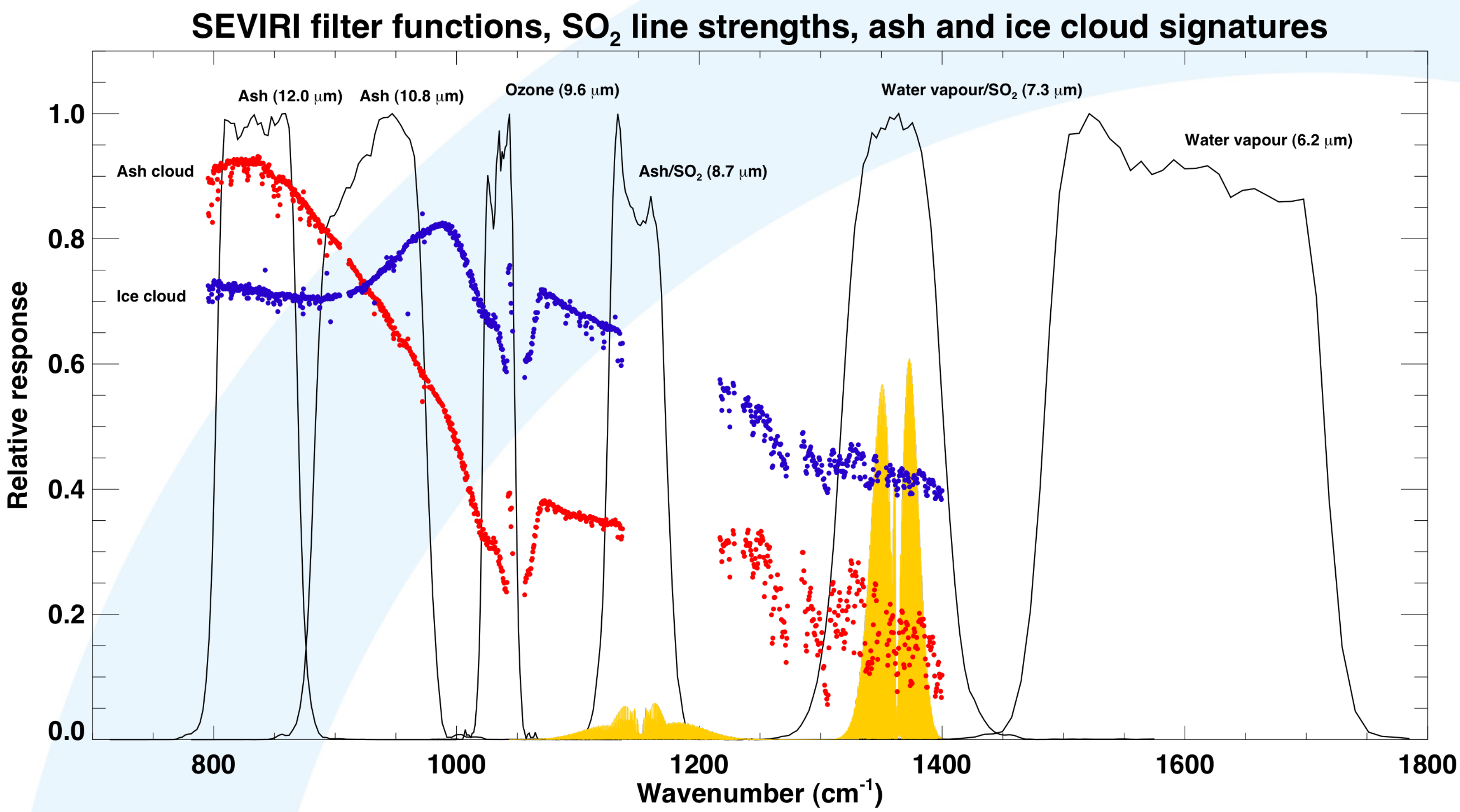

SEVIRI – triple detection

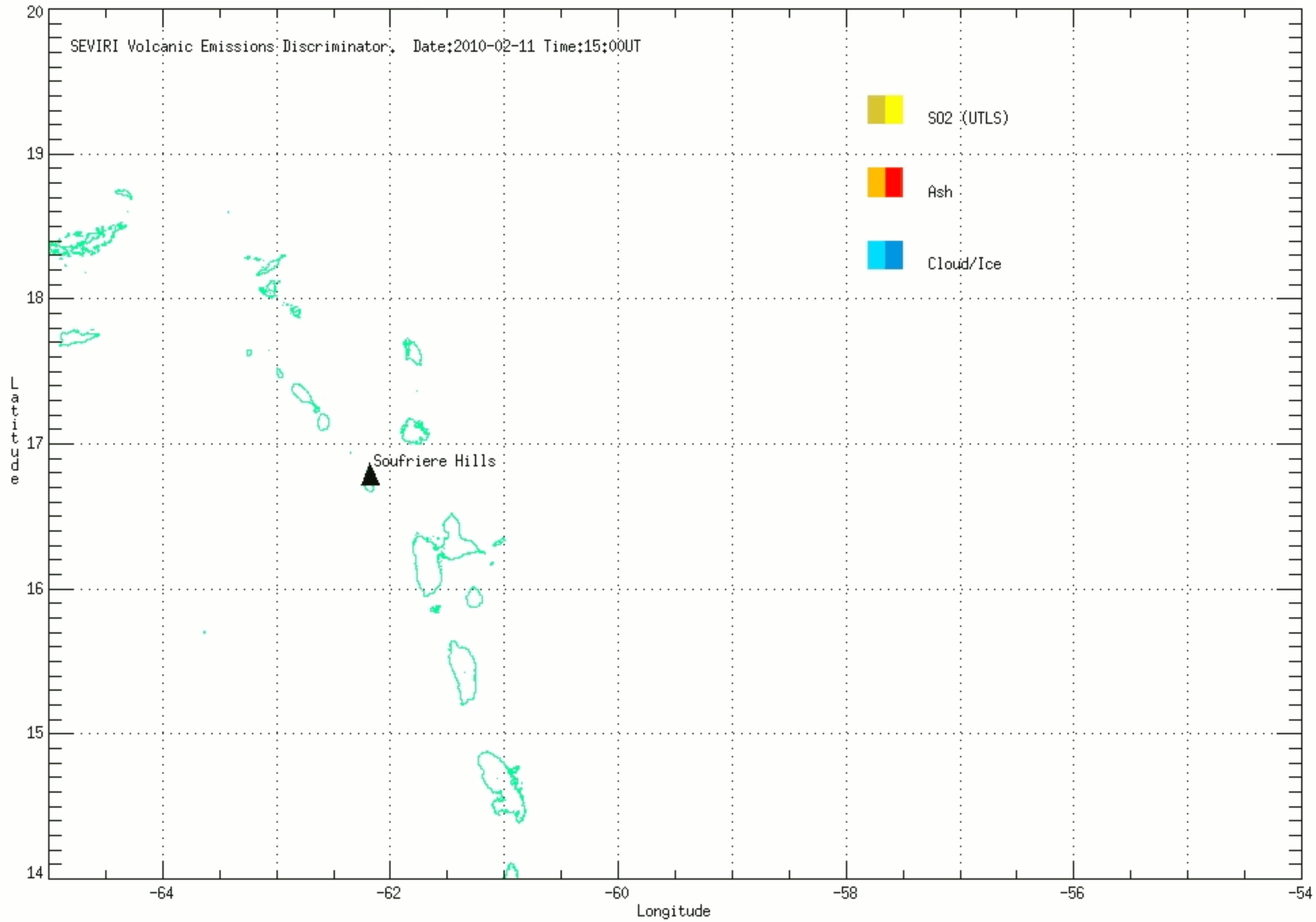

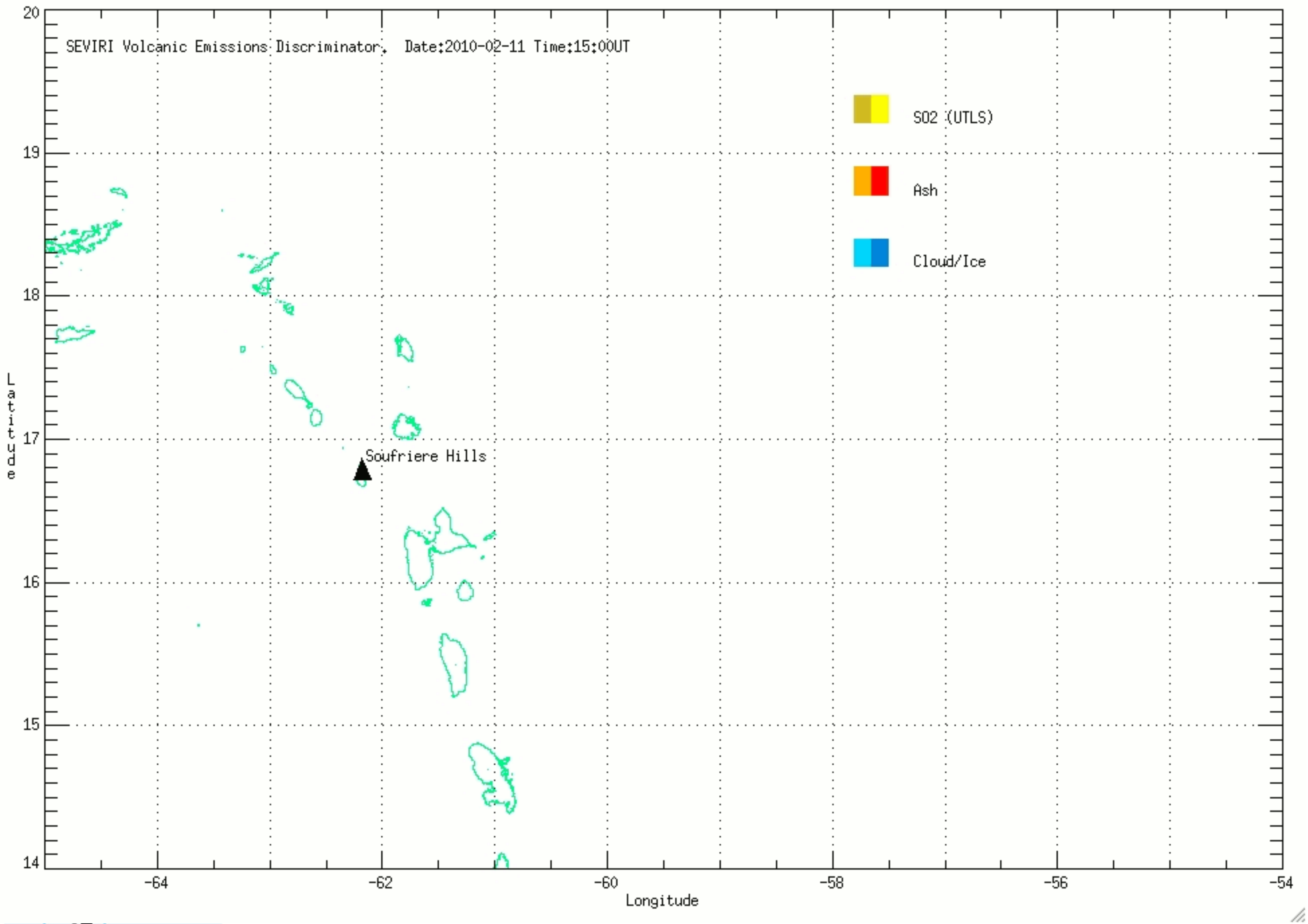
SEVIRI Volcanic Emissions Discriminator. Date:2010-02-11 Time:15:00UT
SO2 (UTLS)
Ash
Cloud/Ice
Soufriere Hills
Latitude
Longitude
20
19
18
17
16
15
14
-64
-62
-60
-58
-56
-54

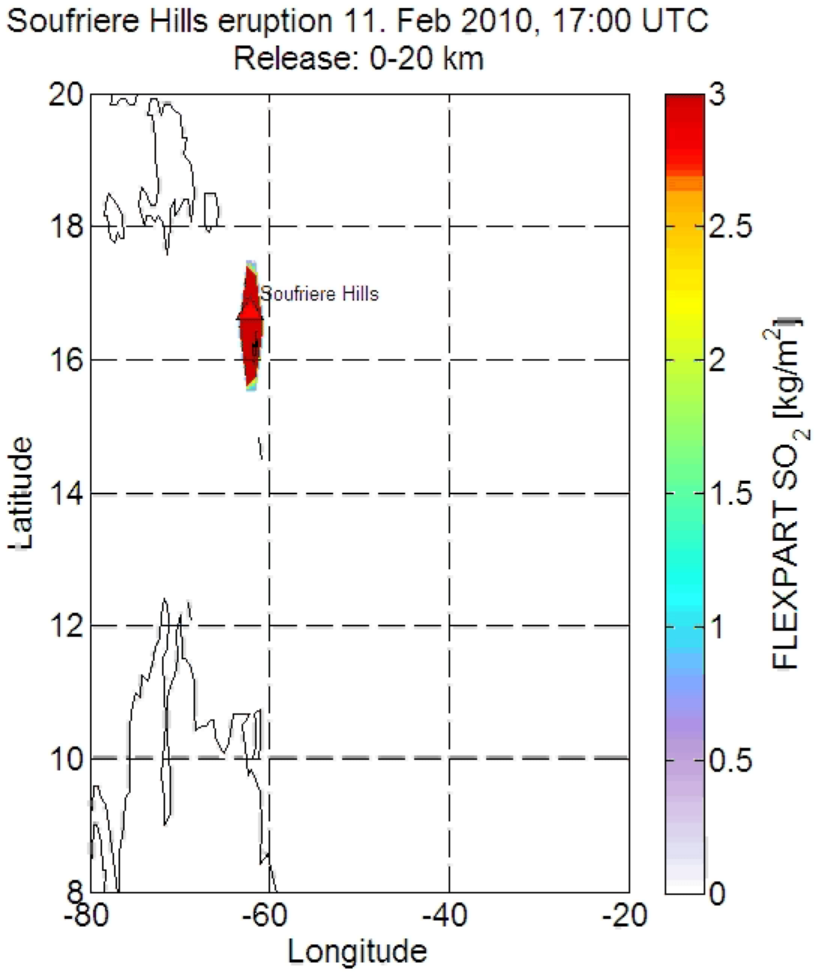

Soufriere Hills eruption 11. Feb 2010, 17:00 UTC
Release: 0-20 km
Soufriere Hills
Latitude
Longitude
FLEXPART SO2 [kg/m2]

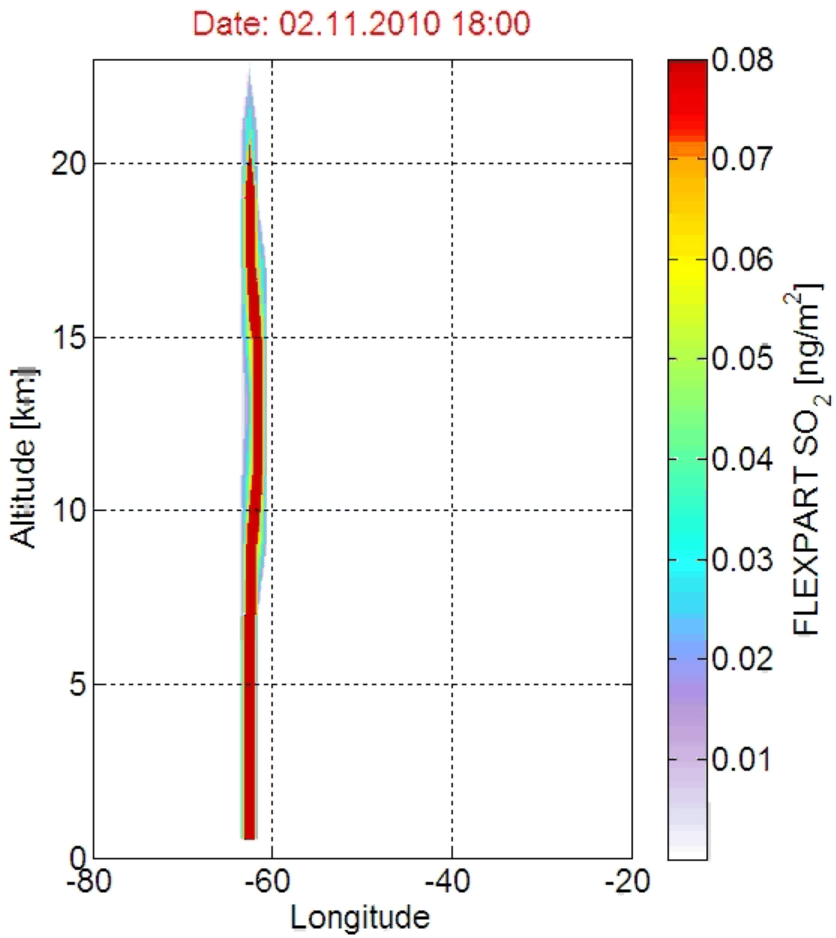

Date: 02.11.2010 18:00
Altitude [km]
Longitude
FLEXPART SO2 [ng/m2]

SEVIRI T_{12}

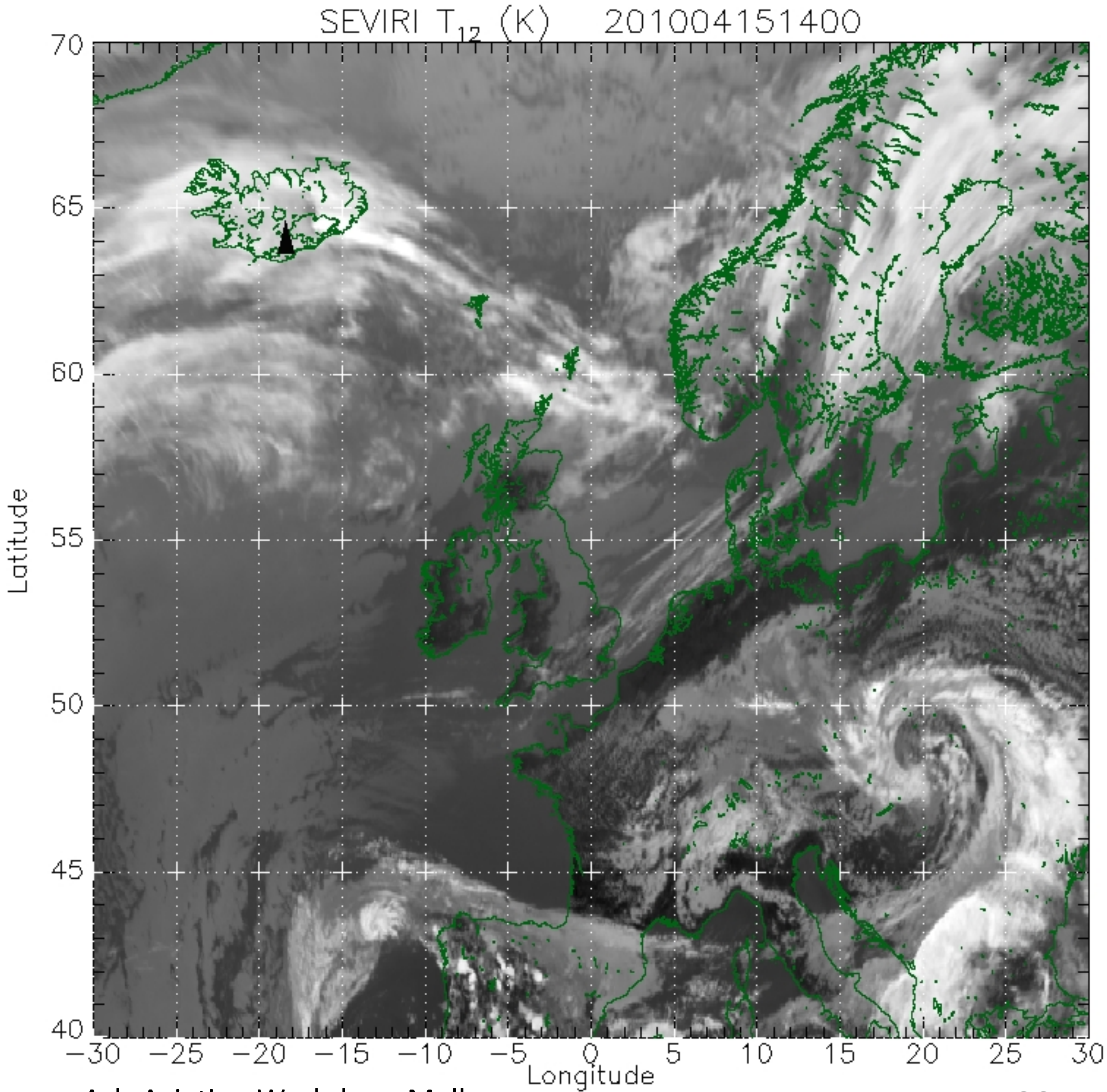
SEVIRI T_{12} (K) 201004151400
Latitude
Longitude
70
65
60
55
50
45
40
−30 −25 −20 −15 −10 −5 0 5 10 15 20 25 30

SEVIRI $T_{11}–T_{12}$

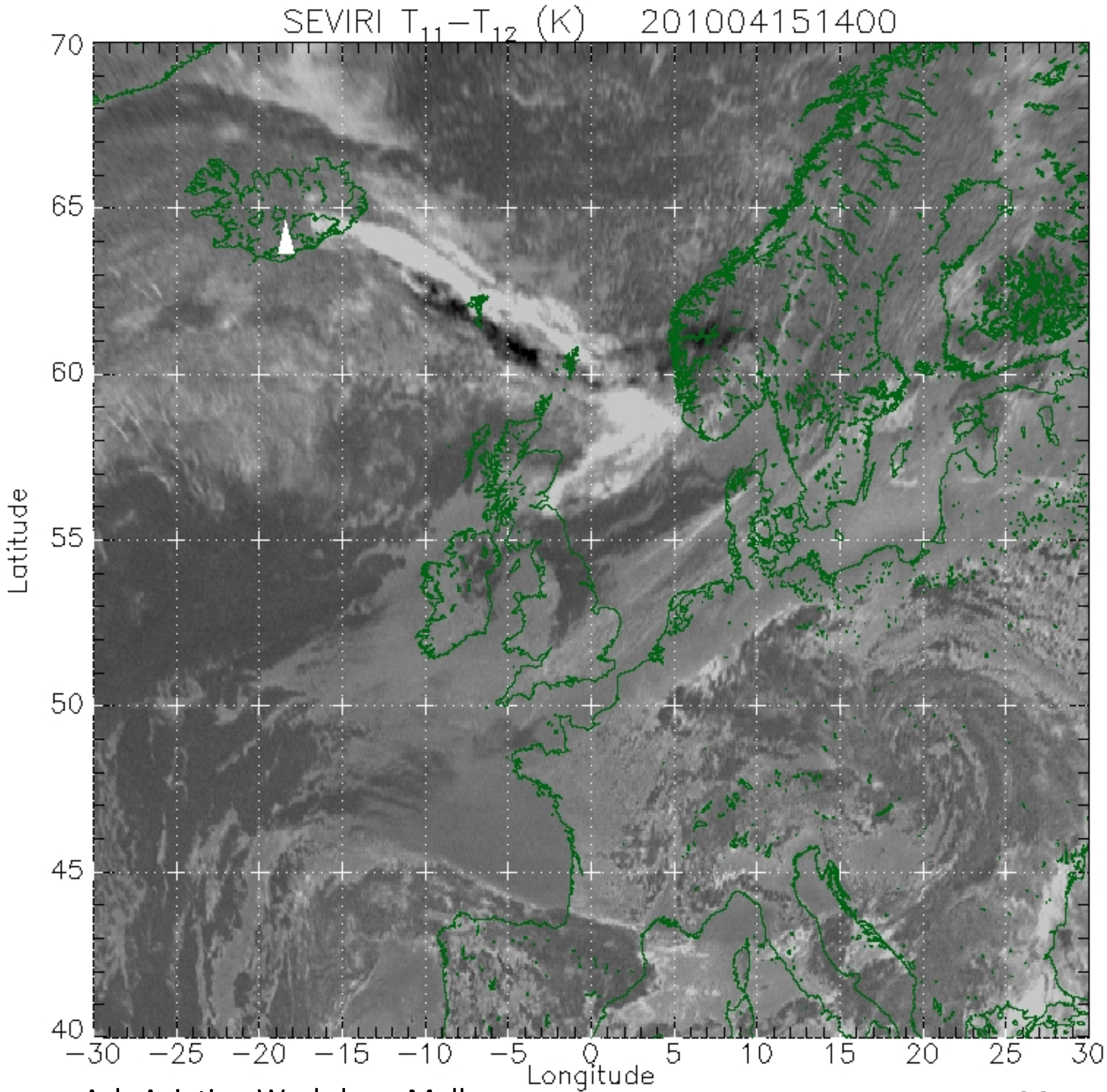

"Theoretical behaviour of spherical water droplets with radii >50 μm"

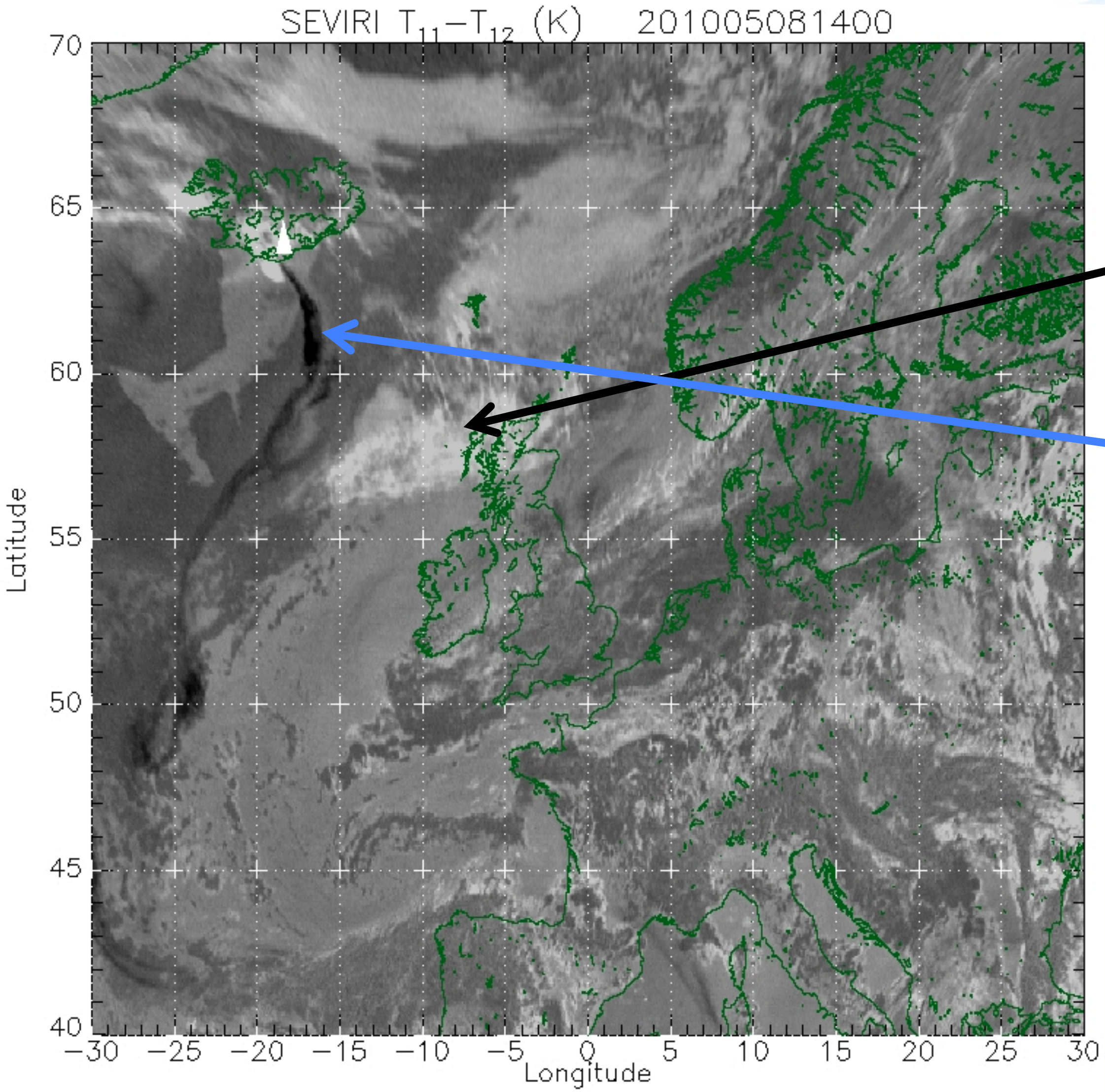

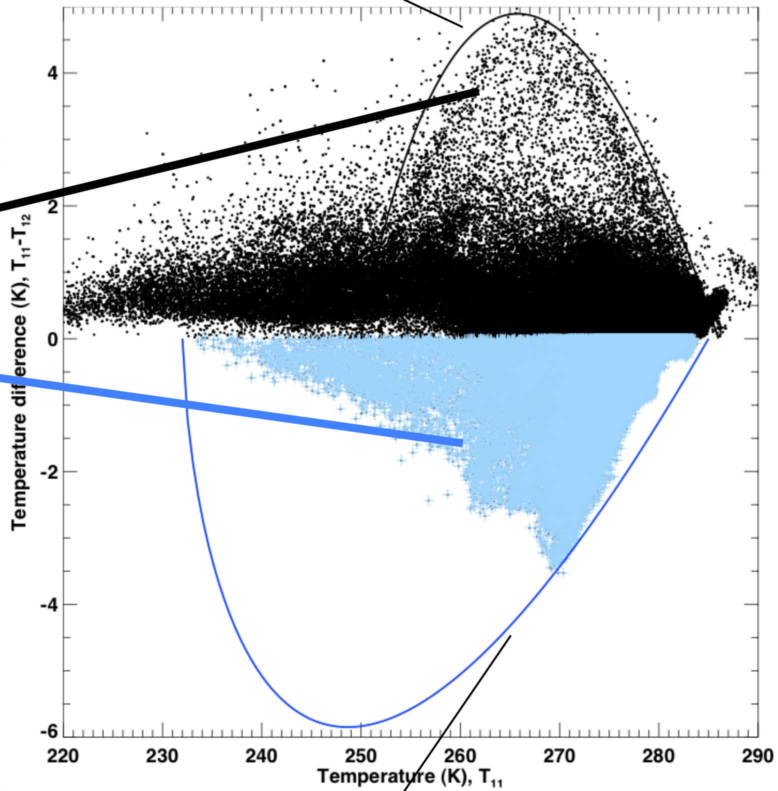

"Theoretical behaviour of spherical silicate particles with radii 1–10 μm"

Volcanic ash – Detection and discrimination

Prata, A. J., 1989, Infrared radiative transfer calculations for volcanic ash, Geophys. Res. Lett., 16(11), 1293-1296

$$T_{11} - T_{12} < 0$$

"reverse absorption" algorithm

$$\Delta T = \Delta T_c [X - X^{\beta}],$$

$$X = 1 - \frac{\Delta T_4}{\Delta T_c},$$

$$\Delta T = T_4 - T_5, \quad \Delta T_c = T_s - T_c, \quad \Delta T_4 = T_s - T_4.$$

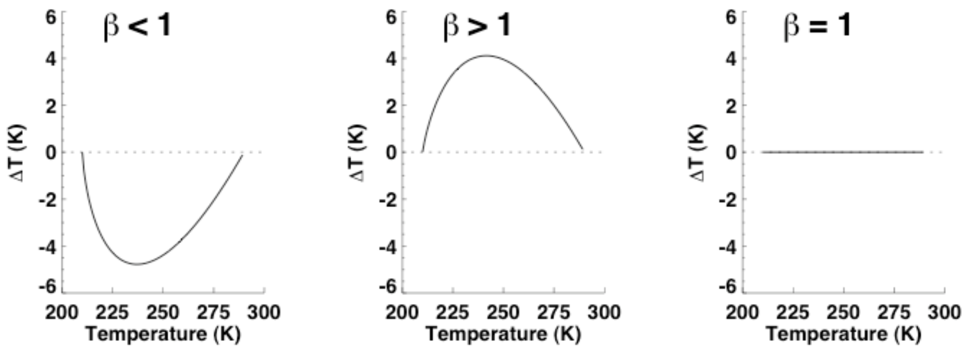

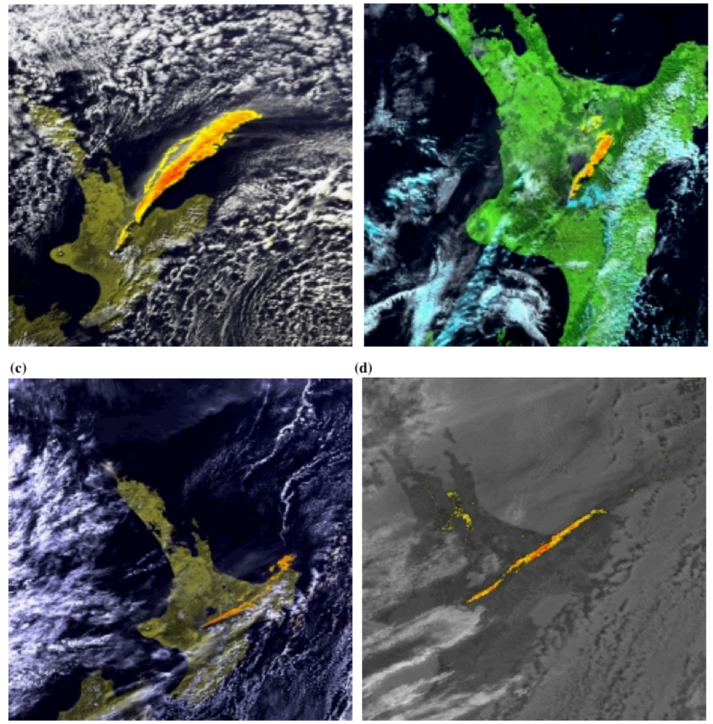

Parametric equations

$$T_4 = \epsilon_4 T_c + (1 - \epsilon_4) T_s$$

$$T_5 = \epsilon_5 T_c + (1 - \epsilon_5) T_s$$

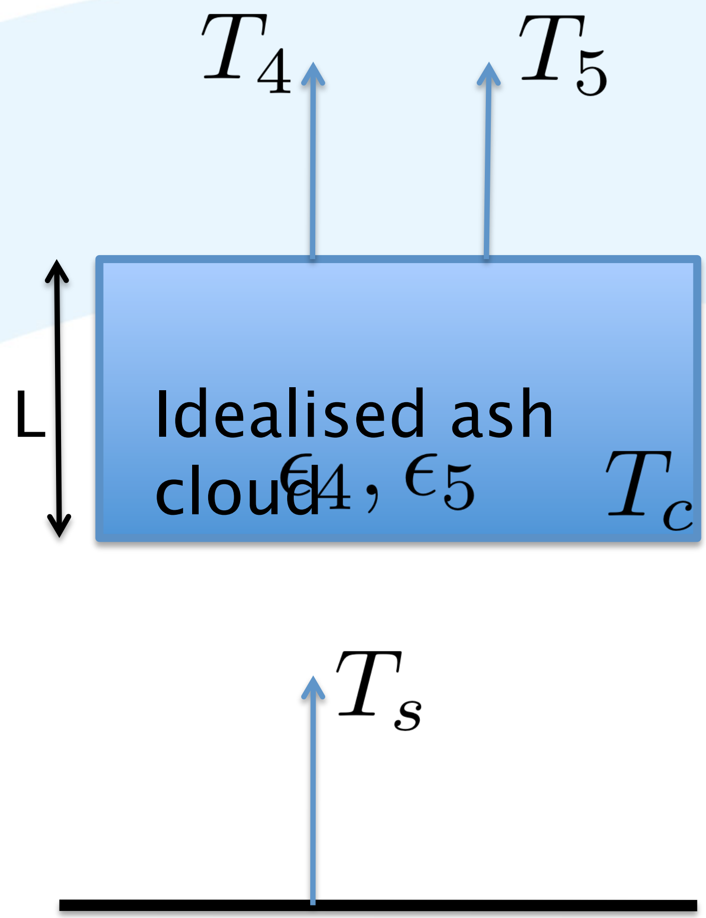

Solve these for:

$$\Delta T = T_4 - T_5$$

Denoting:

$$\Delta T_4 = T_s - T_4$$

$$\Delta T_{tcon} = T_s - T_c$$

$$\Psi = 1 - \frac{\Delta T_4}{\Delta T_{tcon}}$$

$$\epsilon_i = 1 - \exp(-k_i L)$$

$$\Psi_i = 1 - \epsilon_i$$

"like" cloud optical depth

$$\beta = \frac{k_j}{k_i} \qquad \lambda_j > \lambda_i$$

Particle microphysics – radius

Solution

$$\Delta T = \Delta T_{tcon}(\Psi - \Psi^{\beta})$$

$\beta > 1$ $\quad ice/water - cloud$

$\beta < 1$ $\quad ash - cloud$

Note that: $\Psi < 1$

Ash cloud

Ice/water cloud

Opaque cloud

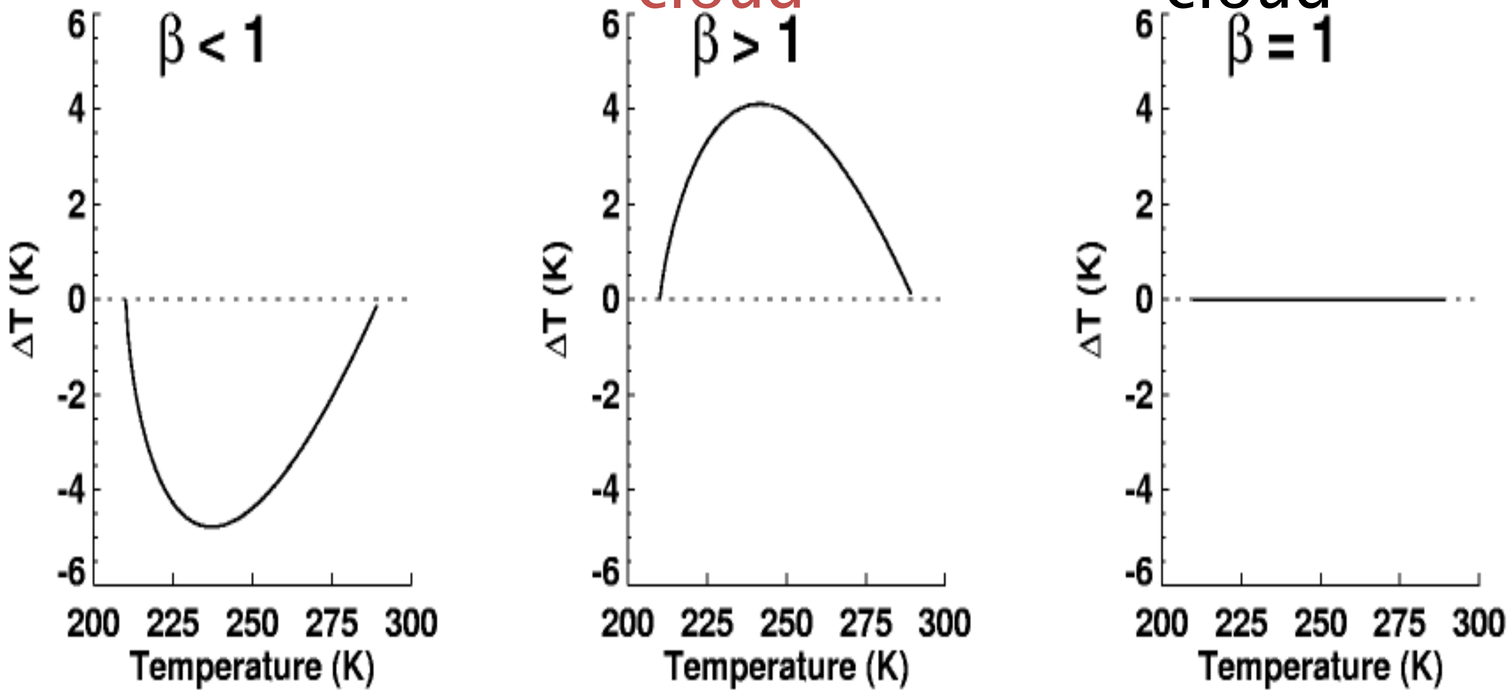

β=ratio of extinction coefficients at 11 μm and 12 μm

Solving for radius and optical depth

Given T_4 and Ψ it is possible to construct "theoretical curves" that suggest the behaviour of "real" measurements on a plot of T_4 vs ΔT

Theory and Measurement

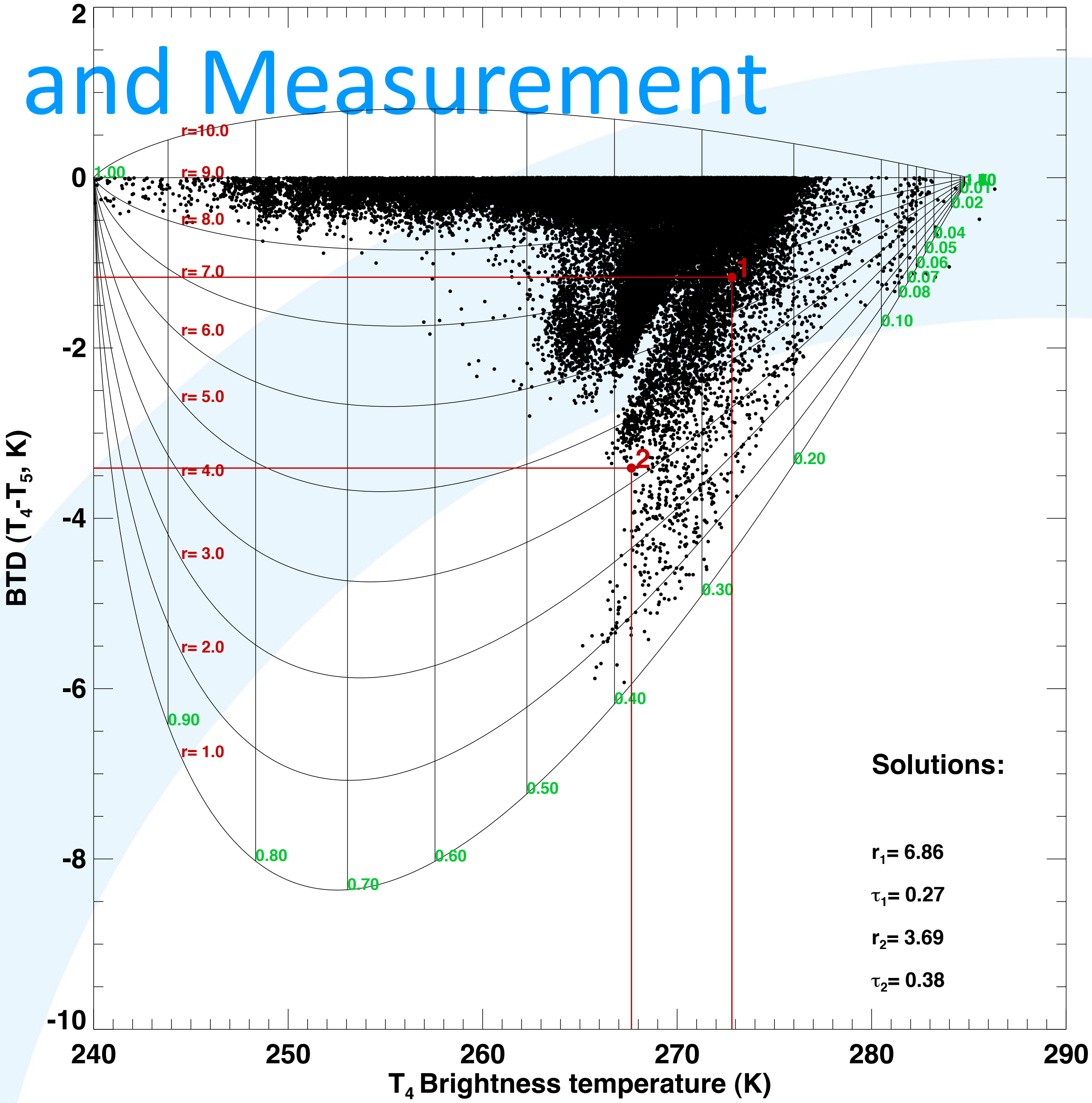

Going quantitative

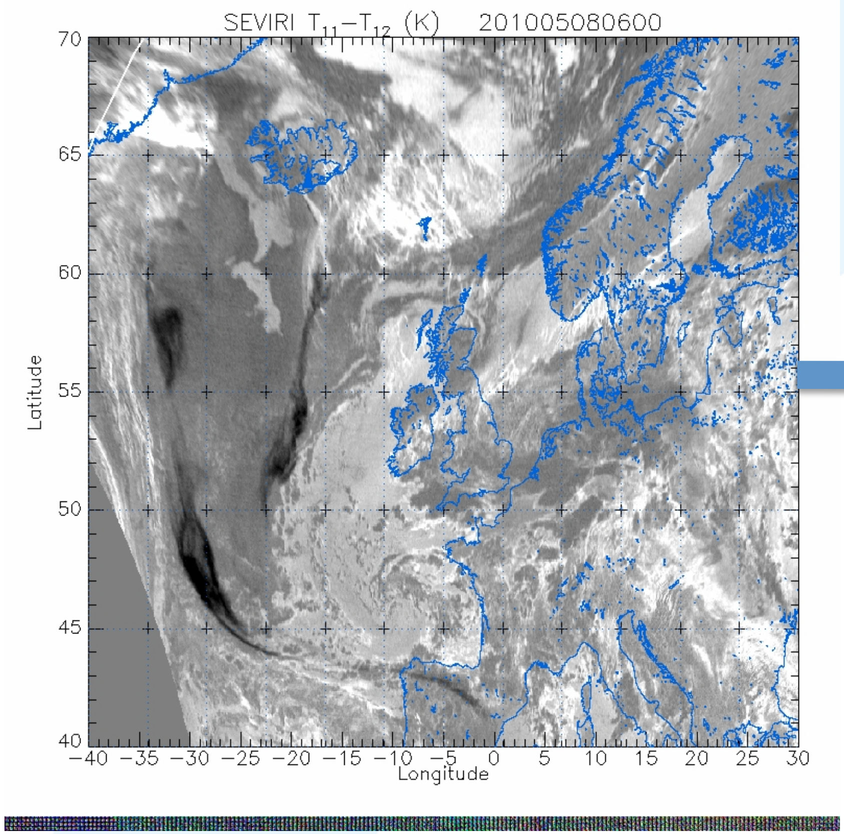

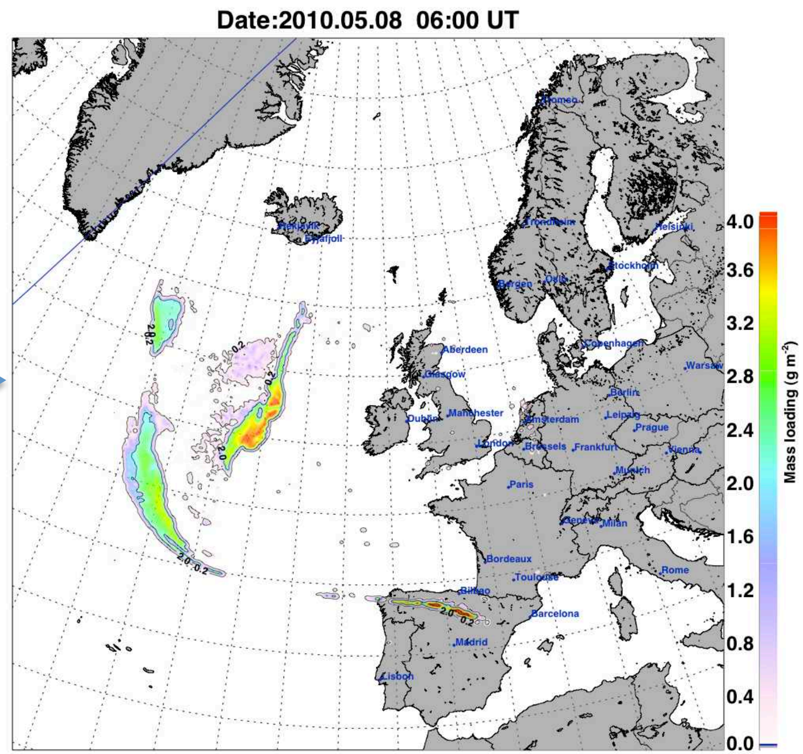

Calculating the mass loading (gm^{-2})

$$M_l = \frac{4}{3}\rho\frac{r\tau}{Q_{ext}}$$

ρ	Density	Units: kg m^{-3}
Q_{ext}	Extinction efficiency	none
τ	Optical depth	none
r	Effective radius	µm

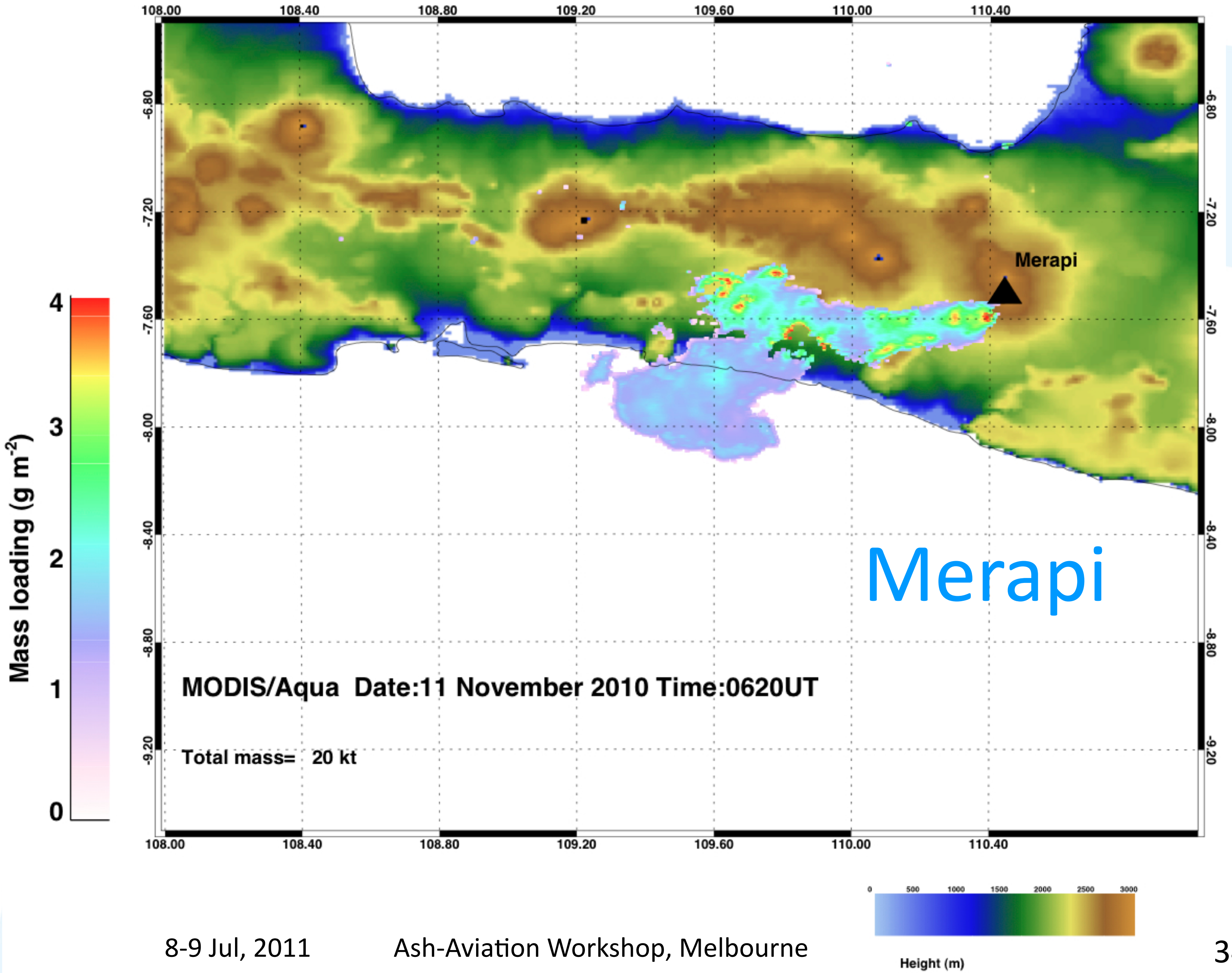

Mass loading (g m^{-2})
4
3
2
1
0
108.00
108.40
108.80
109.20
109.60
110.00
110.40
-6.80
-7.20
-7.60
-8.00
-8.40
-8.80
-9.20
Merapi
MODIS/Aqua Date:11 November 2010 Time:0620UT
Total mass= 20 kt
Merapi
0
500
1000
1500
2000
2500
3000
Height (m)

Methodology

- Data source: SEVIRI 12-channel 15-minute data for 30W-30E, 40N-70N, from 14.04.2010 to 24.05.2010. Only use IR channels.
- Automatically detect pixels affected by ash
- Apply water vapour correction
- Apply parallax correction
- Retrieve effective particle radius, IR optical depth and mass loading (g m^{-2})
- Validate
- Determine concentrations using coincident CALIOP space-based lidar measurements
- Present results

Some problems with ash detection

Water vapour makes $T_{11}-T_{12} > 0$

Correction applied based on Yu et al. (2003)

Clear land at night gives $T_{11}-T_{12} < 0$

No good correction algorithm available

Mixed pixels

Difficult to correct for without sub-pixel data

Improvement possible for some pixels by using spatial information

What do we know about ash particles?

Atmospheric and Environmental Impacts of Volcanic Particulates

Adam J. Durant[1], Costanza Bonadonna[2], and Claire J. Horwell[3]

1811-5209/10/0006-0235$2.50 DOI: 10.2113/gselements.6.4.235

A single ash particle erupted during the 18 May 1980 eruption of Mount St. Helens, USA. The dark voids are vesicles formed as gases escaped. Image width is about 75 μm. USGS image by A. Sarna-Wojcicki

High silicate content
Particle size (radius) ranges from 0.01–500 μm (typically)
Irregular shape
Melting point ~1100 °
(800–1200 ºC).

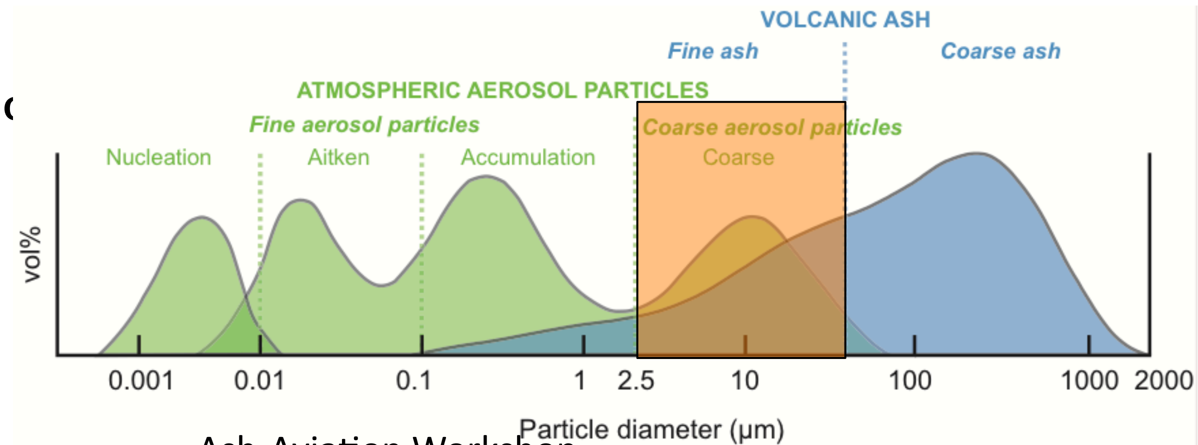

Microphysics

Refractive index as a function of wavelength.
Spherical particles.
Mie scattering equation solver

Modified-gamma and log-normal size distributions

$$\frac{dn(r)}{dr} = \frac{Nb^7}{6!} r^6 exp(-br)$$

$$\frac{dn(r)}{dr} = \frac{N}{r\sigma\sqrt{2\pi}} exp\left\{\frac{-(Ln[r] - Ln[r_o])^2}{2\sigma^2}\right\}$$

Efficiency factors for polydispersions:

$$\hat{Q}_f = \frac{\int_o^\infty \pi r^2 Q_f(\frac{2\pi r}{\lambda}, m) \frac{dn(r)}{dr} dr}{\int_o^\infty \pi r^2 \frac{dn(r)}{dr} dr}$$

Refractive indices

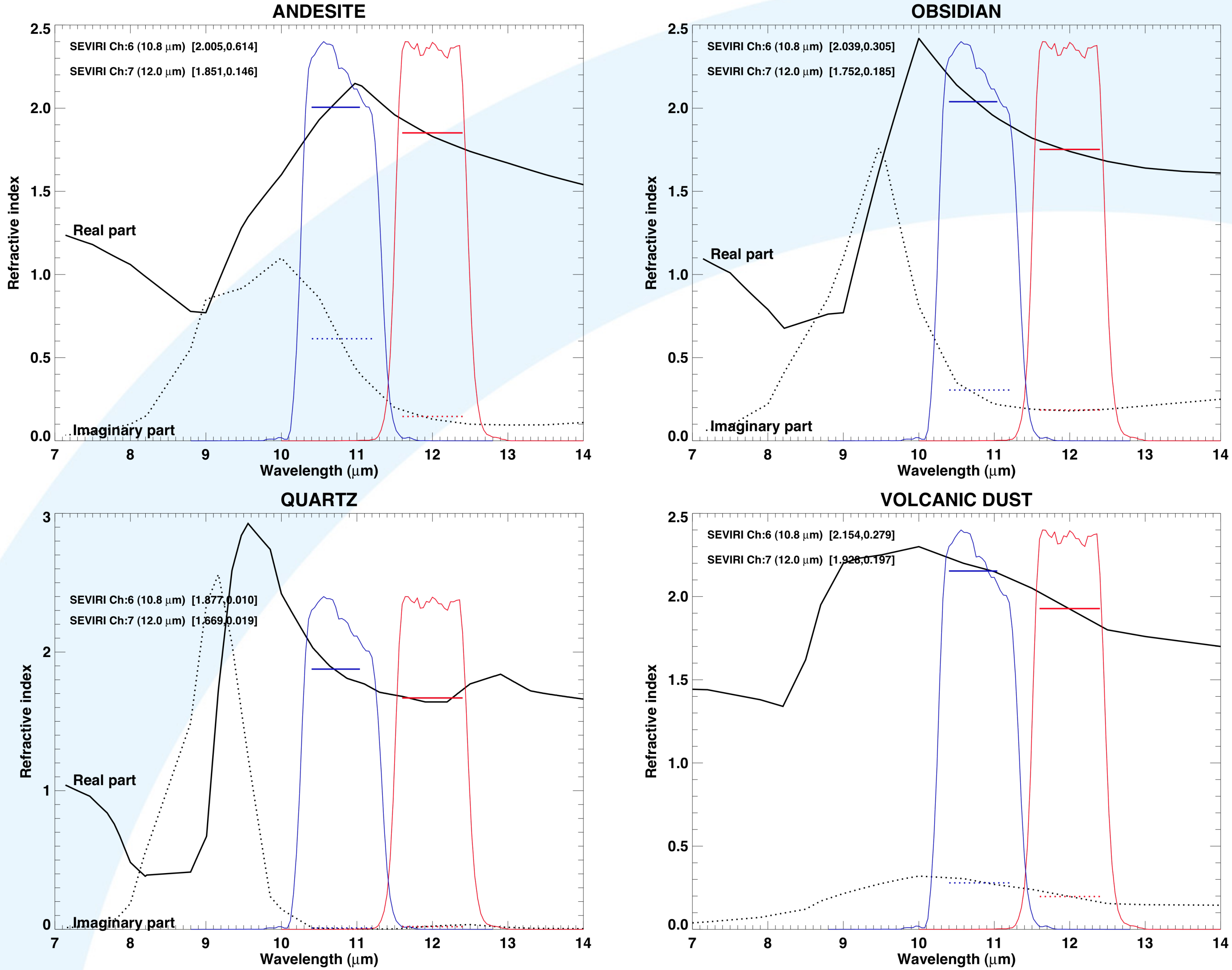

Procedure

Run Mie code for particle sizes from 0.2 to 32 µm in steps of 0.2 µm

Run RT code for all particle sizes, optical depths from 0.02 to 8, in steps of 0.02, 16 streams, and cloud-top and surface temperatures from Tc±10 K, Ts ±10 K

Generate very large look-up table containing simulated top-of-atmosphere (no water vapour) brightness temperatures at 10.8, 12.0 µm

Use ash-identified pixels with measured BTs at 10.8 and 12.0 µm to find "best fit" to simulations.

(Sometimes several values found).

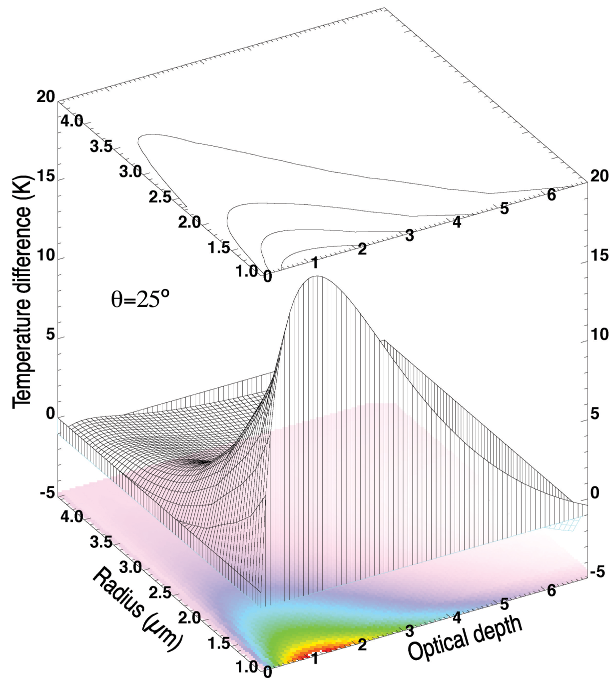

In practice the radiative transfer equation with scattering is solved

$$\mu \frac{\partial I}{\partial \tau}(\tau, \mu) = I(\tau, \mu) - (1 - \varpi_o)B(T) - \frac{\varpi_o}{2} \int_{-1}^{1} P(\mu; \mu') I(\tau, \mu') d\mu'$$

Boundary conditions:

$$I(0, -\mu) = 0$$

$$I(\tau_1, +\mu) = B(T_s)$$

Standard Mie code used to solve for the scattering efficiencies. Need complex refractive indices.

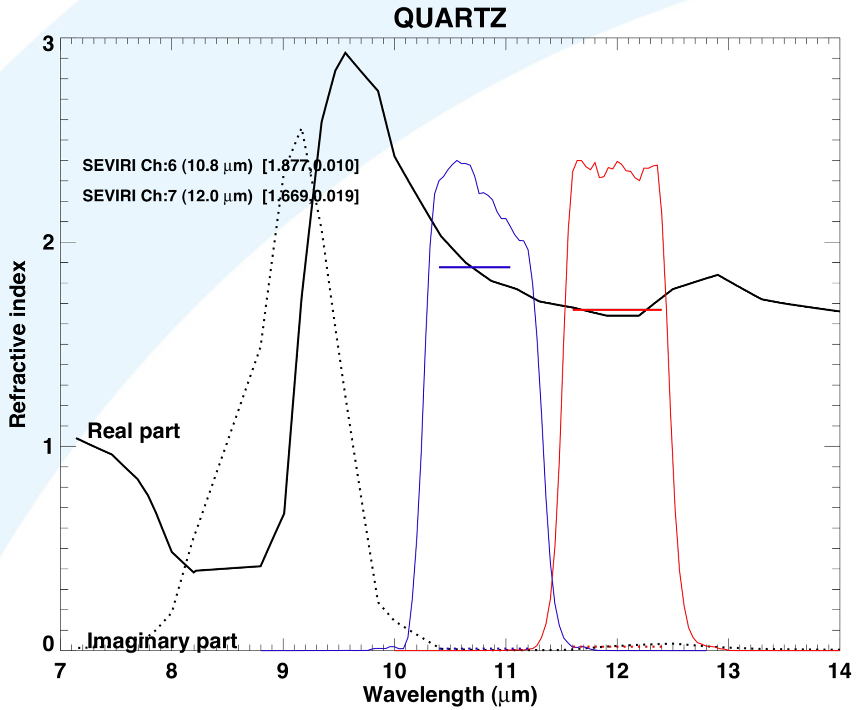

What is all the fuss about?

- Erosion of edges
- Ash build-up on turbine blades
- Plugged cooling holes

Why Is Operation In Volcanic Ash An Issue ?

- Erodes compressor blades and linings
- Ash melts in Combustor and deposits in HP Turbine
  - Reduced HPNGV throat area
  - Increased HPC pressure
  - Engine surge
  - Internal cooling airflow blockage
- Fine particles can get in to oil system and damage transmissions components
- Pneumatic controls blocked by small particles

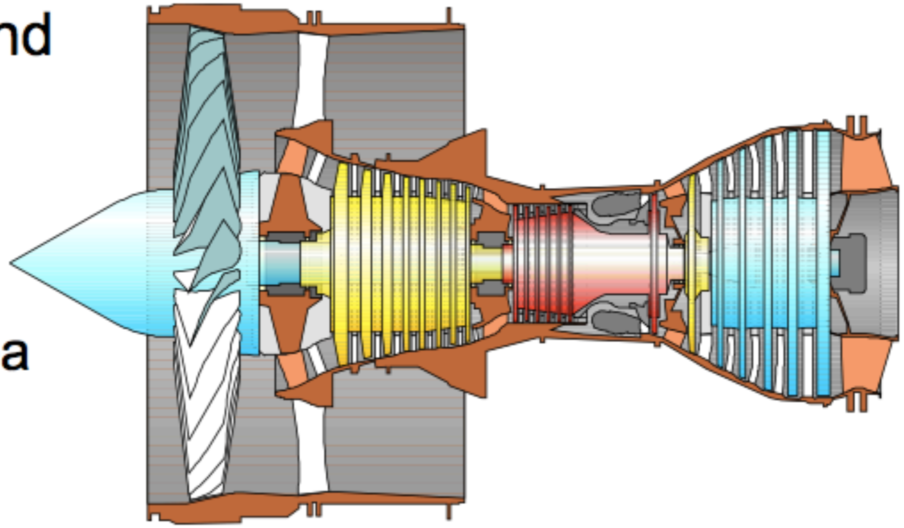

Heavy HP NGV contamination (BA747, Jarkarta 1982)

Threat to Aviation from Volcanoes

- Most danger in 1st 3hrs after eruption
- Highest risk is at night or in low visibility conditions
- Hazard is from micron-size silicate particles
- Volcanoes are globally distributed, often in remote locations, unpredictable, and most are not monitored
- Winds can rapidly spread ash into regions previously clear
- Ash can be distributed from the ground to 50, 000 ft (or higher), but generally forms into thin layers (100's m to a few km's)
- There remains some risk days to weeks following an eruption

Global aviation threat

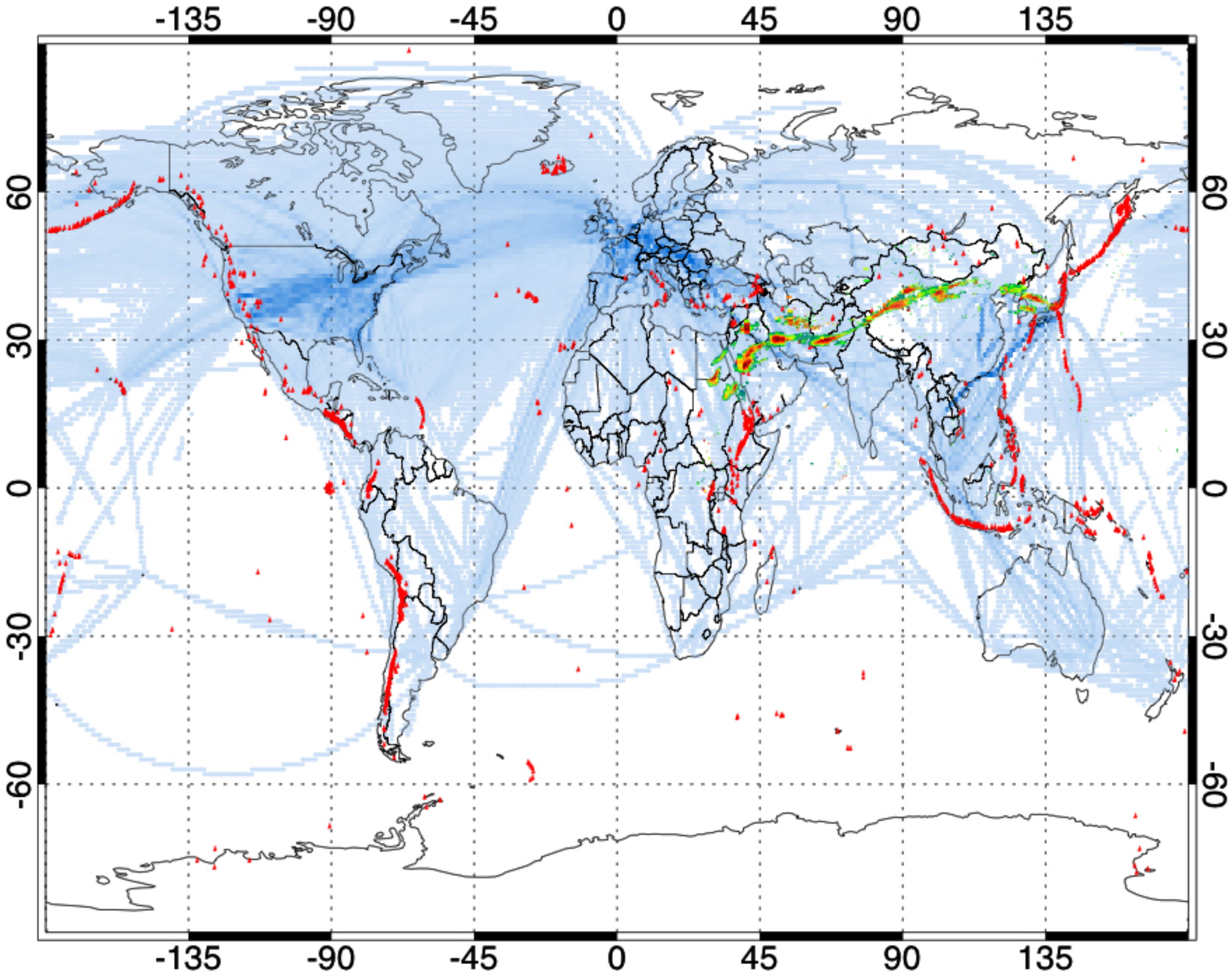

Growth in aviation traffic

Region	Annual average growth rate of passengers (percentage) 2001-2005	
Europe	2.3	4.5
Africa	3.3	5.0
Middle East	6.4	4.0
Asia and Pacific	4.1	7.5
North America	1.8	5.0
Latin America and Caribbean	2.9	4.5
World	2.7	6.0

Freight & mail
(% change in ton-km)

Source: International Civil Aviation Organisation

VAACs

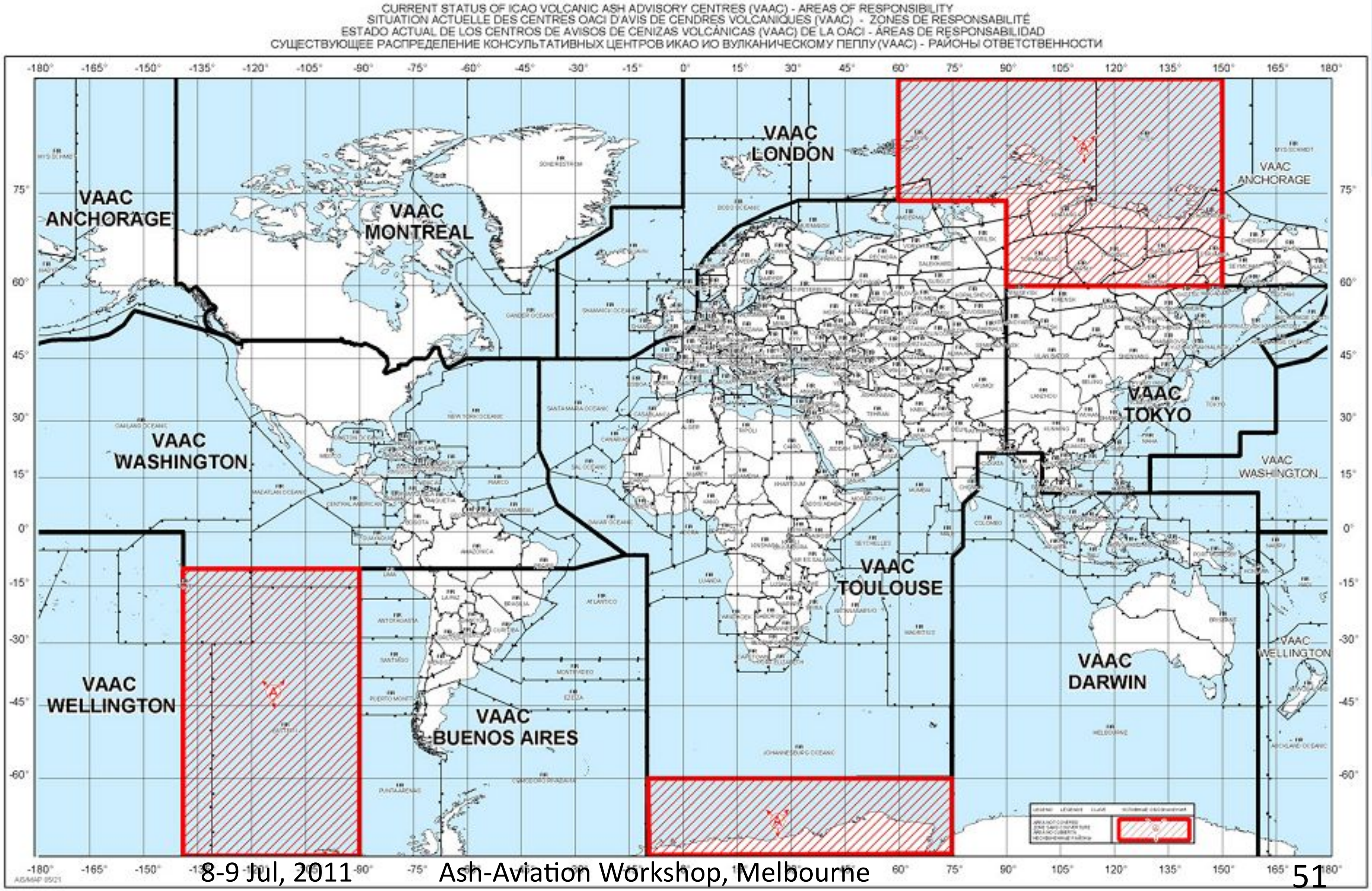
CURRENT STATUS OF ICAO VOLCANIC ASH ADVISORY CENTRES (VAAC) - AREAS OF RESPONSIBILITY
SITUATION ACTUELLE DES CENTRES OACI D'AVIS DE CENDRES VOLCANIQUES (VAAC) - ZONES DE RESPONSABILITÉ
ESTADO ACTUAL DE LOS CENTROS DE AVISOS DE CENIZAS VOLCÁNICAS (VAAC) DE LA OACI - ÁREAS DE RESPONSABILIDAD
СУЩЕСТВУЮЩЕЕ РАСПРЕДЕЛЕНИЕ КОНСУЛЬТАТИВНЫХ ЦЕНТРОВ ИКАО ПО ВУЛКАНИЧЕСКОМУ ПЕПЛУ (VAAC) - РАЙОНЫ ОТВЕТСТВЕННОСТИ
VAAC ANCHORAGE
VAAC MONTREAL
VAAC LONDON
VAAC ANCHORAGE
VAAC WASHINGTON
VAAC TOKYO
VAAC WASHINGTON
VAAC TOULOUSE
VAAC WELLINGTON
VAAC BUENOS AIRES
VAAC DARWIN
VAAC WELLINGTON

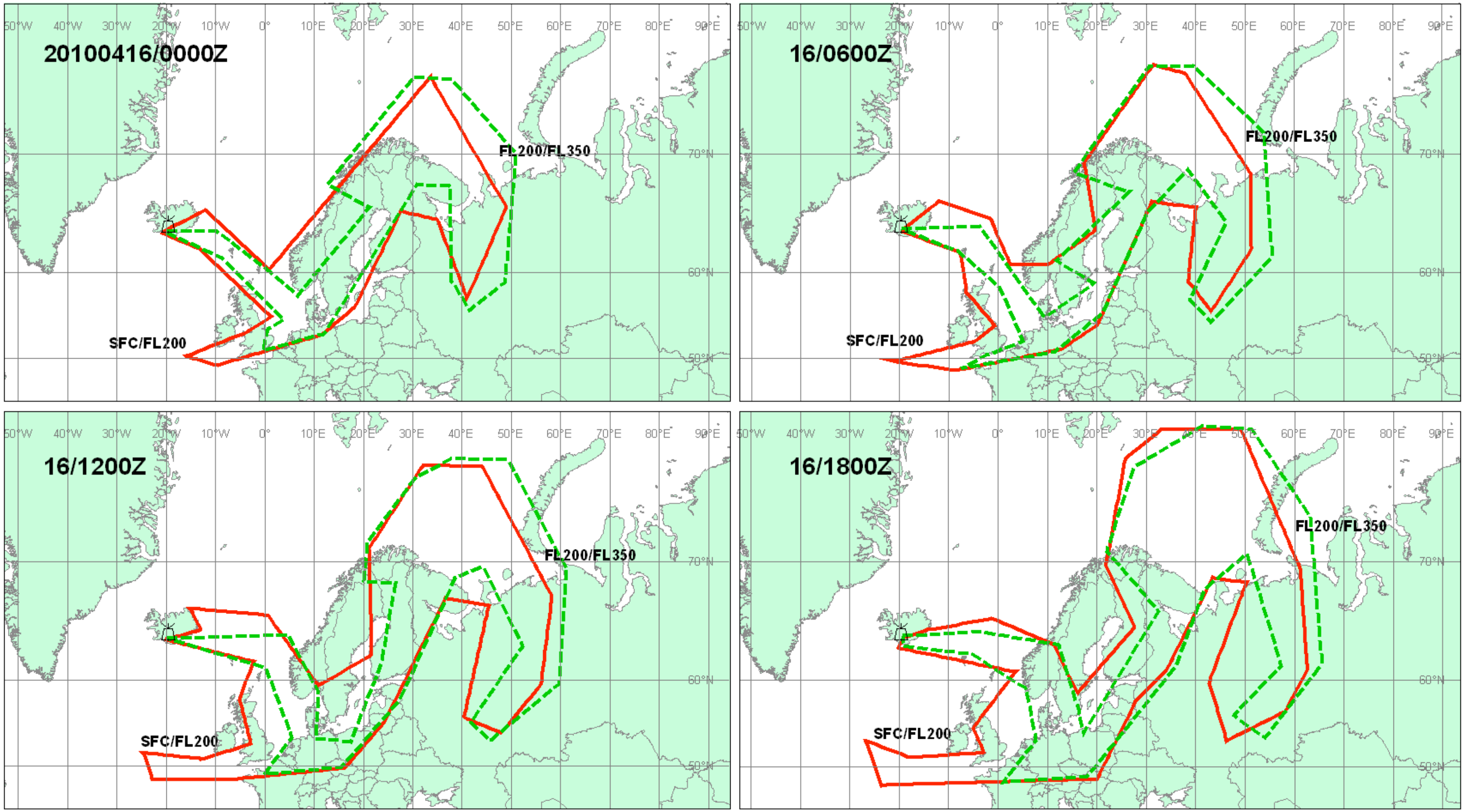

VA ADVISORY
DTG: 20100416/0000Z
VAAC: LONDON
VOLCANO:
EYJAFJALLAJOKULL
PSN: N6338 W01937
AREA: ICELAND

SUMMIT ELEV: 1666M
ADVISORY NR: 2010/008
INFO SOURCE: ICELAND MET OFFICE
AVIATION COLOUR CODE: RED
ERUPTION DETAILS: SIGNIFICANT ERUPTION CONTINUING. PLUME REACHING FL180, BUT POSSIBLY OCCASIONALLY TO FL240.

RMK: ASH CONCENTRATIONS WITHIN INDICATED AREAS ARE UNKNOWN. NO SIGNIFICANT ASH RISK ABOVE FL350.
NXT ADVISORY: 20100416/0600Z

The Safe to Fly – Chart: 17th May 2010

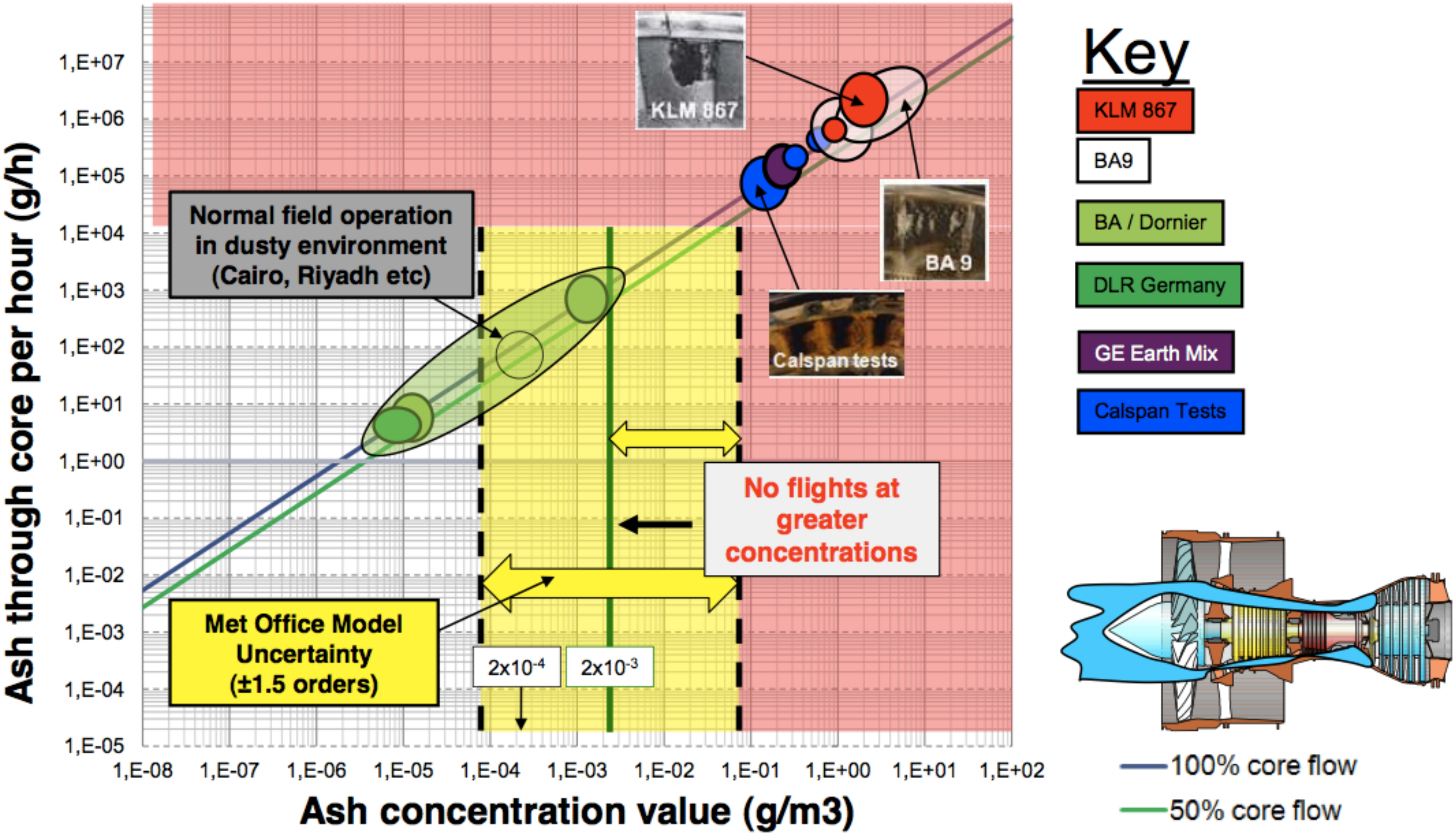

15-17 May 2010

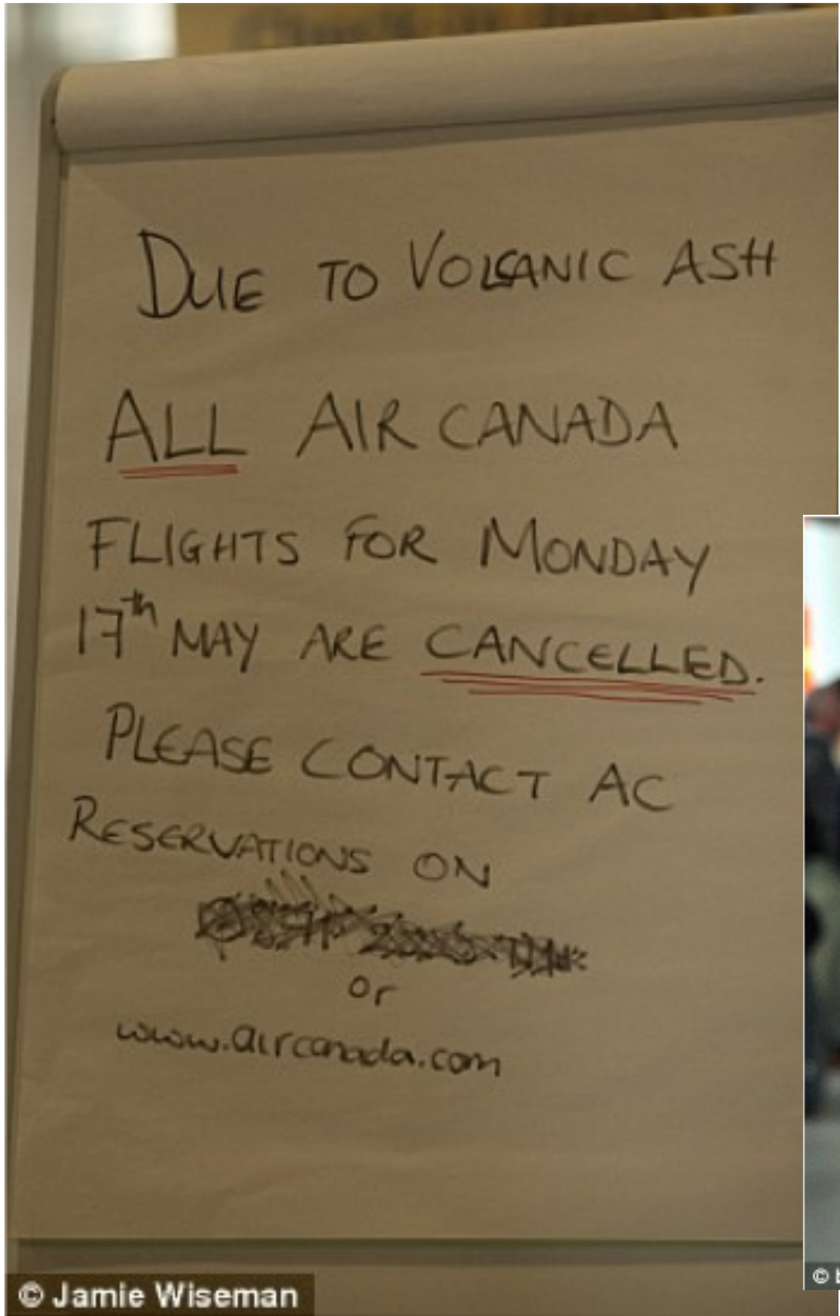

Mail Online News

The ash cloud that never was: Inaccurate Met Office forecast causes airport chaos for 50,000

Michael O'Leary, Ryanair's chief executive, said: 'It is frankly ridiculous that the flight plans of millions of air passengers are being disrupted on a daily basis by an outdated, inappropriate and imaginary computer-generated model. It is time these charts were done away with.'

Willie Walsh, boss of British Airways, said the shutdown was a gross over-reaction to a very minor risk. 'I am very concerned that we have decisions on opening and closing of airports based on a theoretical model,' he added.

'There was no evidence of ash in the skies over London yet Heathrow was closed.'

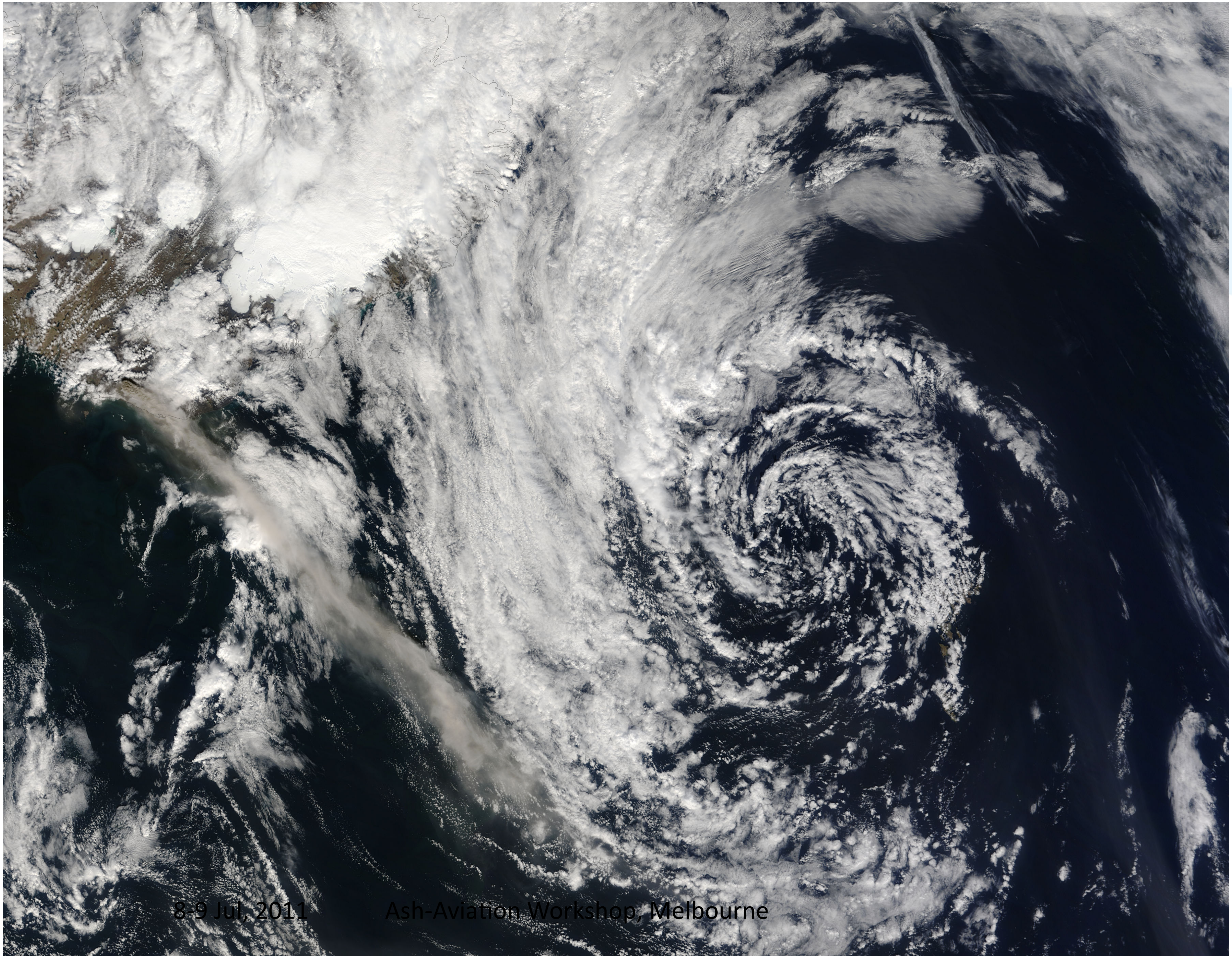

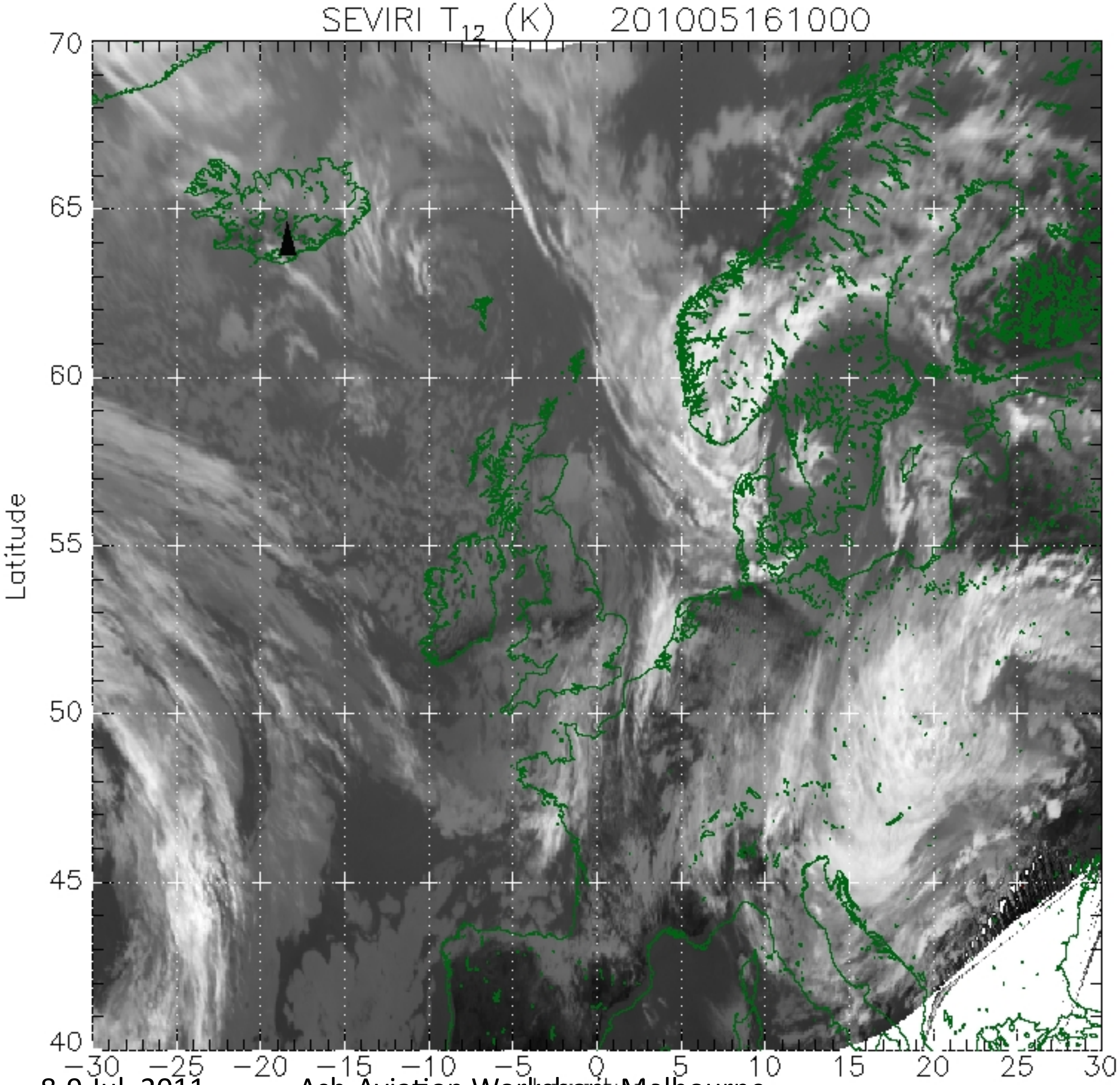
SEVIRI T_{12} (K) 201005161000
Latitude
70
65
60
55
50
45
40
−30 −25 −20 −15 −10 −5 0 5 10 15 20 25 30
Longitude

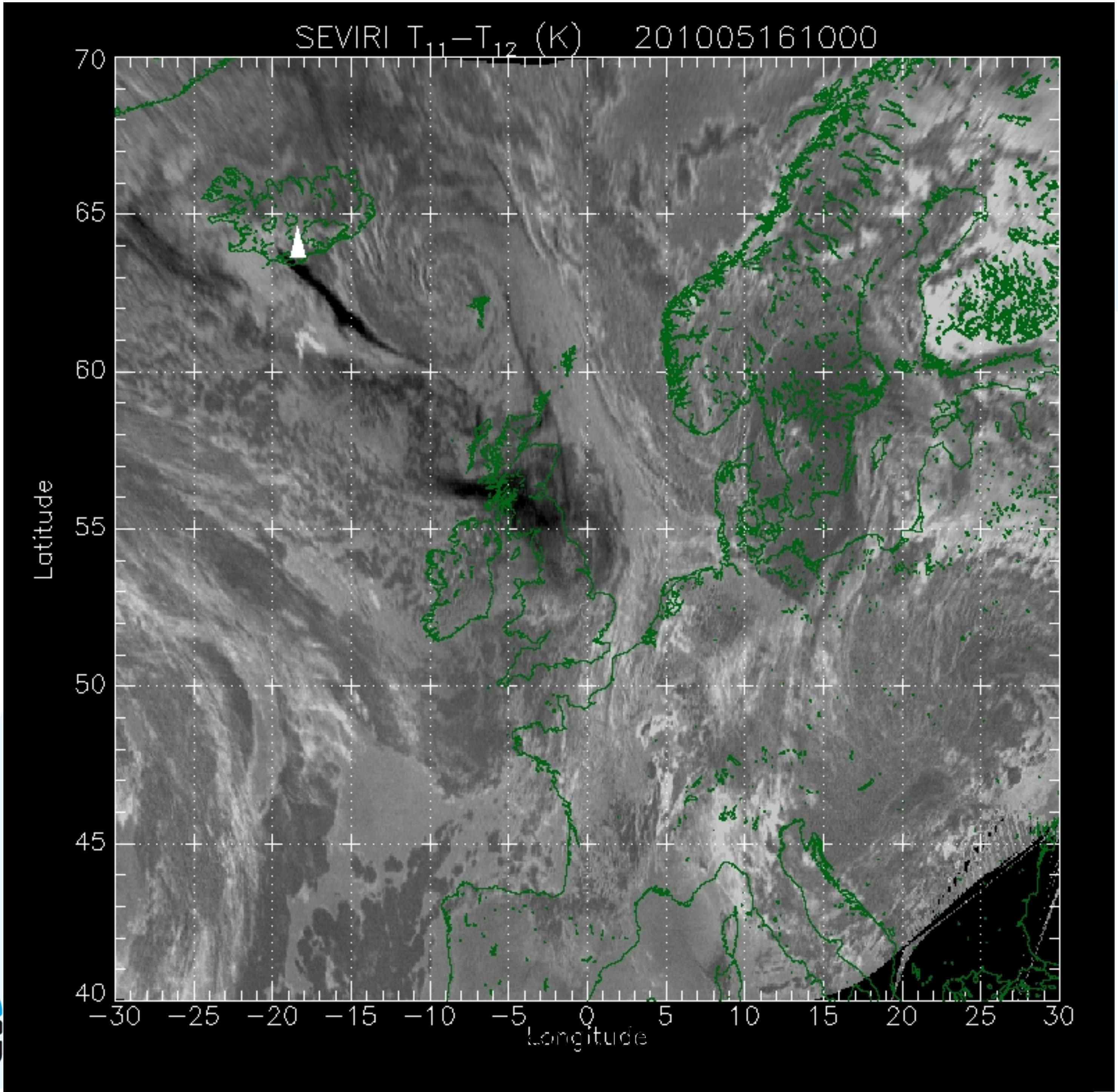
SEVIRI $T_{11}-T_{12}$ (K) 201005161000
70
65
60
55
50
45
40
Latitude
−30 −25 −20 −15 −10 −5 0 5 10 15 20 25 30
Longitude

Date: 2010.05.16
Time: 10:00 UTC

Mean radius (Gaussian)	: 6.22 μm
Mean radius (6-parameter fit)	: 6.36 μm
Total mass	: 0.637 Tg
Maximum mass loading	: 14.84 g m^{-2}
Pixels with mass loading > 6.0	: 104(1.2%)
Pixels with mass loading > 4.0	: 1240(14.5%)
Pixels with mass loading > 2.0 and < 4.0	: 6802(79.5%)
Pixels with mass loading > 0.2 and < 2.0	: 510(6.0%)
Pixels with mass loading > 0.0	: 8552(1.1%)

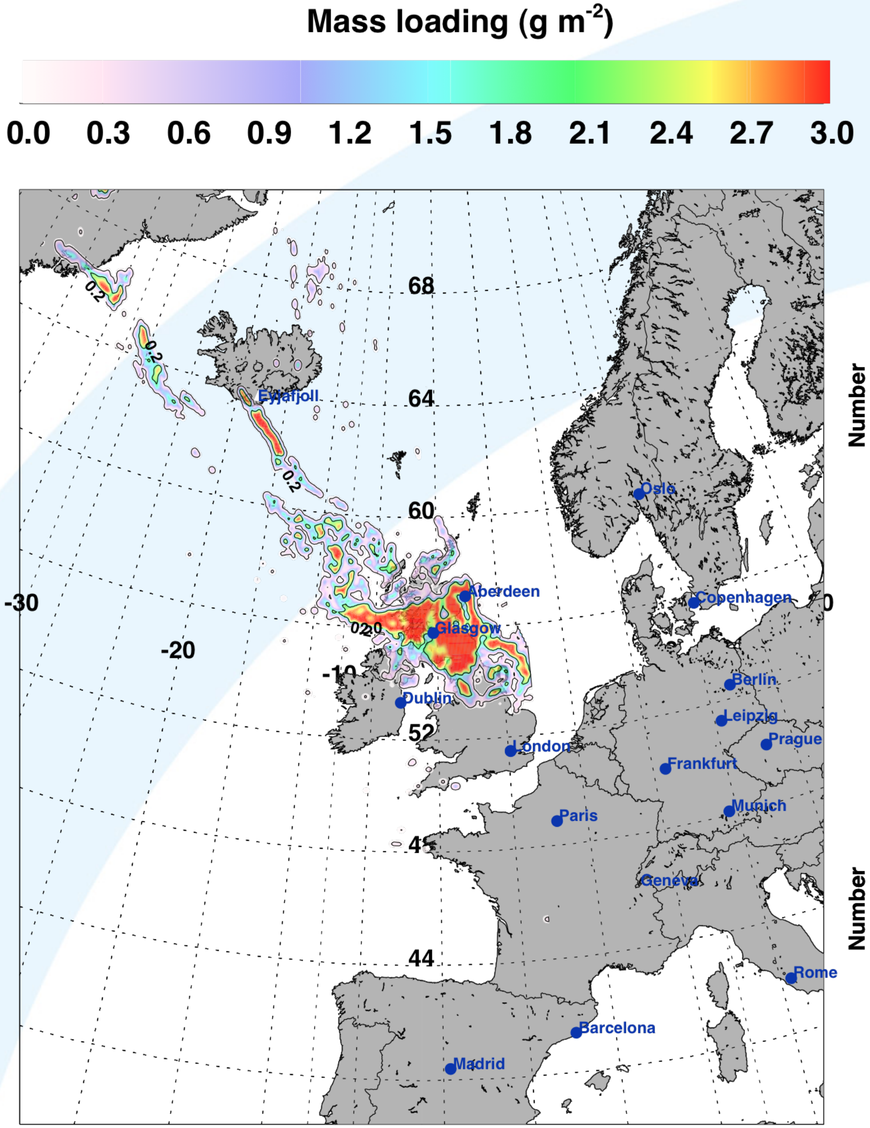

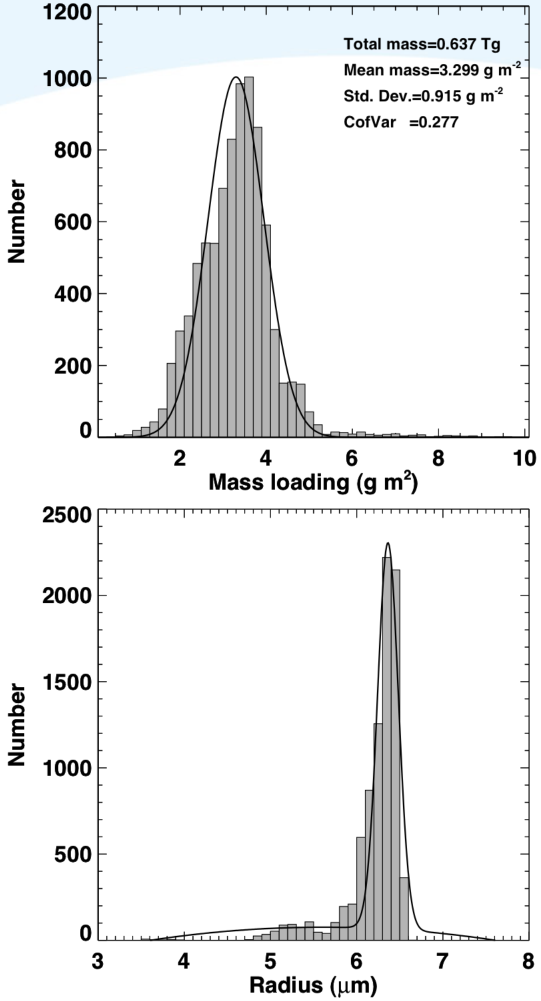

16 April 20:00 UT

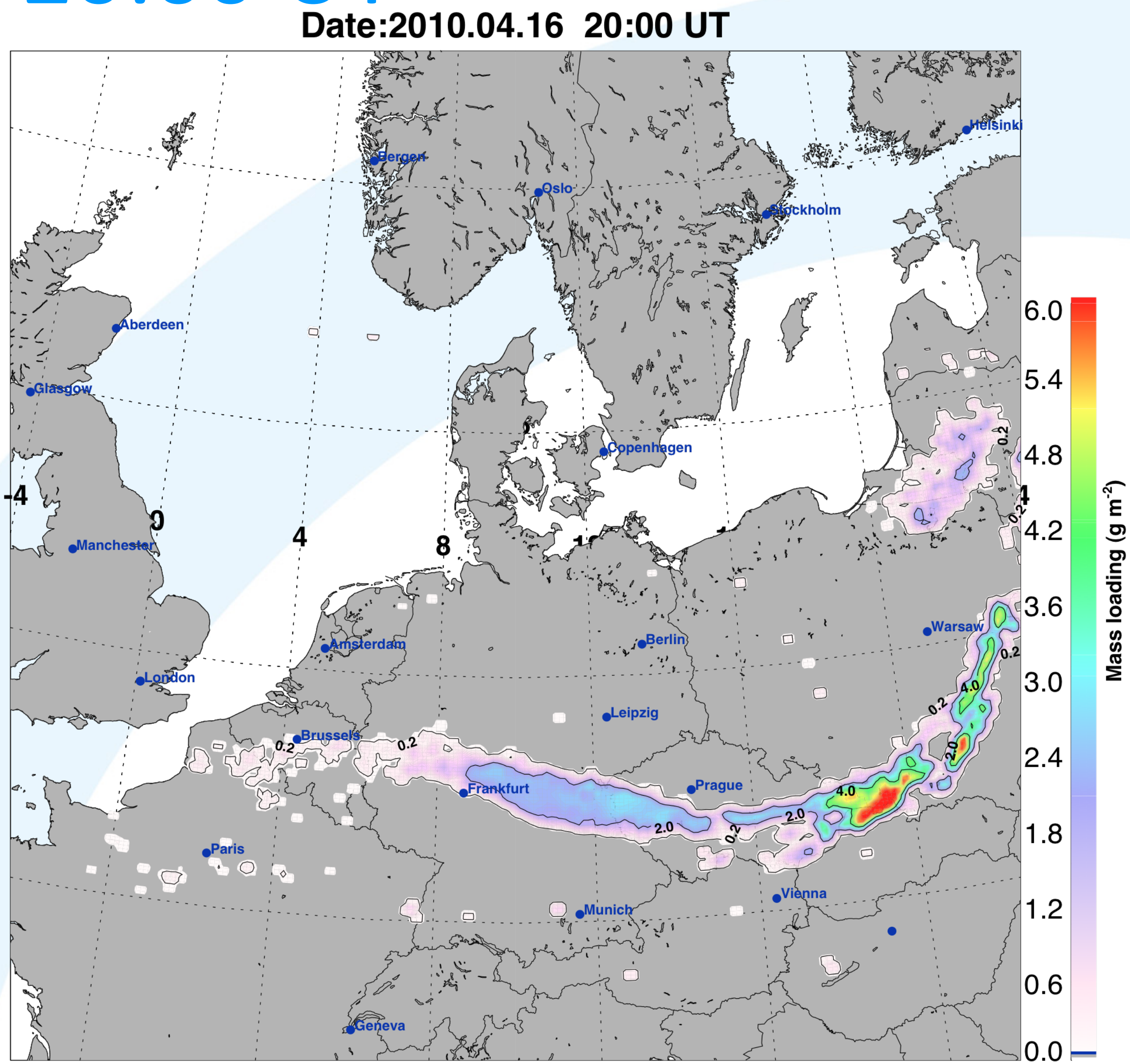

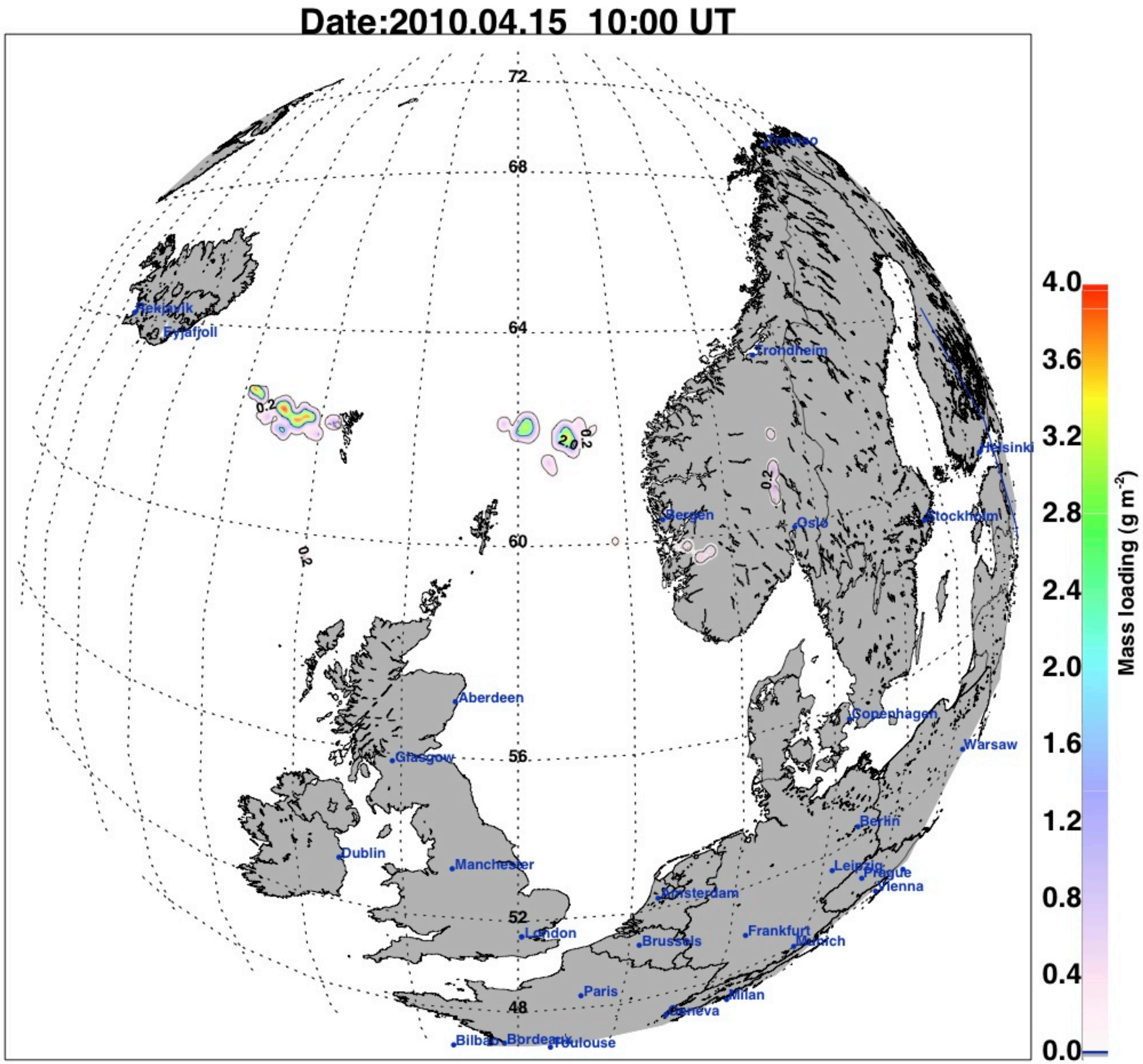
Date:2010.04.15 10:00 UT
72
68
64
60
56
52
48
Reykjavik
Eyjafjoll
Tromso
Trondheim
Helsinki
Bergen
Oslo
Stockholm
Aberdeen
Copenhagen
Warsaw
Glasgow
Berlin
Dublin
Manchester
Leipzig
Prague
Vienna
Amsterdam
London
Brussels
Frankfurt
Munich
Paris
Milan
Geneva
Bilbao
Bordeaux
Toulouse
0.2
2.0
4.0
3.6
3.2
2.8
2.4
2.0
1.6
1.2
0.8
0.4
0.0
Mass loading (g m-2)

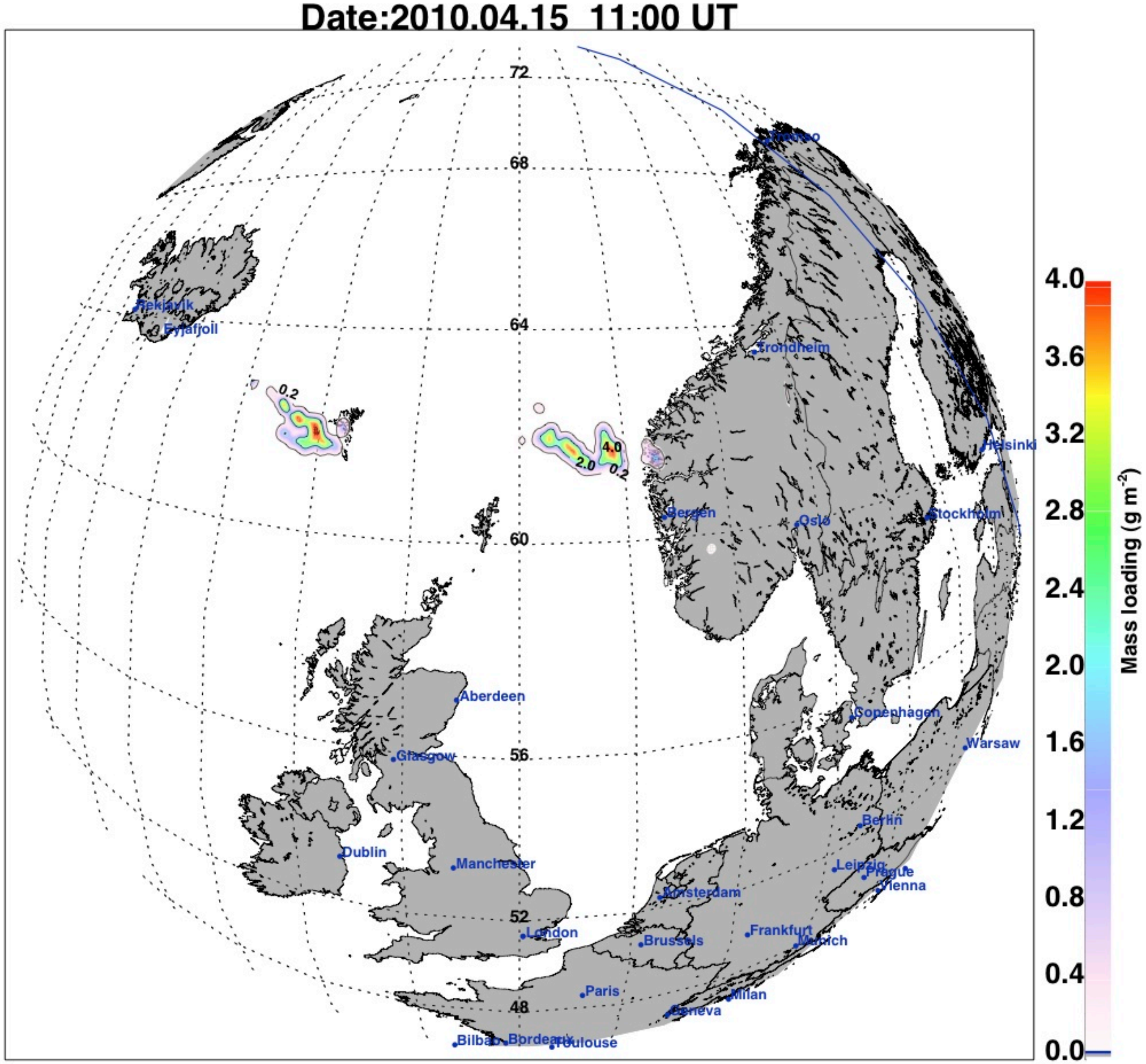
Date:2010.04.15 11:00 UT
72
68
64
60
56
52
48
Reykjavik
Eyjafjoll
Tromso
Trondheim
Helsinki
Bergen
Oslo
Stockholm
Aberdeen
Copenhagen
Warsaw
Glasgow
Berlin
Dublin
Manchester
Leipzig
Prague
Vienna
Amsterdam
London
Brussels
Frankfurt
Munich
Paris
Milan
Geneva
Bilbao
Bordeaux
Toulouse
0.2
4.0
2.0
4.0
3.6
3.2
2.8
2.4
2.0
1.6
1.2
0.8
0.4
0.0
Mass loading (g m^{-2})

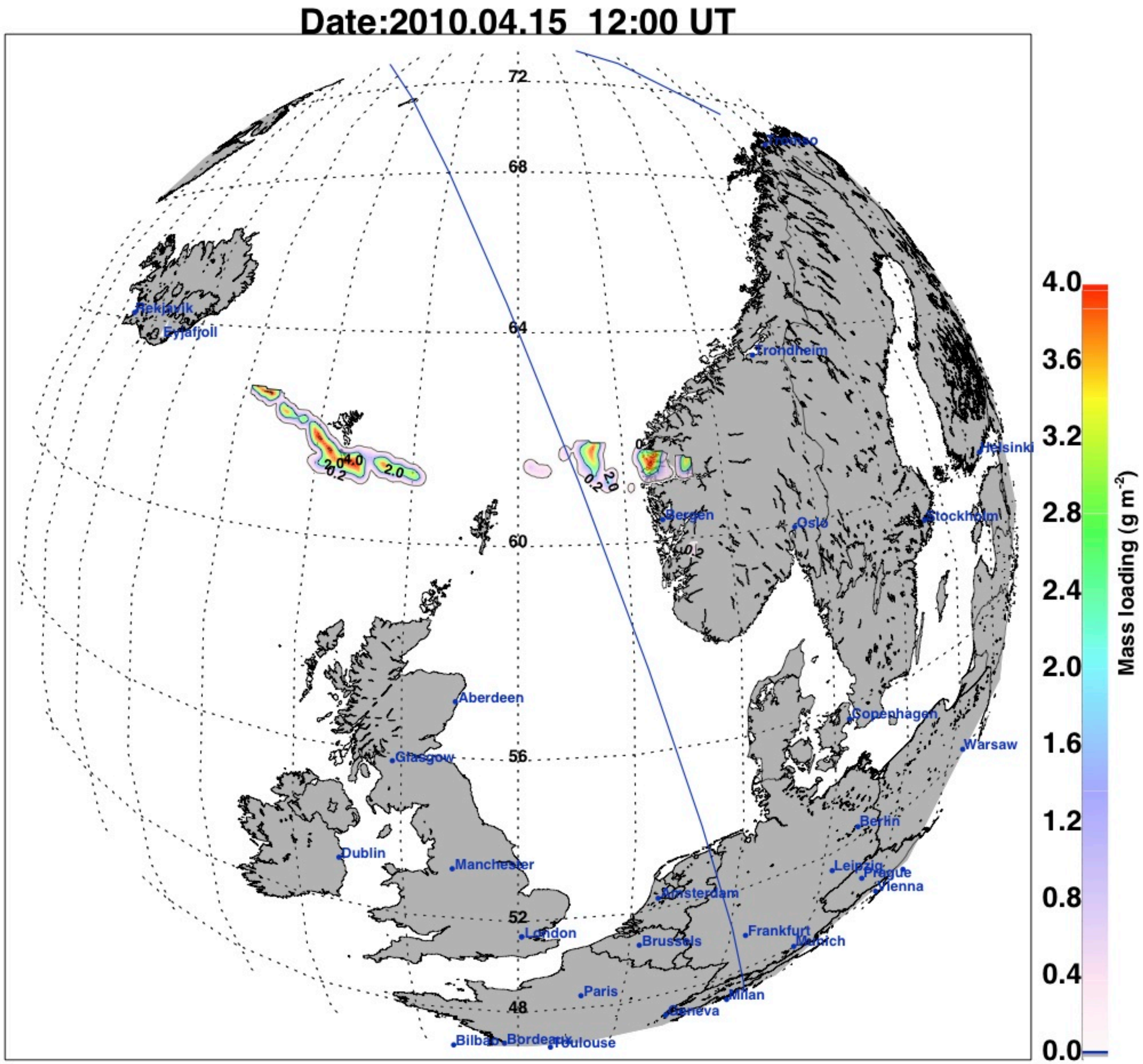
Date:2010.04.15 12:00 UT
Mass loading (g m^{-2})
4.0
3.6
3.2
2.8
2.4
2.0
1.6
1.2
0.8
0.4
0.0
72
68
64
60
56
52
48
Reykjavik
Eyjafjoll
Trondheim
Bergen
Oslo
Stockholm
Helsinki
Copenhagen
Warsaw
Aberdeen
Glasgow
Dublin
Manchester
London
Amsterdam
Berlin
Prague
Vienna
Frankfurt
Brussels
Paris
Milan
Geneva
Bordeaux
Toulouse

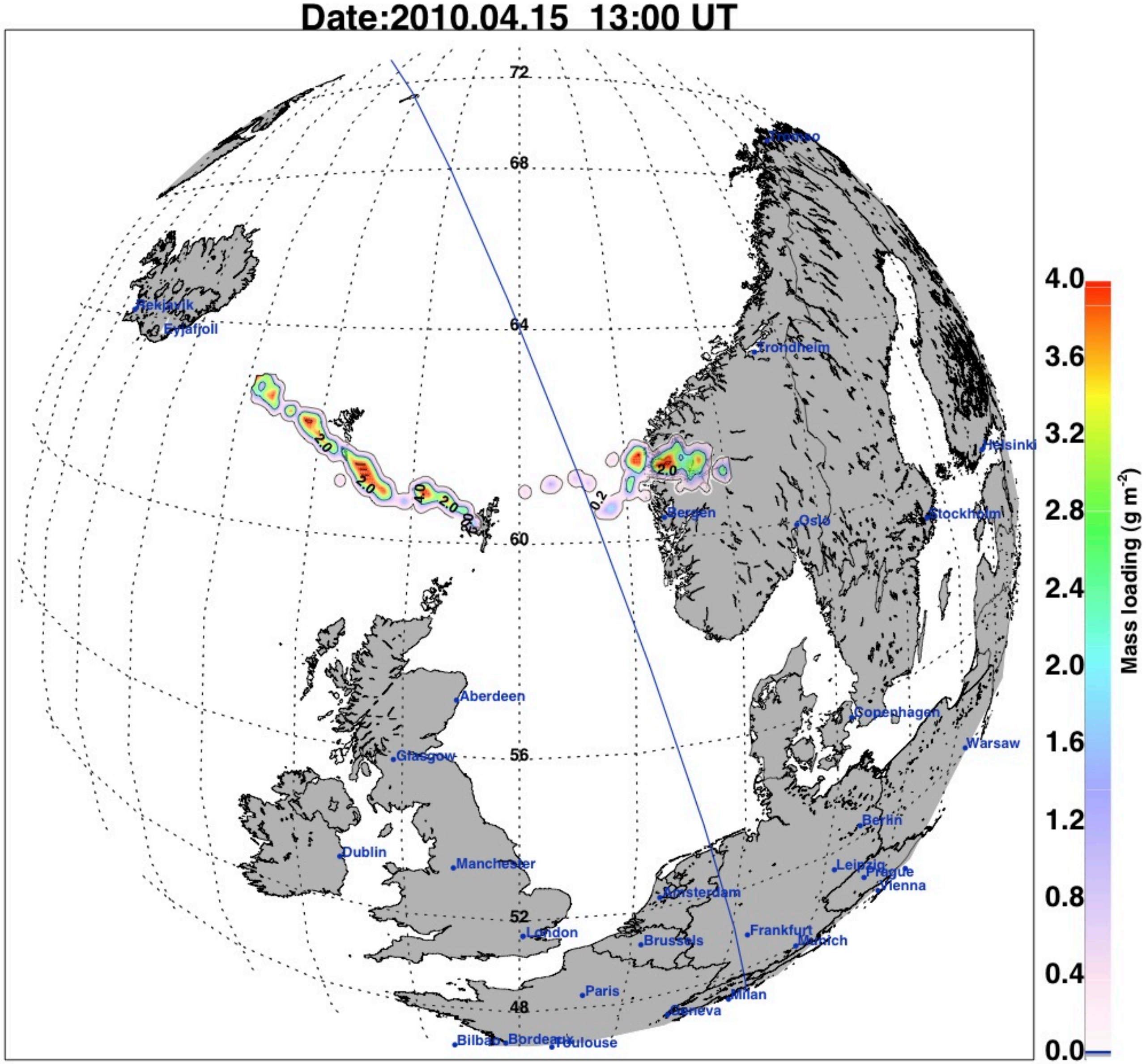
Date:2010.04.15 13:00 UT
Mass loading (g m^{-2})
4.0
3.6
3.2
2.8
2.4
2.0
1.6
1.2
0.8
0.4
0.0
Reykjavik
Eyjafjoll
Trondheim
Bergen
Oslo
Stockholm
Helsinki
Copenhagen
Warsaw
Aberdeen
Glasgow
Dublin
Manchester
London
Amsterdam
Brussels
Berlin
Leipzig
Prague
Vienna
Frankfurt
Munich
Paris
Geneva
Milan
Bilbao
Bordeaux
Toulouse
72
68
64
60
56
52
48

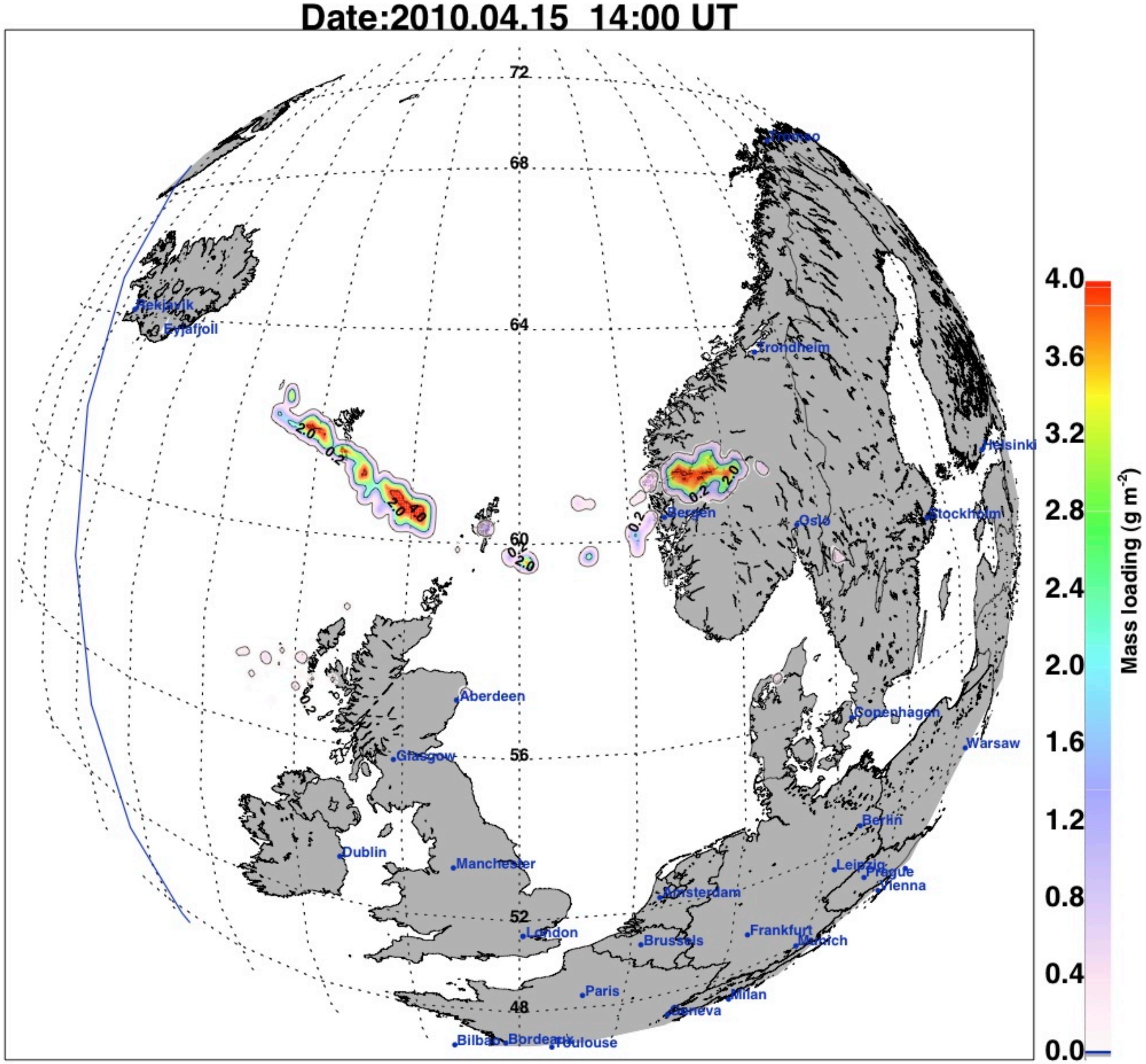

Date:2010.04.15 14:00 UT
72
68
64
60
56
52
48
Reykjavik
Eyjafjoll
Tromso
Trondheim
Helsinki
Bergen
Oslo
Stockholm
Aberdeen
Glasgow
Copenhagen
Warsaw
Dublin
Manchester
Berlin
Leipzig
Prague
Vienna
Amsterdam
London
Brussels
Frankfurt
Munich
Paris
Geneva
Milan
Bilbao
Bordeaux
Toulouse
Mass loading (g m^{-2})
4.0
3.6
3.2
2.8
2.4
2.0
1.6
1.2
0.8
0.4
0.0

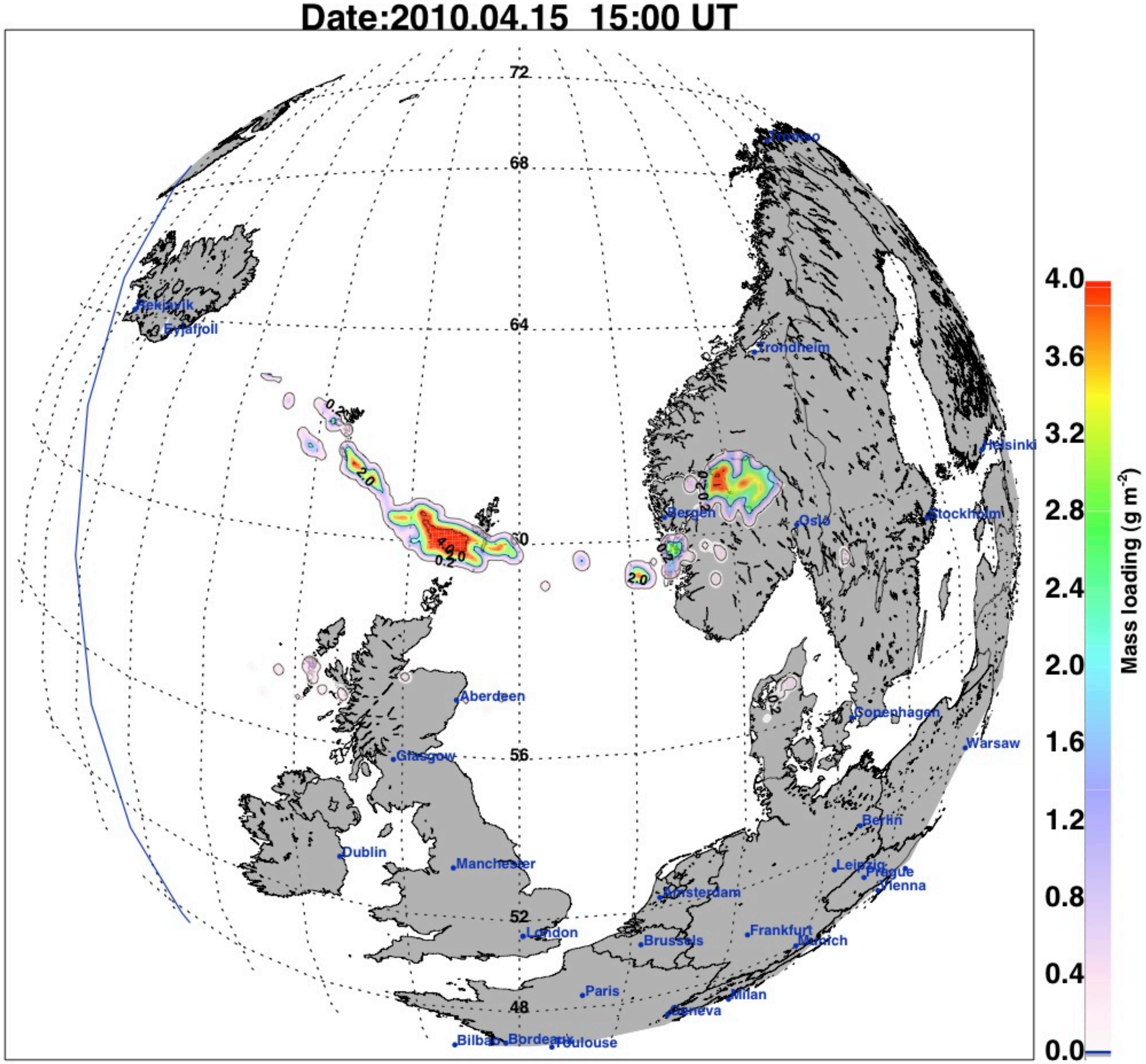
Date:2010.04.15 15:00 UT
72
68
64
60
56
52
48
Reykjavik
Eyjafjoll
Trondheim
Helsinki
Bergen
Oslo
Stockholm
Aberdeen
Copenhagen
Warsaw
Glasgow
Berlin
Dublin
Manchester
Amsterdam
Vienna
London
Brussels
Frankfurt
Paris
Milan
Geneva
Toulouse
4.0
3.6
3.2
2.8
2.4
2.0
1.6
1.2
0.8
0.4
0.0
Mass loading (g m^{-2})

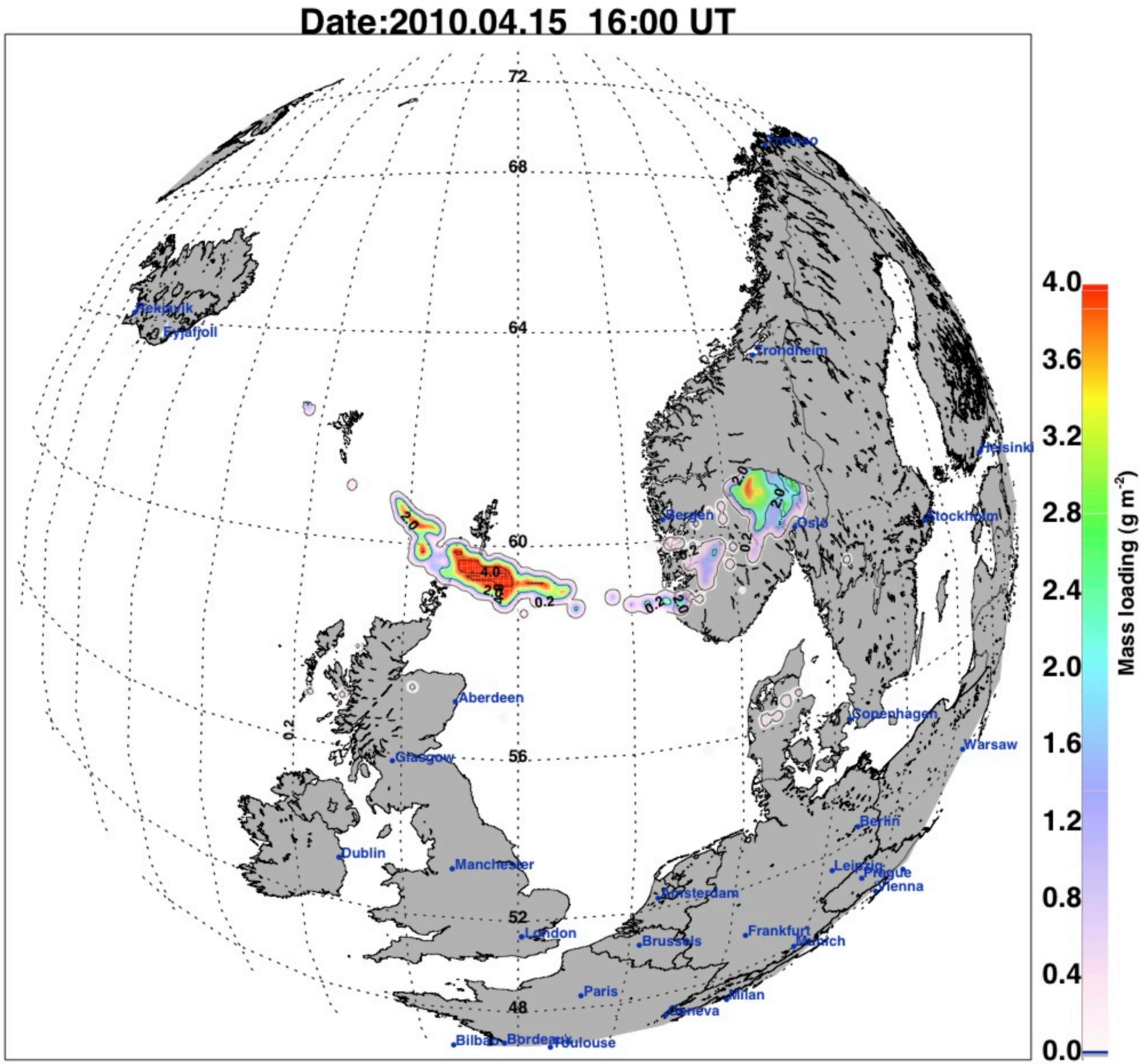
Date:2010.04.15 16:00 UT
72
68
64
60
56
52
48
Reykjavik
Eyjafjoll
Trondheim
Bergen
Oslo
Stockholm
Helsinki
Aberdeen
Glasgow
Copenhagen
Warsaw
Berlin
Dublin
Manchester
Amsterdam
London
Brussels
Frankfurt
Munich
Leipzig
Prague
Vienna
Paris
Geneva
Milan
Bilbao
Bordeaux
Toulouse
4.0
3.6
3.2
2.8
2.4
2.0
1.6
1.2
0.8
0.4
0.0
Mass loading (g m^{-2})

Date:2010.05.16 00:00 UT

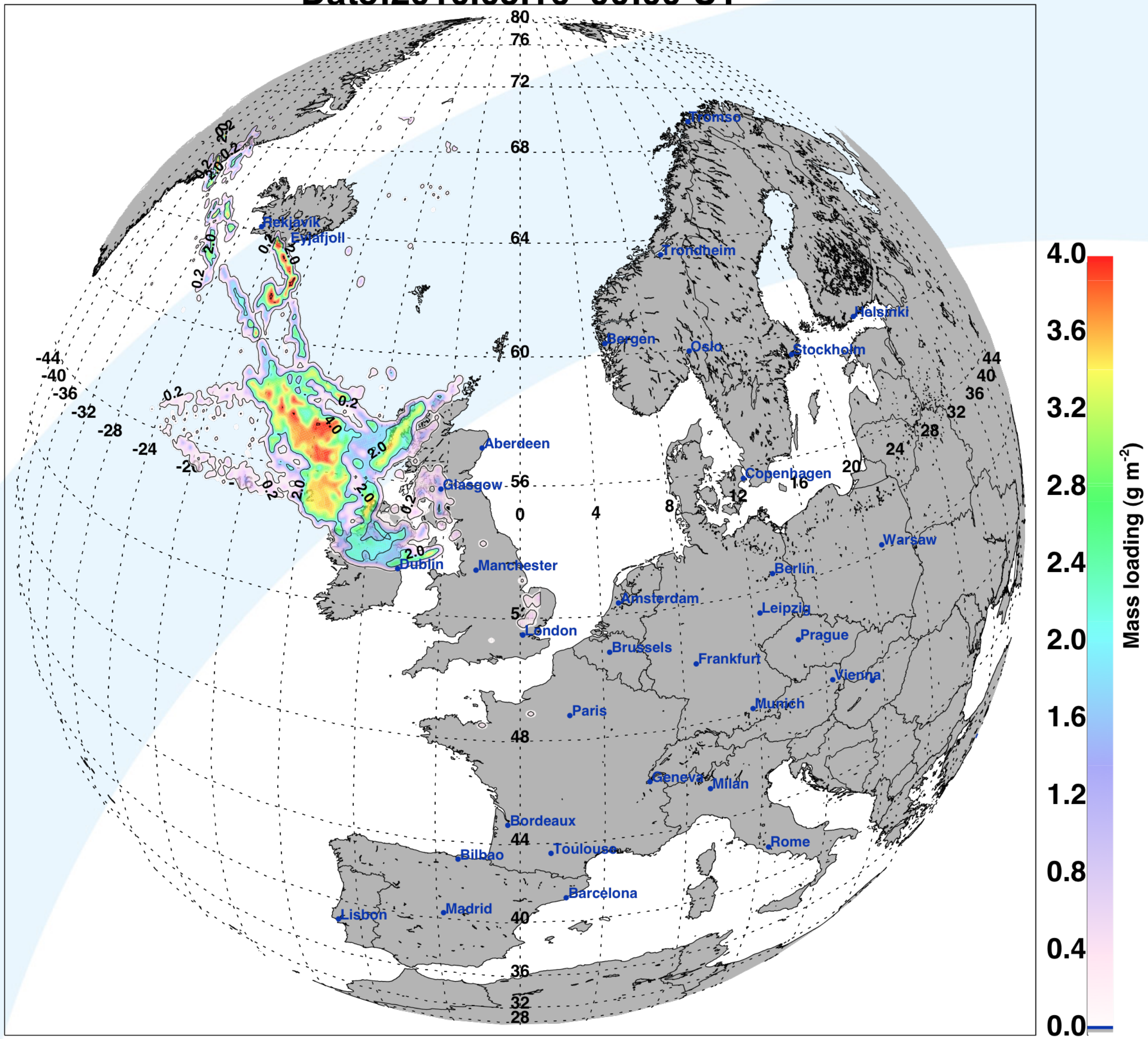

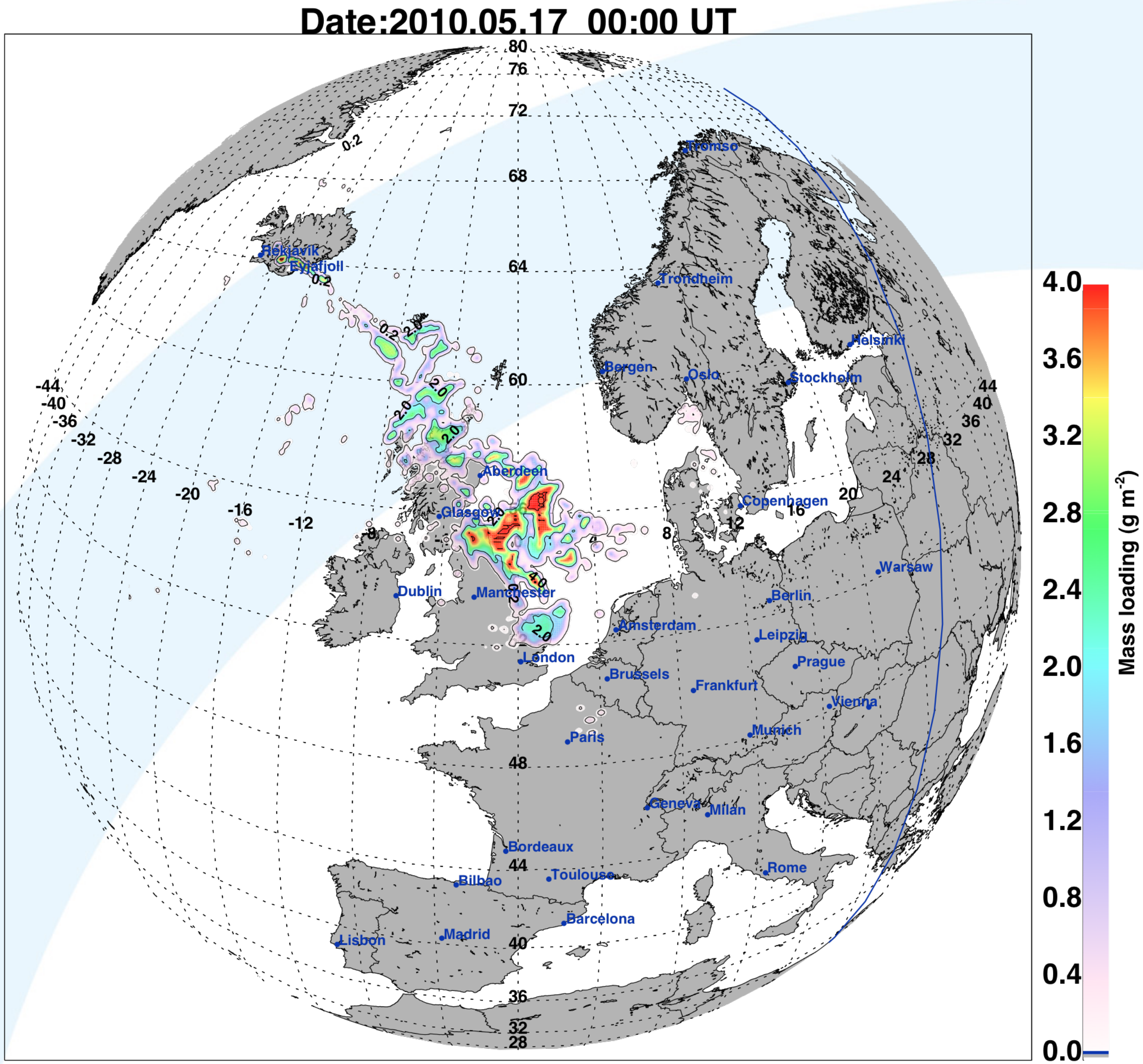
Date:2010.05.17 00:00 UT
Reykjavik
Eyjafjoll
Tromso
Trondheim
Helsinki
Bergen
Oslo
Stockholm
Aberdeen
Copenhagen
Glasgow
Warsaw
Dublin
Manchester
Berlin
Amsterdam
Leipzig
London
Prague
Brussels
Frankfurt
Vienna
Munich
Paris
Geneva
Milan
Bordeaux
Rome
Bilbao
Toulouse
Barcelona
Lisbon
Madrid
Mass loading (g m^-2)
4.0
3.6
3.2
2.8
2.4
2.0
1.6
1.2
0.8
0.4
0.0

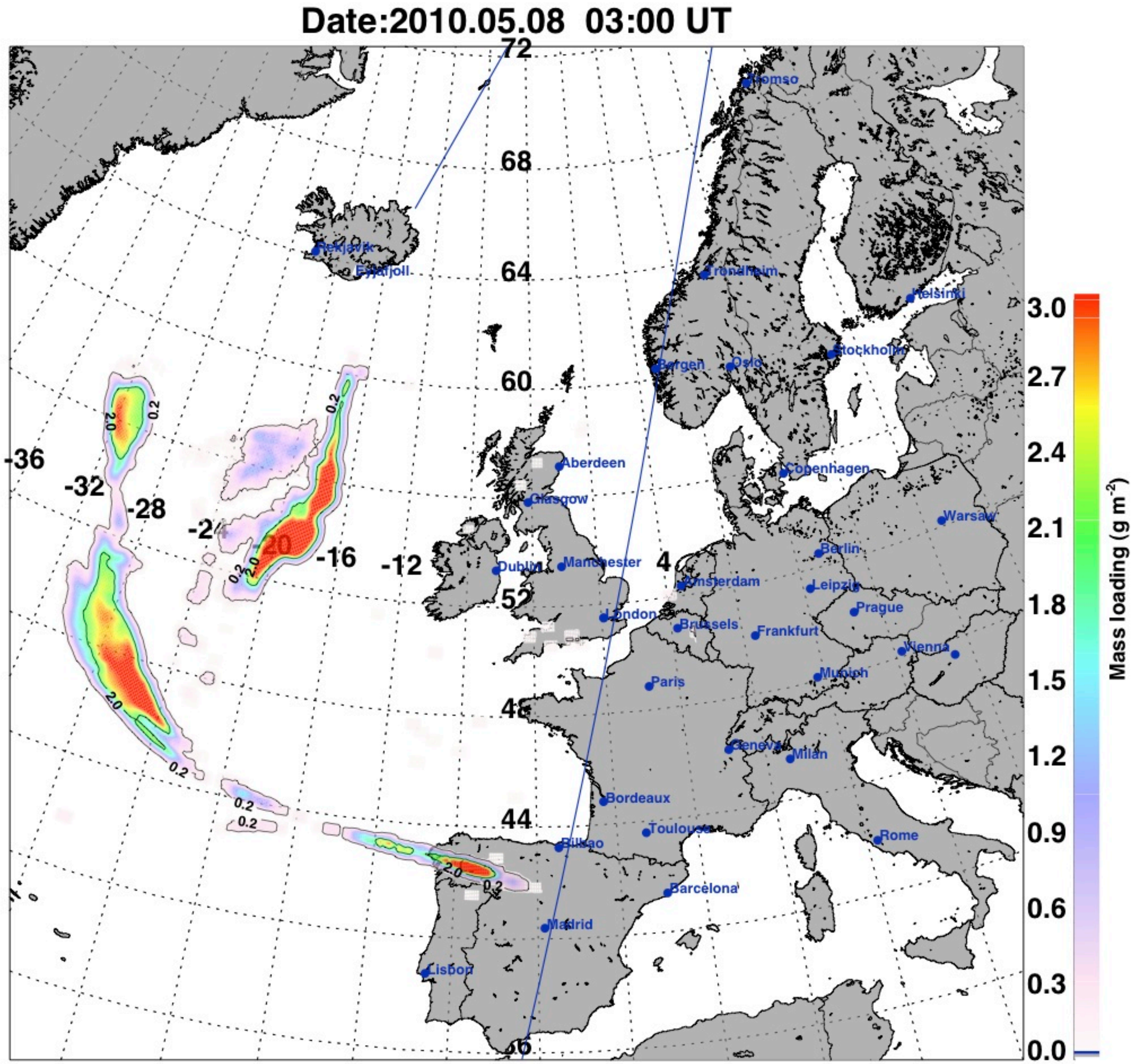
Date:2010.05.08 03:00 UT
72
68
64
60
52
48
44
-36
-32
-28
-24
-20
-16
-12
4
0.2
2.0
Aberdeen
Glasgow
Dublin
Manchester
London
Amsterdam
Brussels
Paris
Frankfurt
Leipzig
Berlin
Prague
Vienna
Munich
Warsaw
Copenhagen
Stockholm
Oslo
Bergen
Trondheim
Helsinki
Tromso
Reykjavik
Geneva
Milan
Bordeaux
Toulouse
Bilbao
Barcelona
Madrid
Lisbon
Rome
3.0
2.7
2.4
2.1
1.8
1.5
1.2
0.9
0.6
0.3
0.0
Mass loading (g m^{-2})

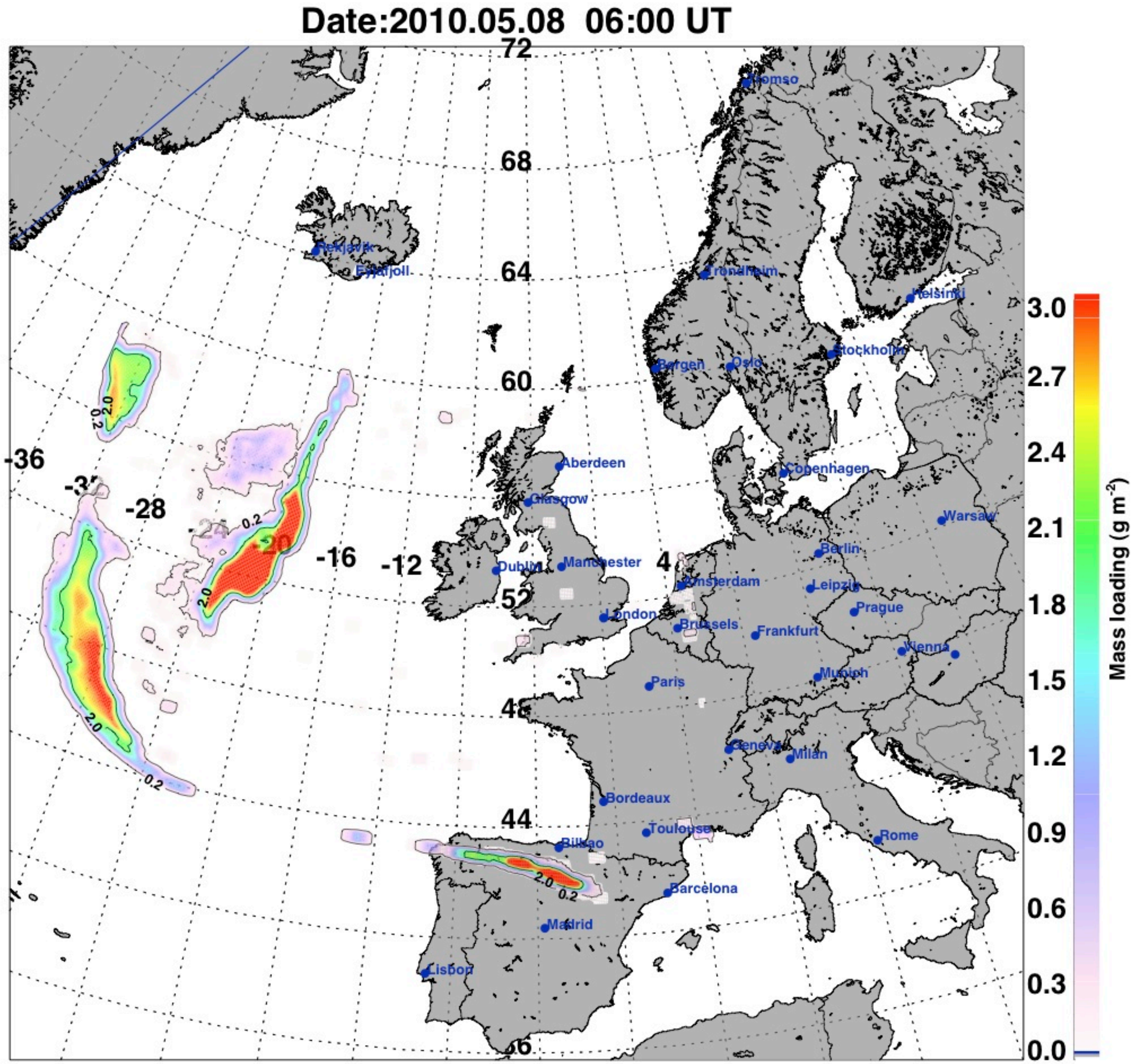

Date:2010.05.08 06:00 UT
Mass loading (g m^{-2})
3.0
2.7
2.4
2.1
1.8
1.5
1.2
0.9
0.6
0.3
0.0
Reykjavik
Eyjafjoll
Tromso
Trondheim
Helsinki
Stockholm
Bergen
Oslo
Copenhagen
Aberdeen
Glasgow
Dublin
Manchester
London
Amsterdam
Brussels
Berlin
Warsaw
Leipzig
Prague
Frankfurt
Vienna
Munich
Paris
Geneva
Milan
Bordeaux
Toulouse
Bilbao
Barcelona
Rome
Madrid
Lisbon

Date:2010.05.08 09:00 UT

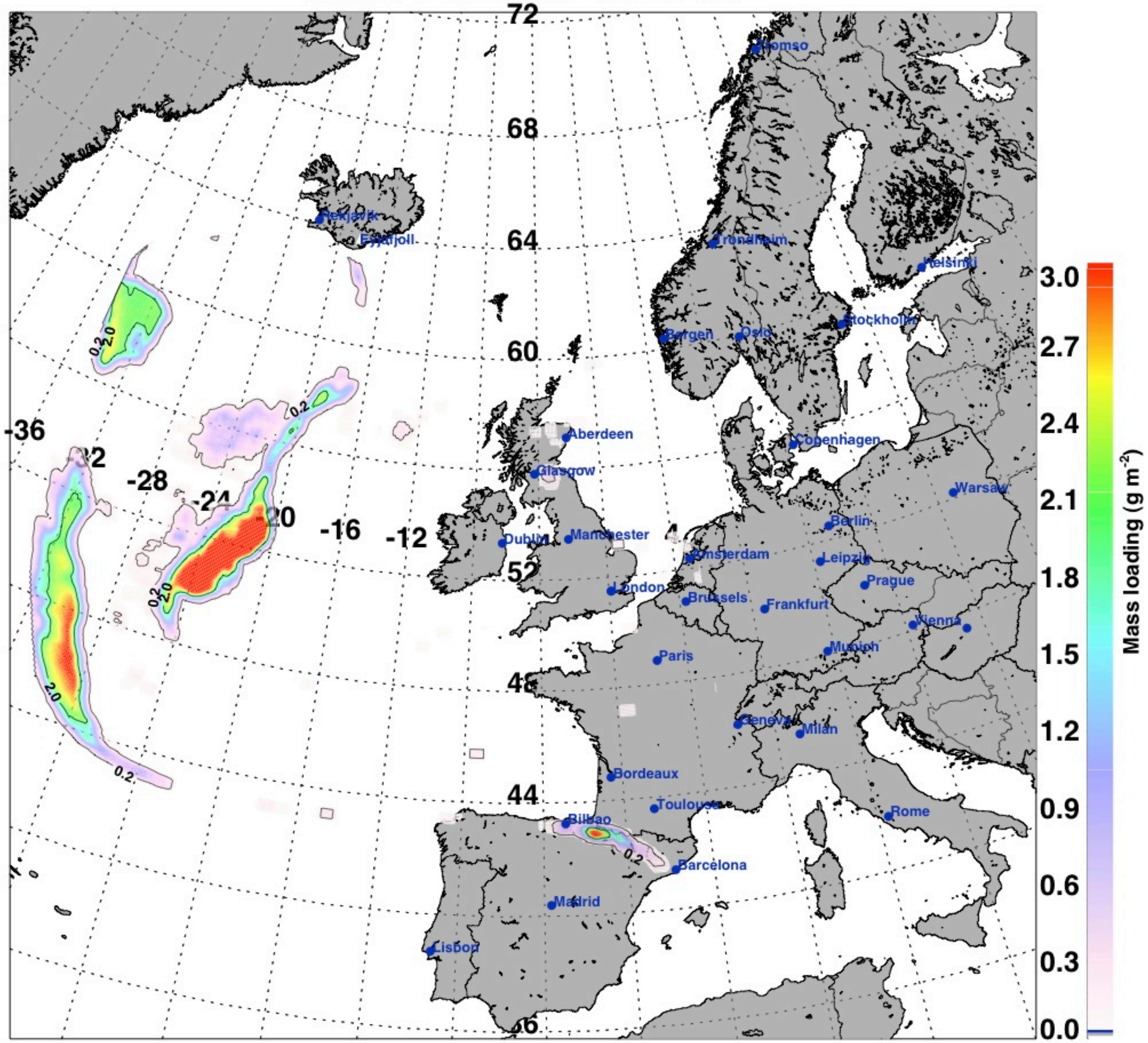

Date:2010.05.08 09:00 UT

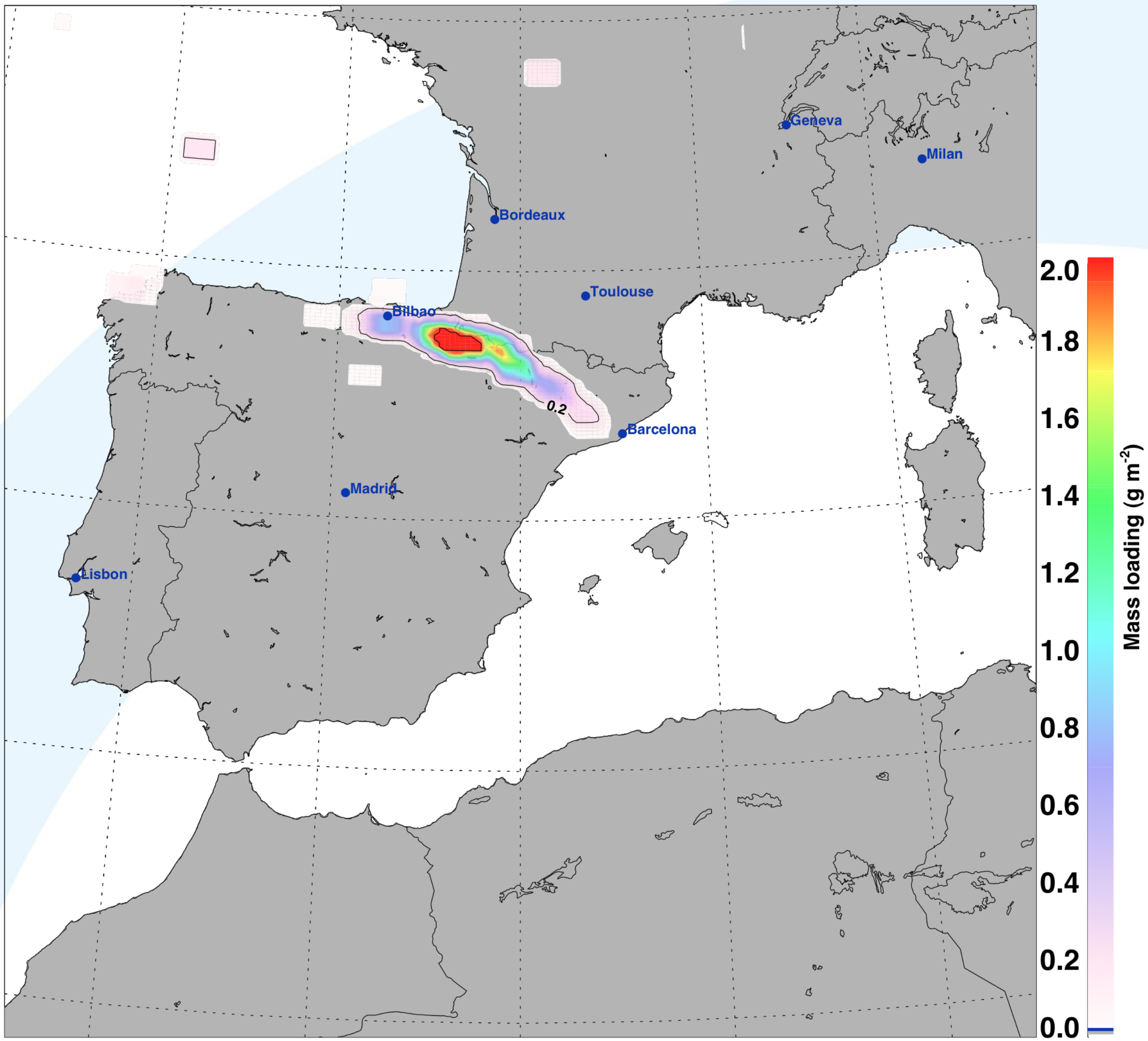

Date:2010.05.08 09:30 UT

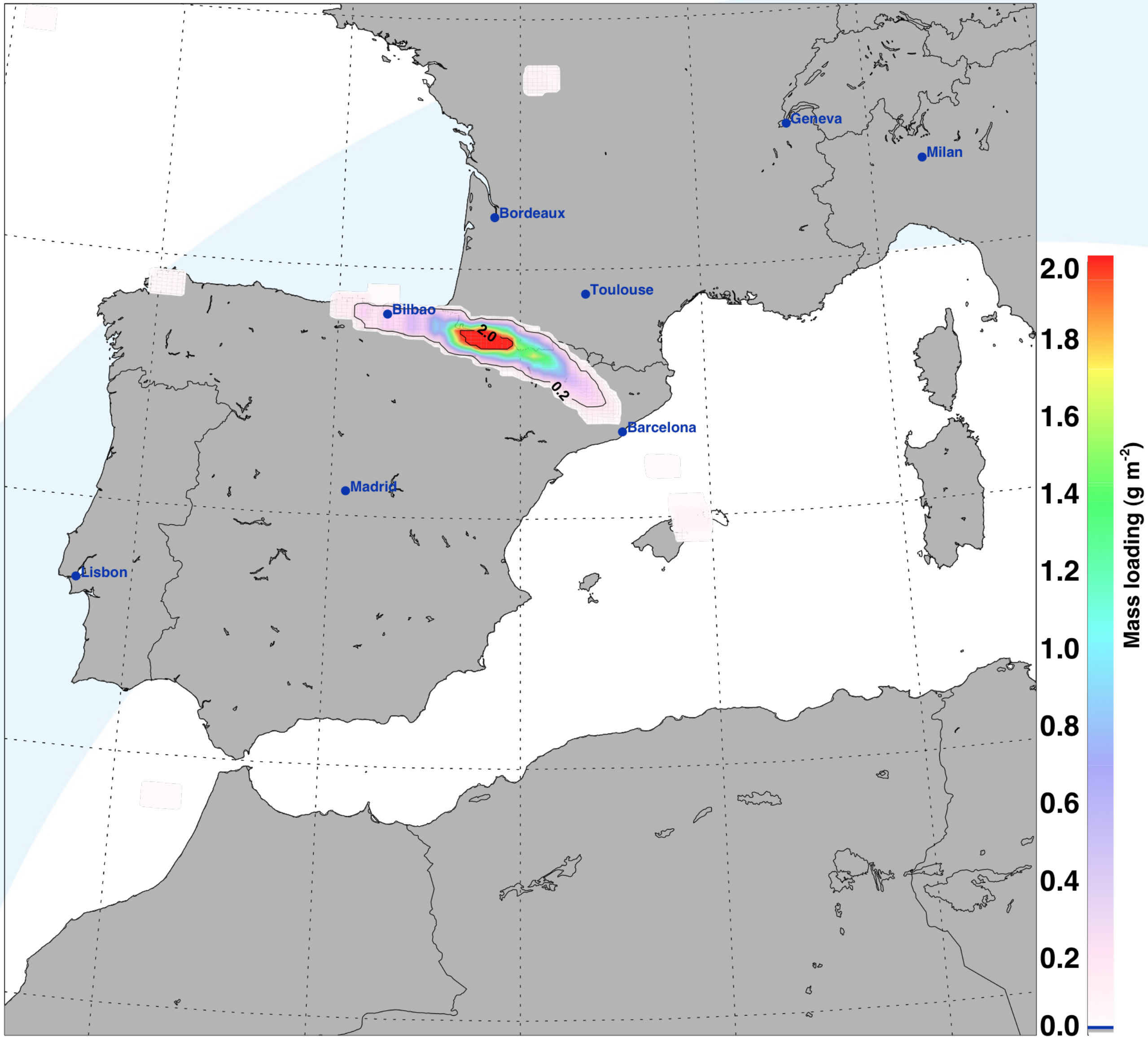

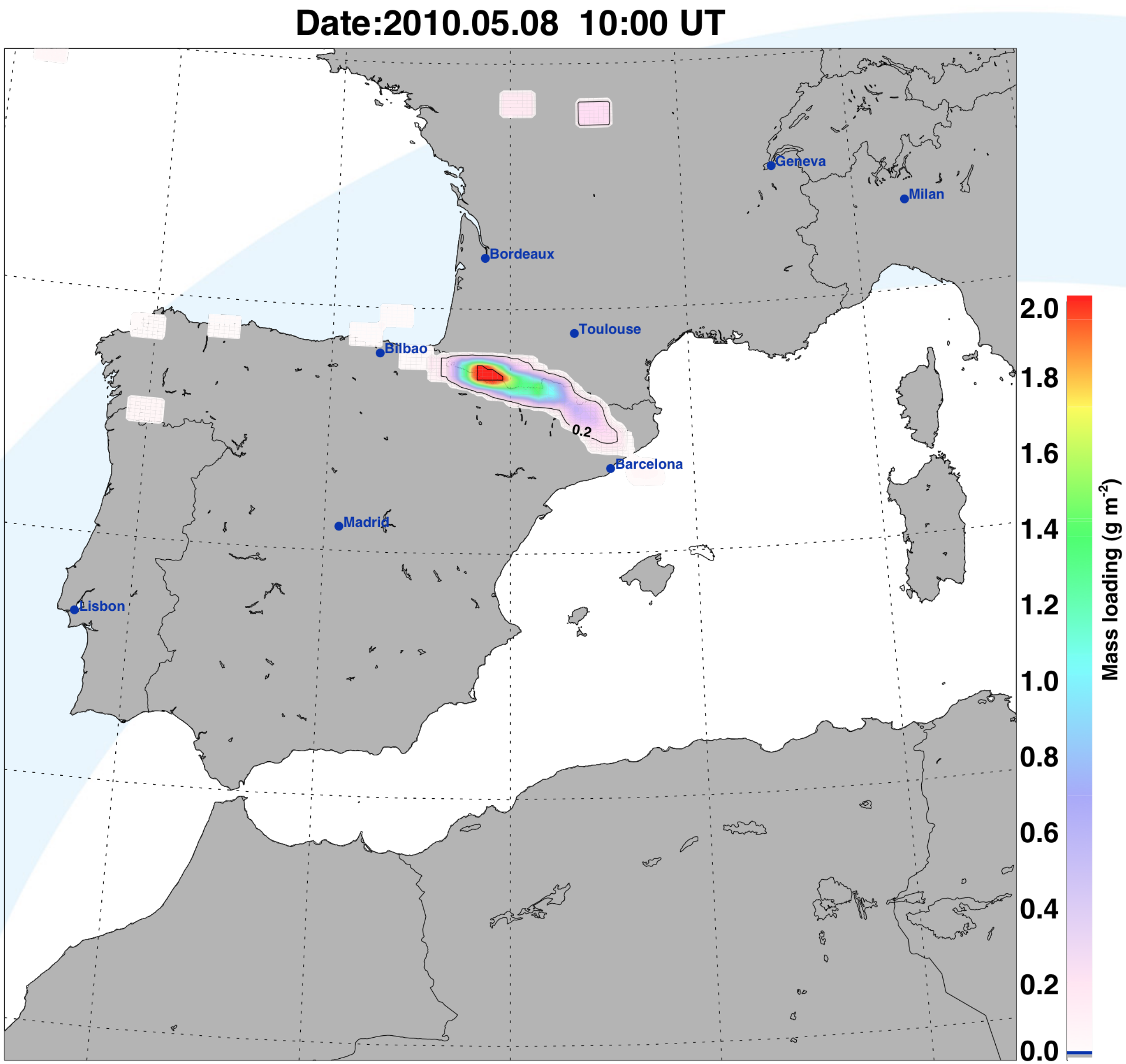
Date:2010.05.08 10:00 UT
Geneva
Milan
Bordeaux
Toulouse
Bilbao
0.2
Barcelona
Madrid
Lisbon
2.0
1.8
1.6
1.4
1.2
1.0
0.8
0.6
0.4
0.2
0.0
Mass loading (g m-2)

Sun photometer at Barcelona

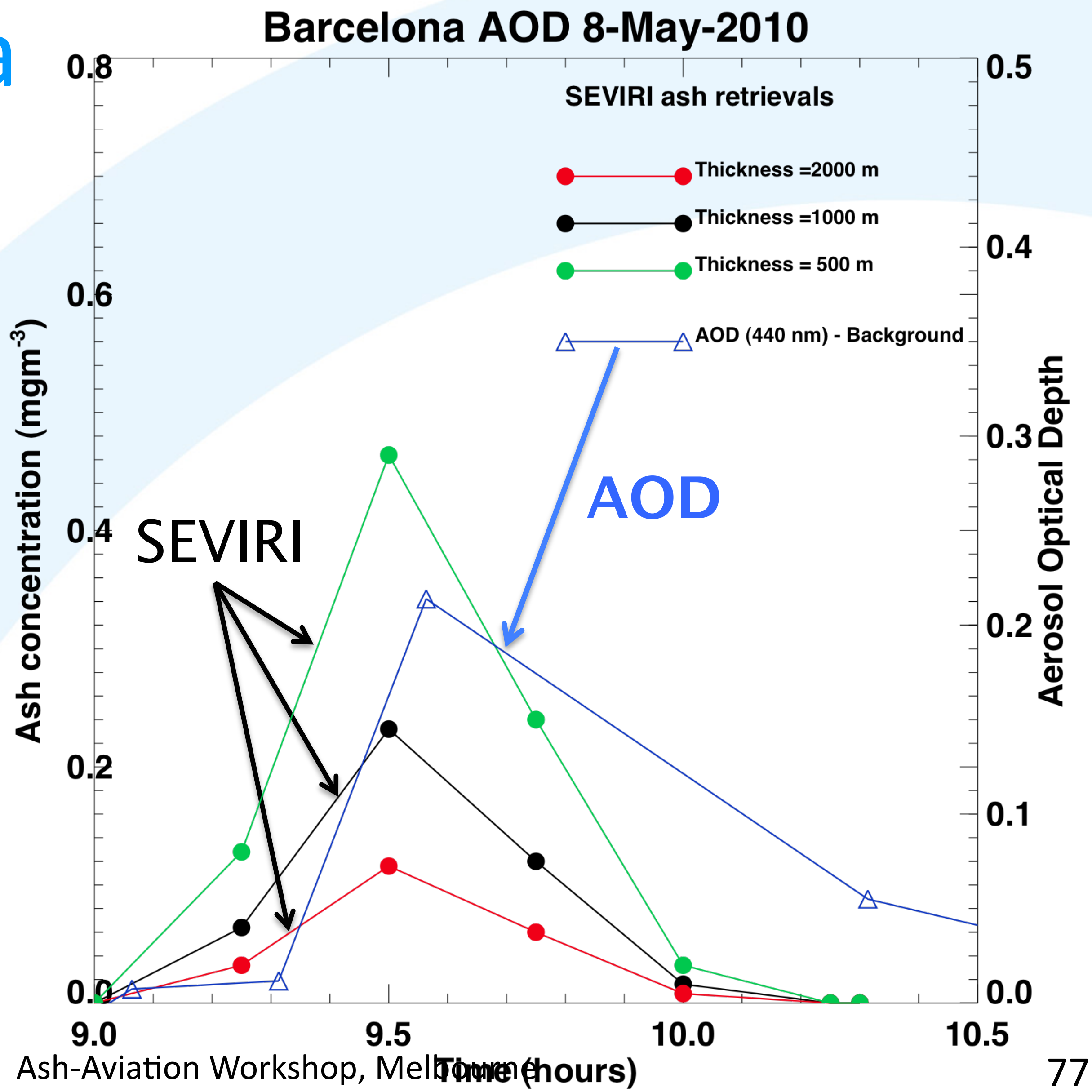

Date:2010.04.15 13:30 UT

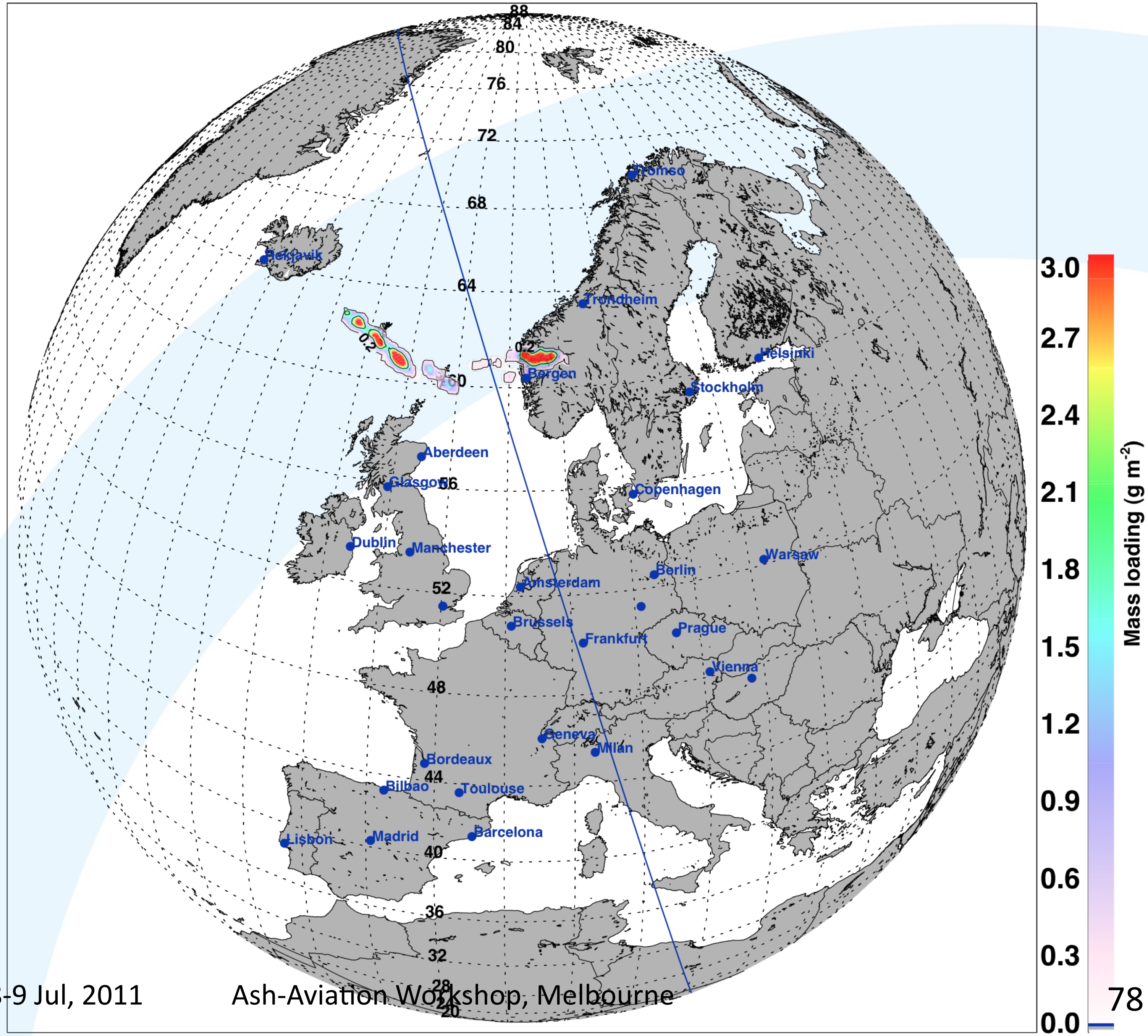

CALIPSO

15 April 2010 – Daytime

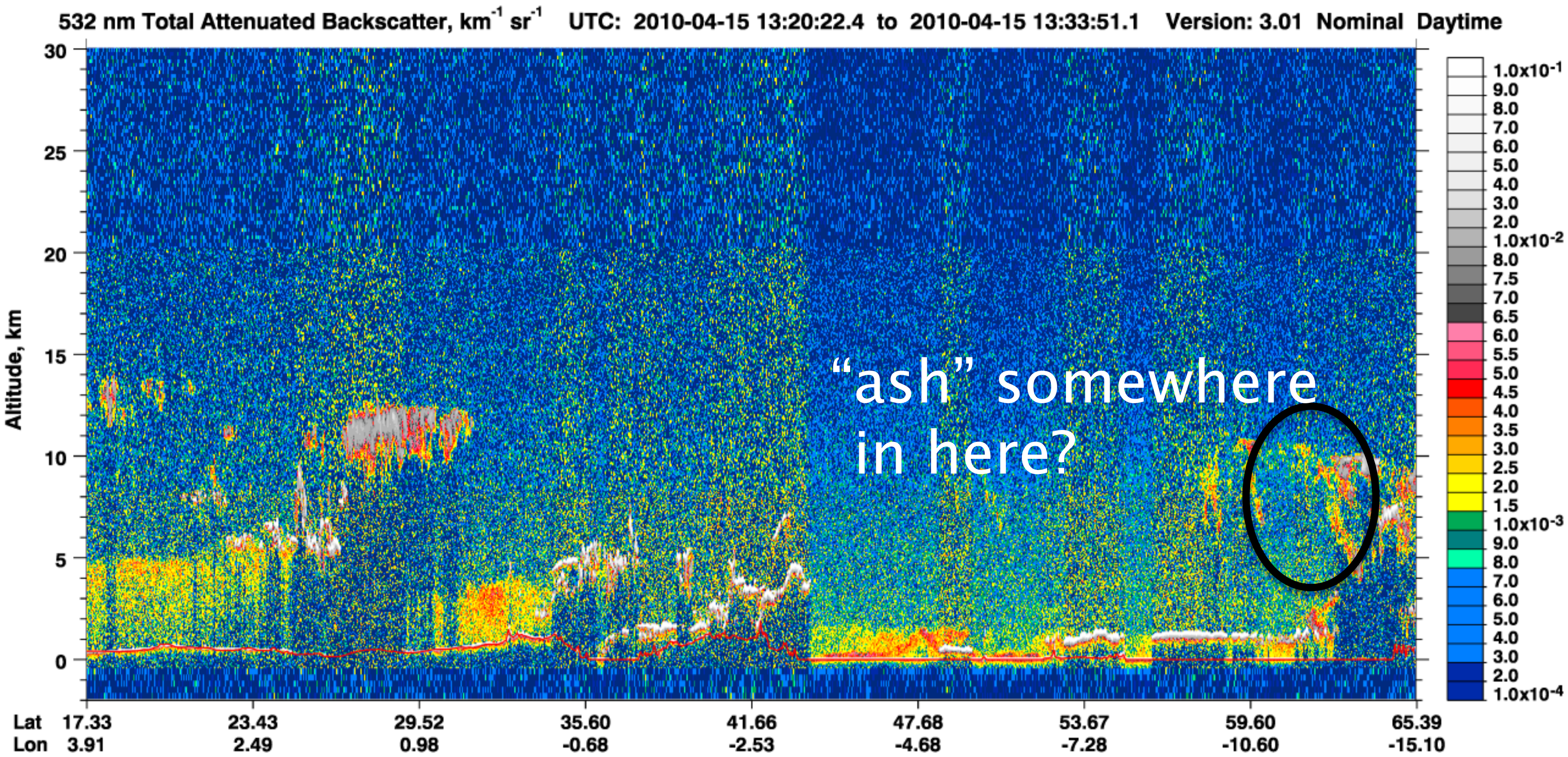

CALIOP "curtain" 532 nm Total Backscatter

Date:2010.05.12 03:30 UT

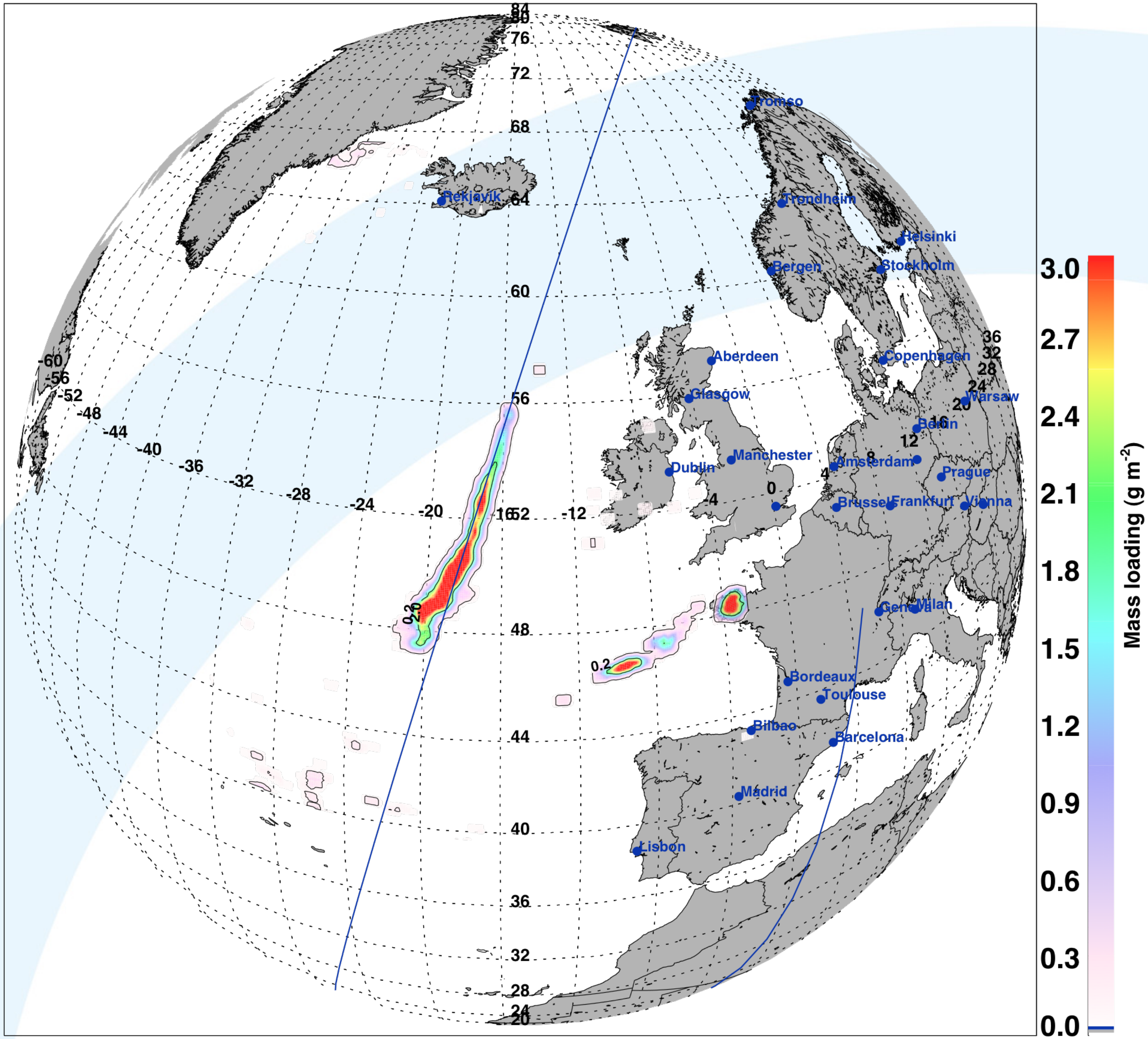

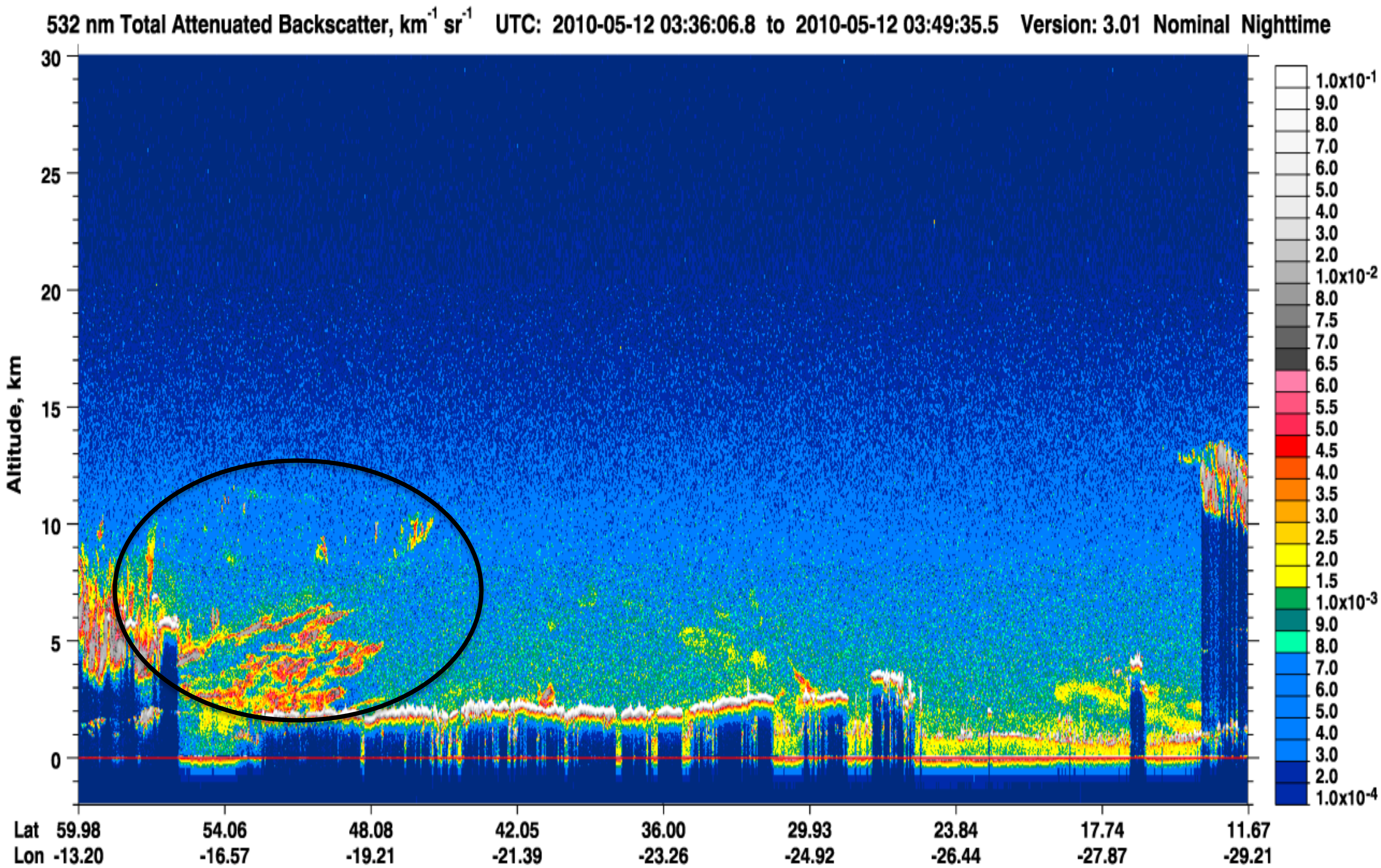
532 nm Total Attenuated Backscatter, km⁻¹ sr⁻¹ UTC: 2010-05-12 03:36:06.8 to 2010-05-12 03:49:35.5 Version: 3.01 Nominal Nighttime
Altitude, km
30
25
20
15
10
5
0
Lat 59.98 54.06 48.08 42.05 36.00 29.93 23.84 17.74 11.67
Lon -13.20 -16.57 -19.21 -21.39 -23.26 -24.92 -26.44 -27.87 -29.21
1.0x10-1
9.0
8.0
7.0
6.0
5.0
4.0
3.0
2.0
1.0x10-2
8.0
7.5
7.0
6.5
6.0
5.5
5.0
4.5
4.0
3.5
3.0
2.5
2.0
1.5
1.0x10-3
9.0
8.0
7.0
6.0
5.0
4.0
3.0
2.0
1.0x10-4

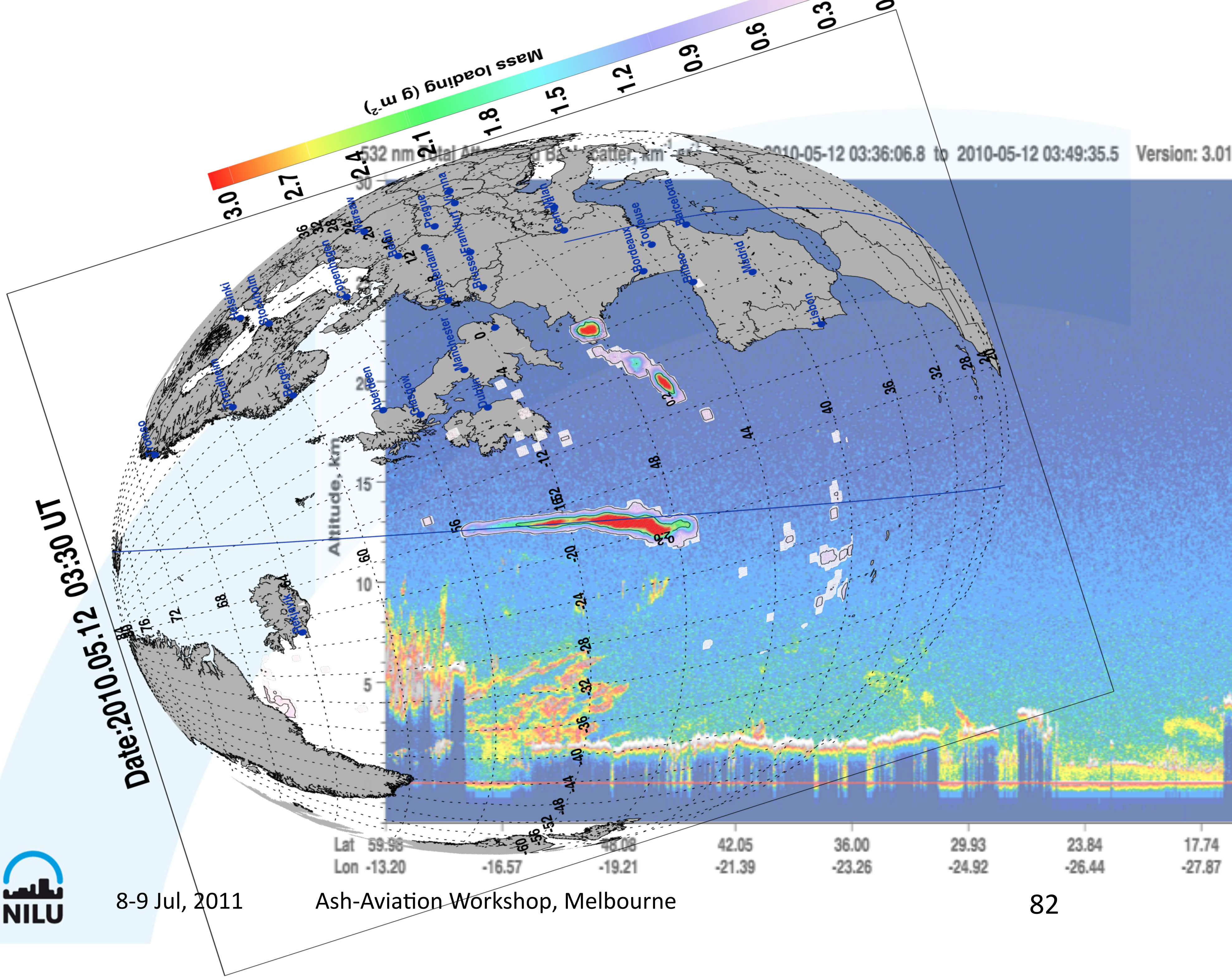
Mass loading (g m-2)
3.0
2.7
2.4
2.1
1.8
1.5
1.2
0.9
0.6
0.3
0
532 nm Total Attenuated Backscatter, km-1 sr-1 2010-05-12 03:36:06.8 to 2010-05-12 03:49:35.5 Version: 3.01
Altitude, km
Date:2010.05.12 03:30 UT
Lat 59.98 48.08 42.05 36.00 29.93 23.84 17.74
Lon -13.20 -16.57 -19.21 -21.39 -23.26 -24.92 -26.44 -27.87
Aberdeen
Glasgow
Dublin
Manchester
Amsterdam
Brussels
Frankfurt
Berlin
Prague
Vienna
Warsaw
Copenhagen
Helsinki
Stockholm
Bergen
Trondheim
Tromso
Bordeaux
Toulouse
Barcelona
Bilbao
Madrid
Lisbon
Geneva
Milan

NILU

For a single aerosol type the mass loading may be written:

$$m_l = \int_{z_1}^{z_2} \rho(z)dz$$

If we assume that the concentration profile is constant over the layer then:

$$\rho = \frac{m_l}{\Delta z}$$

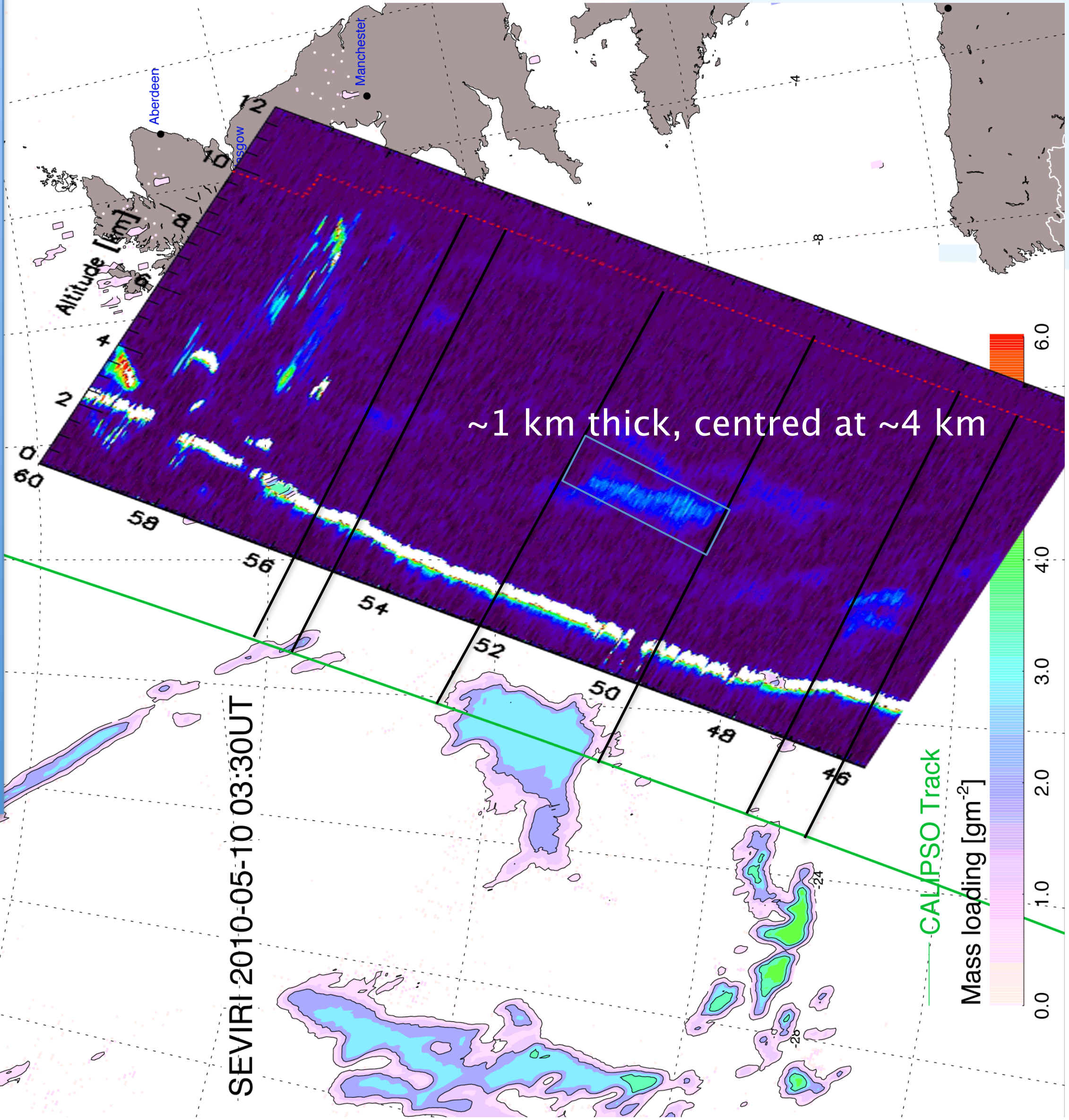

$$m_l = \int_{z_1}^{z_2} \rho(z) dz$$

$m_l \sim 0.4$ g

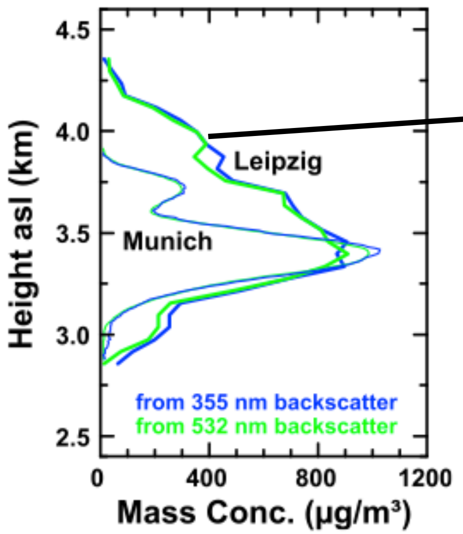

Figure 4. Mass concentrations estimated from the 355 and 532 nm backscatter profiles in Figure 3.

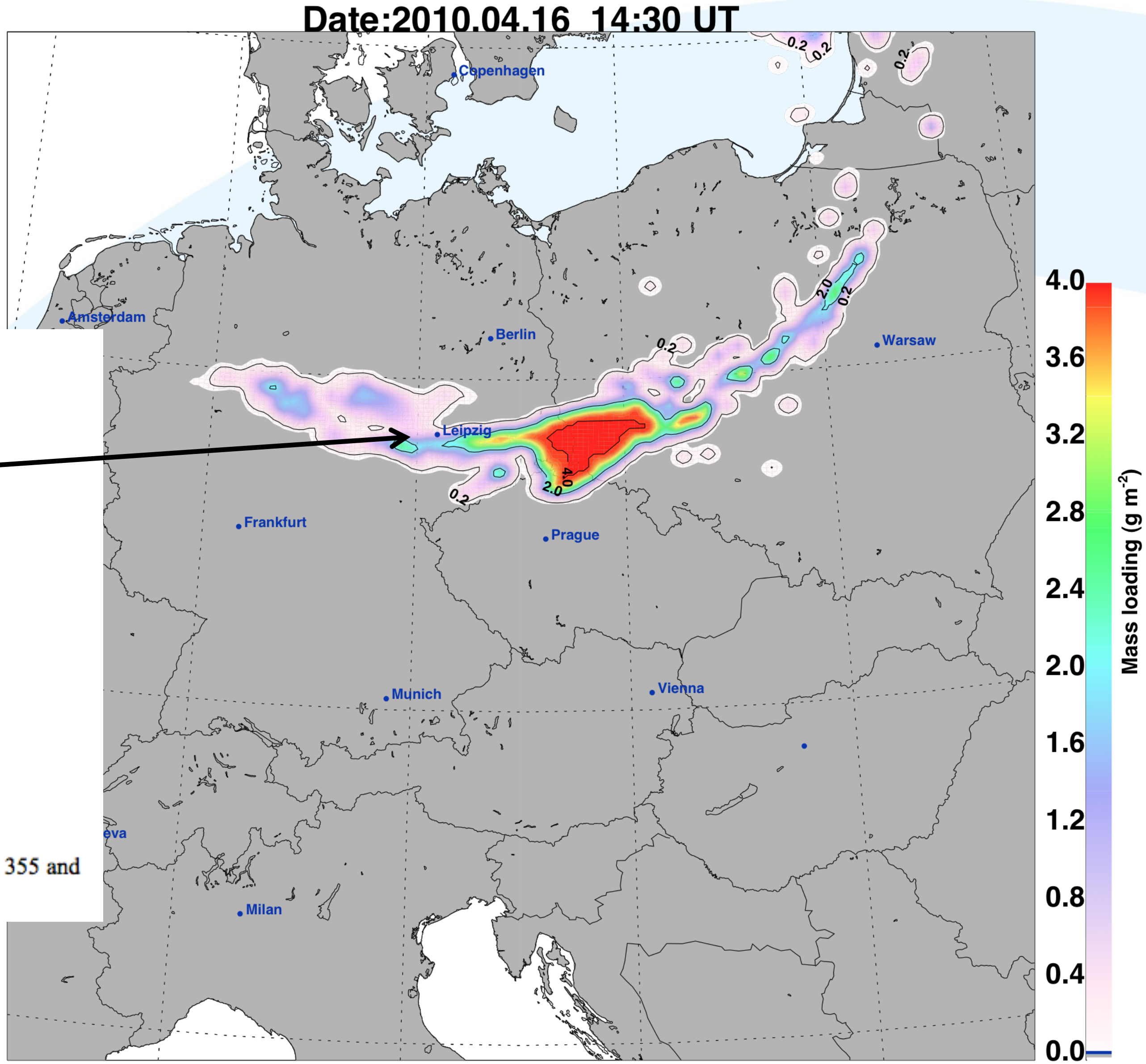

$m_l \sim 0.2$ g

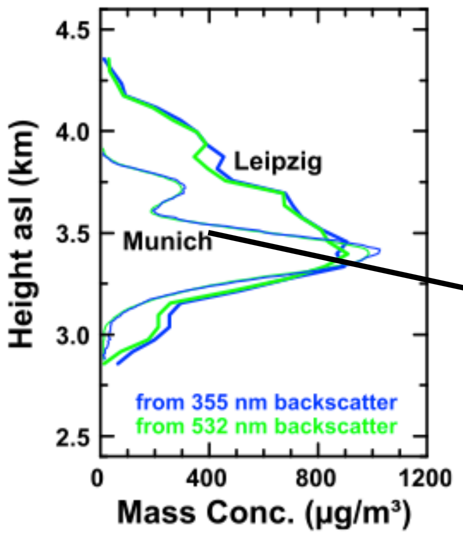

Figure 4. Mass concentrations estimated from the 355 and 532 nm backscatter profiles in Figure 3.

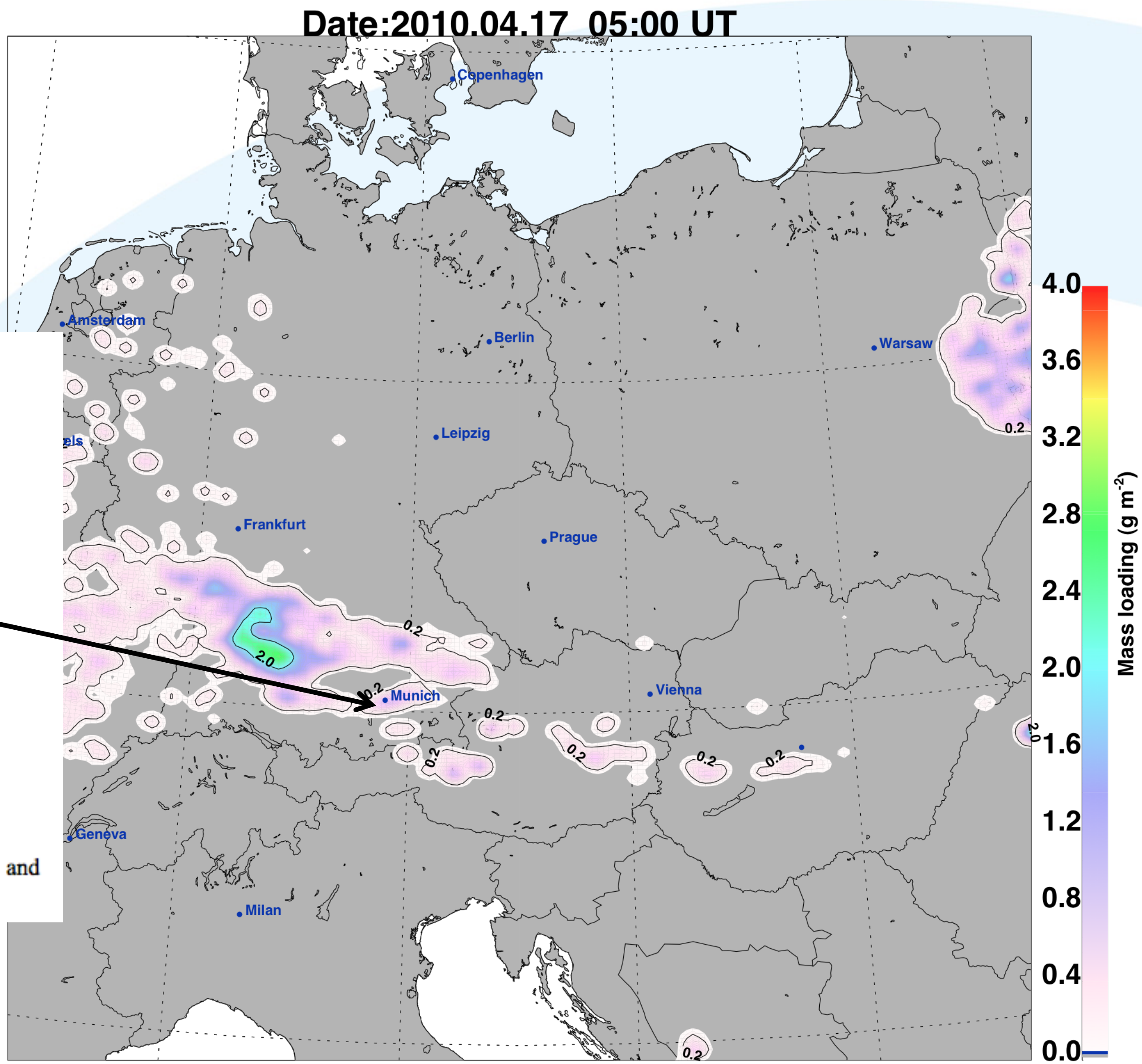

SO_2 as a tracer for Ash

Sulphur dioxide as a volcanic ash proxy during the April–May 2010 eruption of Eyjafjallajökull Volcano, Iceland

H.E.Thomas and A.J. Prata

ACPD submitted

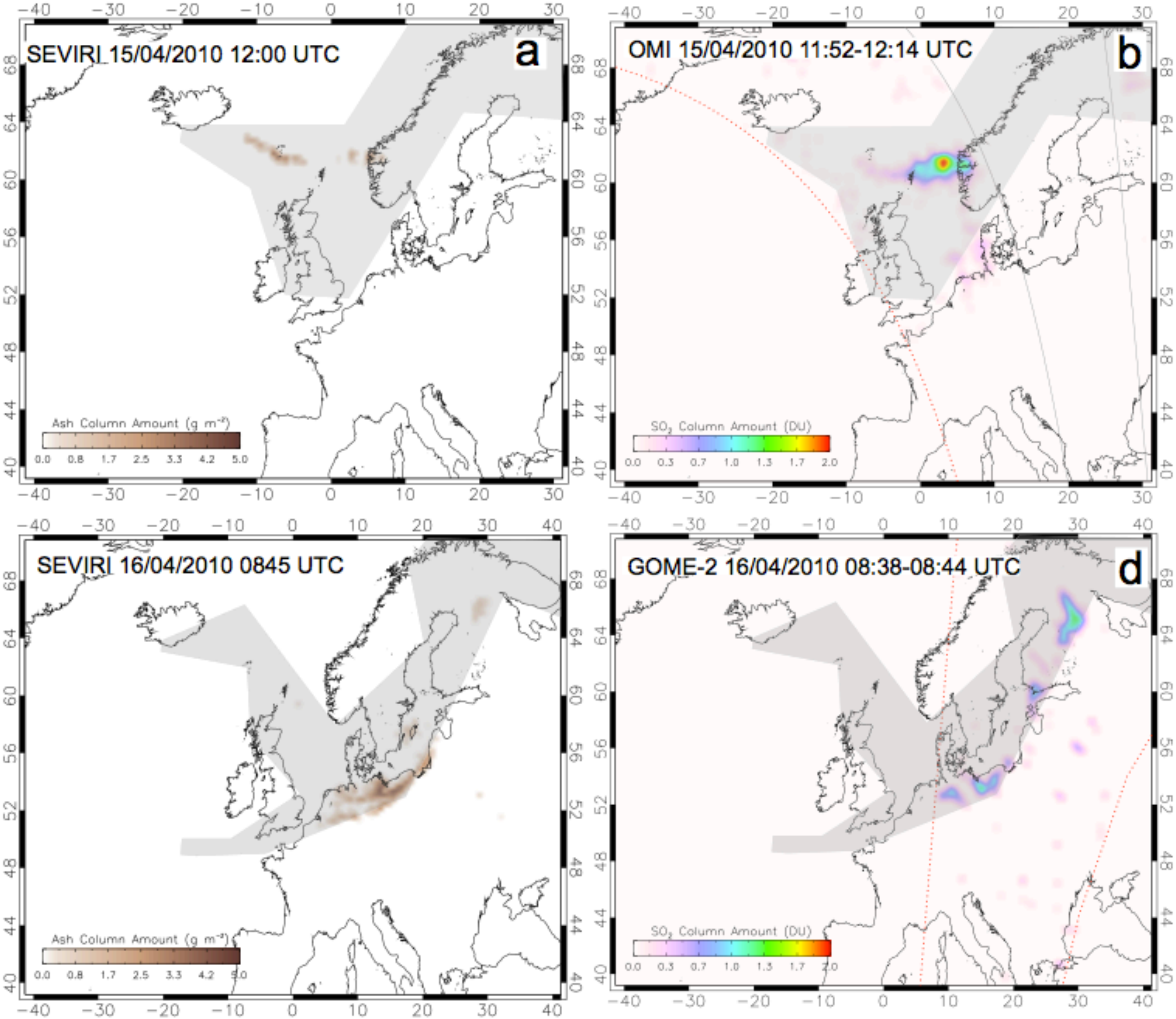
SEVIRI 15/04/2010 12:00 UTC
a
Ash Column Amount (g m⁻²)
OMI 15/04/2010 11:52-12:14 UTC
b
SO_2 Column Amount (DU)
SEVIRI 16/04/2010 0845 UTC
GOME-2 16/04/2010 08:38-08:44 UTC
d

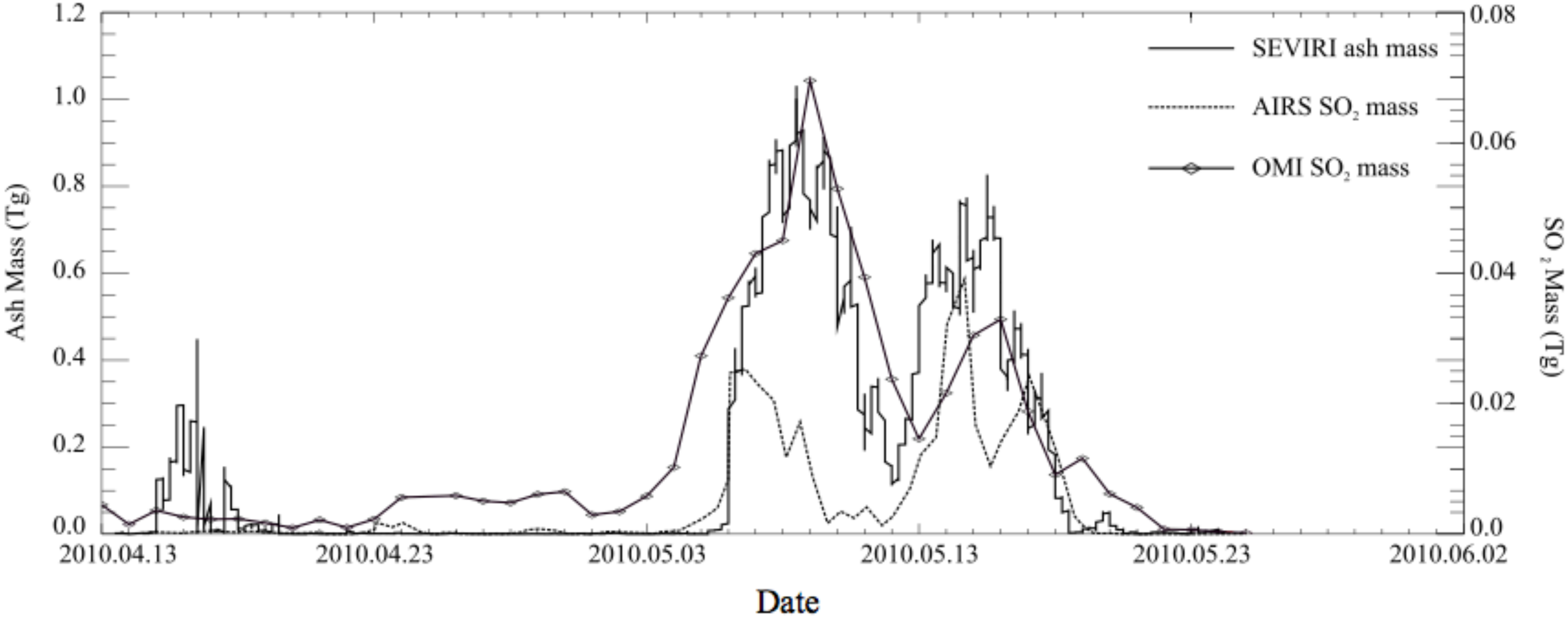

Figure 1: Total tonnage of ash retrieved at 15 minute intervals from the MSG SEVIRI instrment along with the total SO_2 mass detected by the OMI and AIRS instruments for the entire eruption period.

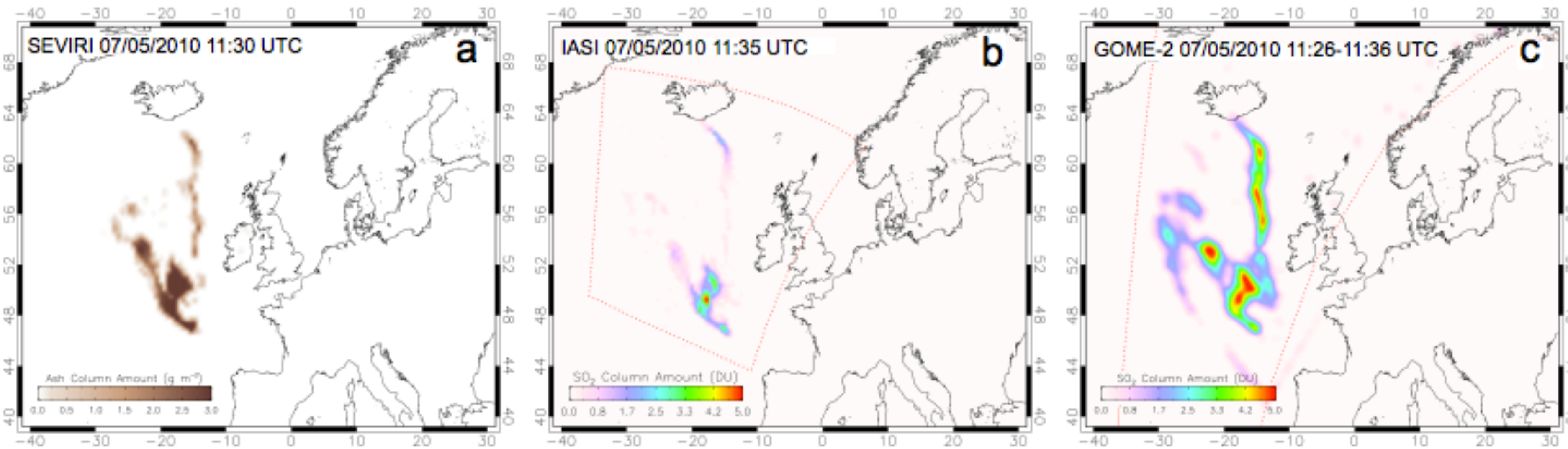
SEVIRI 07/05/2010 11:30 UTC
a
Ash Column Amount (g m⁻²)
IASI 07/05/2010 11:35 UTC
b
SO2 Column Amount (DU)
GOME-2 07/05/2010 11:26-11:36 UTC
c
SO2 Column Amount (DU)

Inversion Modelling and Satellite Data

Determination of time- and height-resolved volcanic ash emissions for quantitative ash dispersion modeling: The 2010 Eyjafjallajö̈kull eruption

A. Stohl, A. J. Prata, S. Eckhardt, L. Clarisse, A. Durant, S. Henne, N. I. Kristiansen, A. Minikin, U. Schumann, P. Seibert, K. Stebel, H. E. Thomas, T. Thorsteinsson, K. Tørseth, and B. Weinzierl

ACPD, January, 2011.

The FLEXPART model

Lagrangian particle dispersion model, similar to the one used at the London VAAC

Meteorological input data:
Forecasts use NCEP GFS data, Analyses ECMWF data

Simulation of volcanic ash in 31 size bins

- gravitational settling
- dry deposition
- wet deposition

Transport of 15 million ash particles by mean winds, turbulence, convection, sedimentation

Inversion Method

Sources x (1..n) x^a a priori profile

Satellite observation y^0 (1..m)

M Emission sensitivity Matrix (m × n), as obtained from FLEXPART

σ standard error of observation

$$\mathbf{M}(\mathbf{x}-\mathbf{x}^a) \approx \mathbf{y}^o - \mathbf{M}\mathbf{x}^a$$

$$\mathbf{M}\tilde{\mathbf{x}} \approx \tilde{\mathbf{y}}.$$

$$J = \underbrace{(\mathbf{M}\tilde{\mathbf{x}}-\tilde{\mathbf{y}})^T \mathbf{diag}(\sigma_o^{-2})(\mathbf{M}\tilde{\mathbf{x}}-\tilde{\mathbf{y}})}_{\text{I) misfit model – observation}} + \underbrace{\tilde{\mathbf{x}}^T \mathbf{diag}(\sigma_{\mathbf{x}}^{-2})\,\tilde{\mathbf{x}}}_{\text{II) deviation from first guess}} + \underbrace{\epsilon\,(\mathbf{D}\tilde{\mathbf{x}})^T \mathbf{D}\tilde{\mathbf{x}}.}_{\text{III) smoothness condition}}$$

NILU

Source-receptor matrix calculation with a Lagrangian particle dispersion model in backward mode, P. Seibert and A. Frank, ACP, 4, 51-63, 2004.

The source term – the great unknown

- Total ash emission highly uncertain
  - Assume 10% of reported tephra production in modeled size range (0.5–290 μm)

- Time variation of emission rate not well known
  - Take what's available, anecdotal evidence

- Eruption column height is variable
  - Reports, satellite data (max. height 11 km?)

- Ash size distribution at point of emission not well known
  - Taken from ground samples around Eyjafjallajökull but they are biased towards larger sizes

All these uncertainties will affect the final model result!

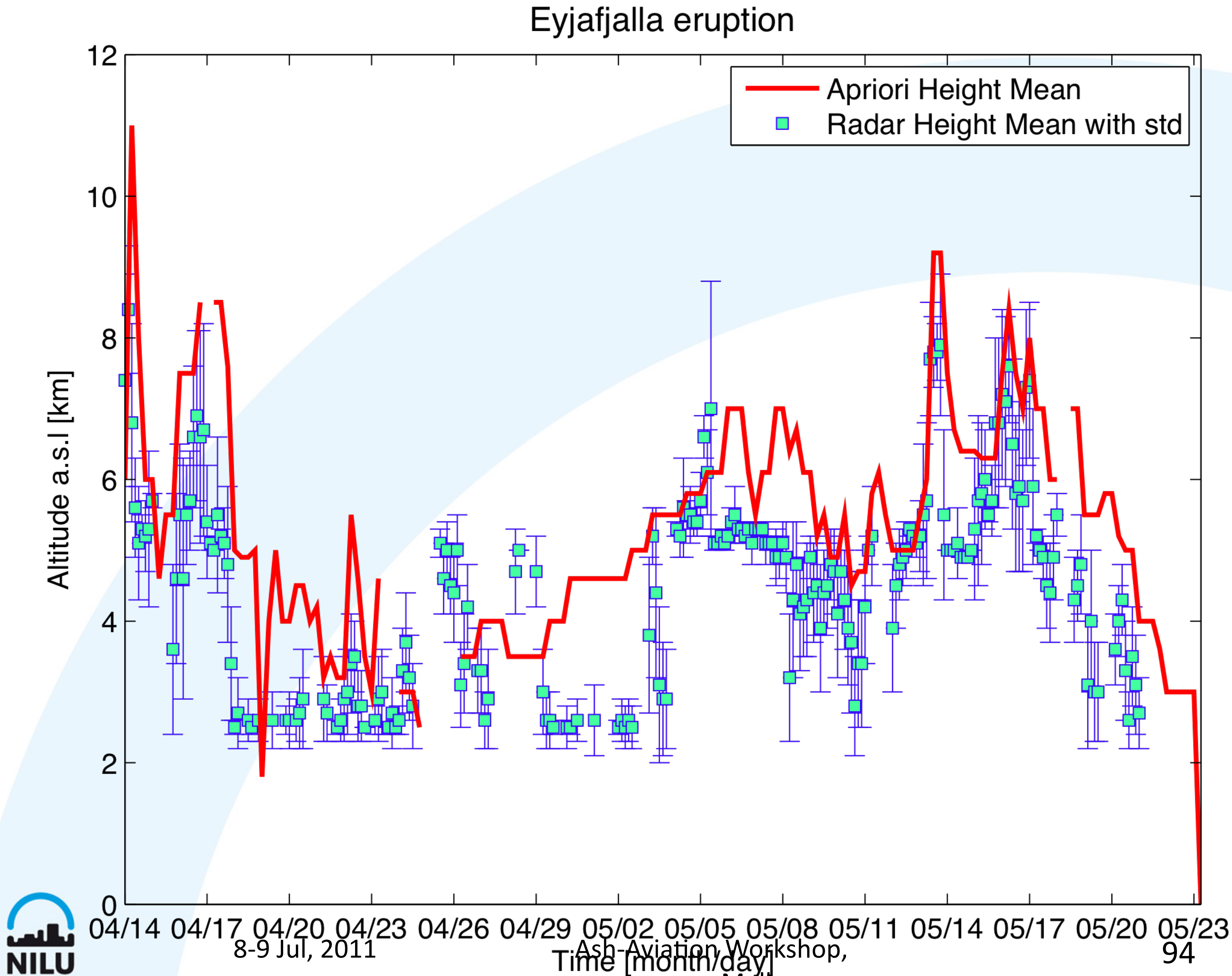
Eyjafjalla eruption
Apriori Height Mean
Radar Height Mean with std
Altitude a.s.l [km]
Time [month/day]
0
2
4
6
8
10
12
04/14
04/17
04/20
04/23
04/26
04/29
05/02
05/05
05/08
05/11
05/14
05/17
05/20
05/23
NILU

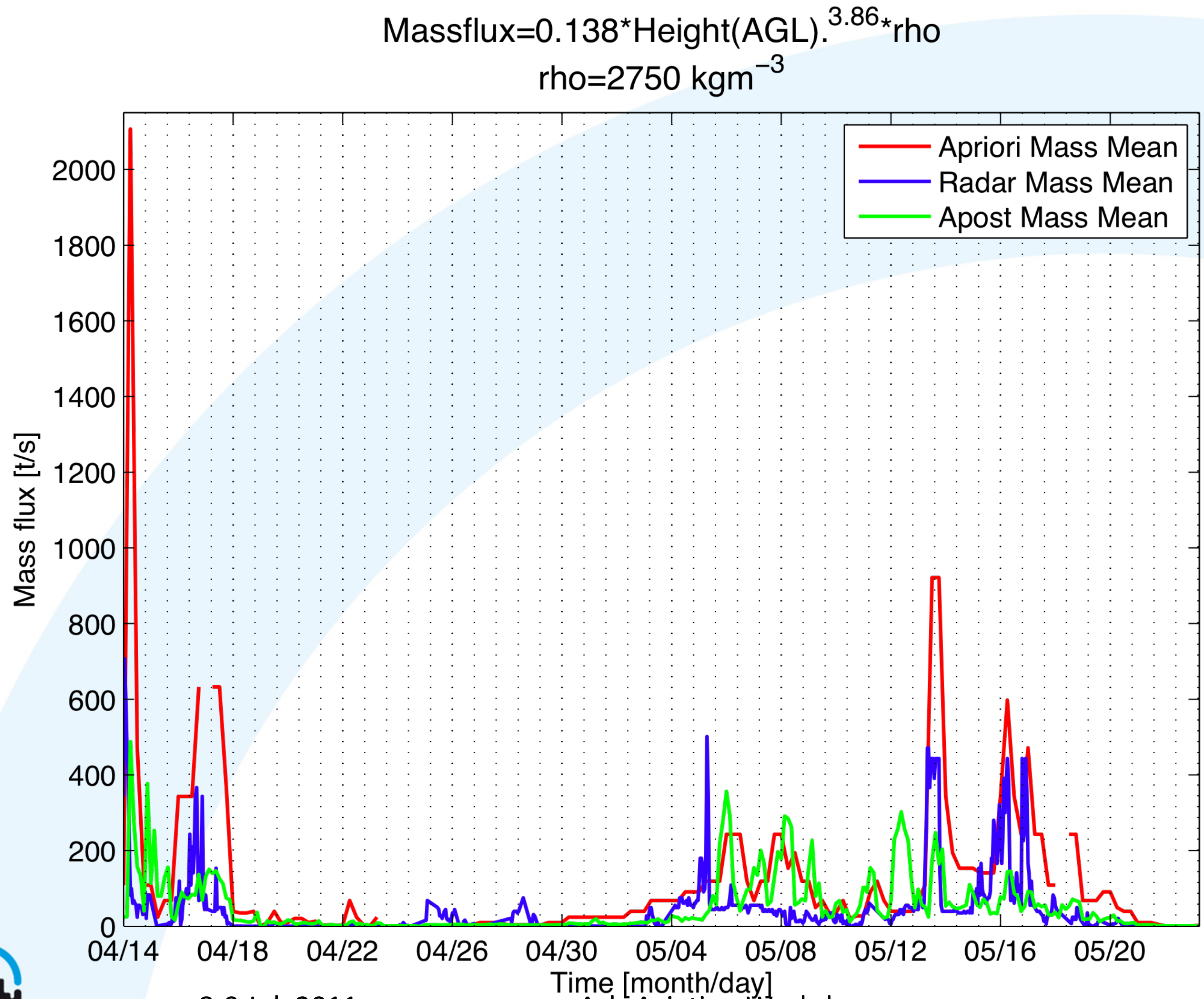

Massflux=0.138*Height(AGL).^3.86*rho
rho=2750 kgm^−3
Apriori Mass Mean
Radar Mass Mean
Apost Mass Mean
Mass flux [t/s]
2000
1800
1600
1400
1200
1000
800
600
400
200
0
04/14
04/18
04/22
04/26
04/30
05/04
05/08
05/12
05/16
05/20
Time [month/day]

Input data

SEVIRI

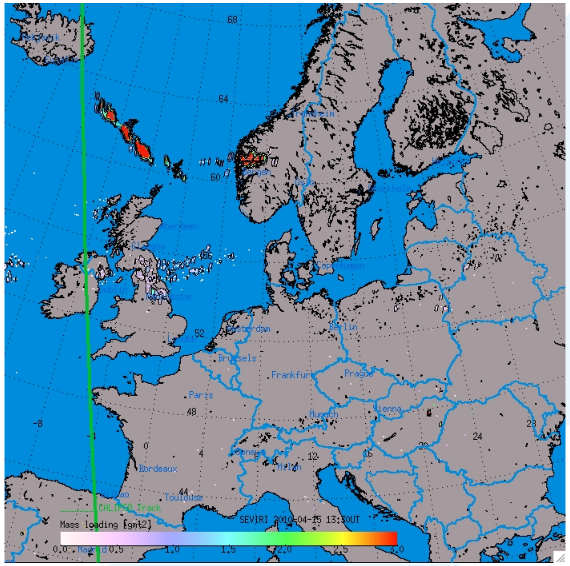

IASI

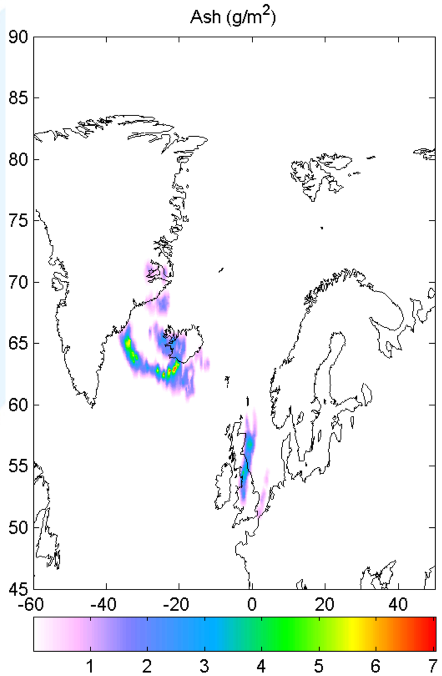

FLEXPART

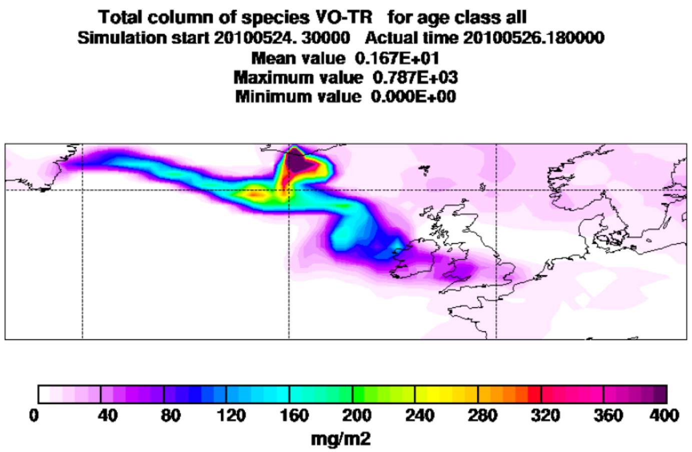

3840 Images

122 Images

6232 Runs

Size distributions

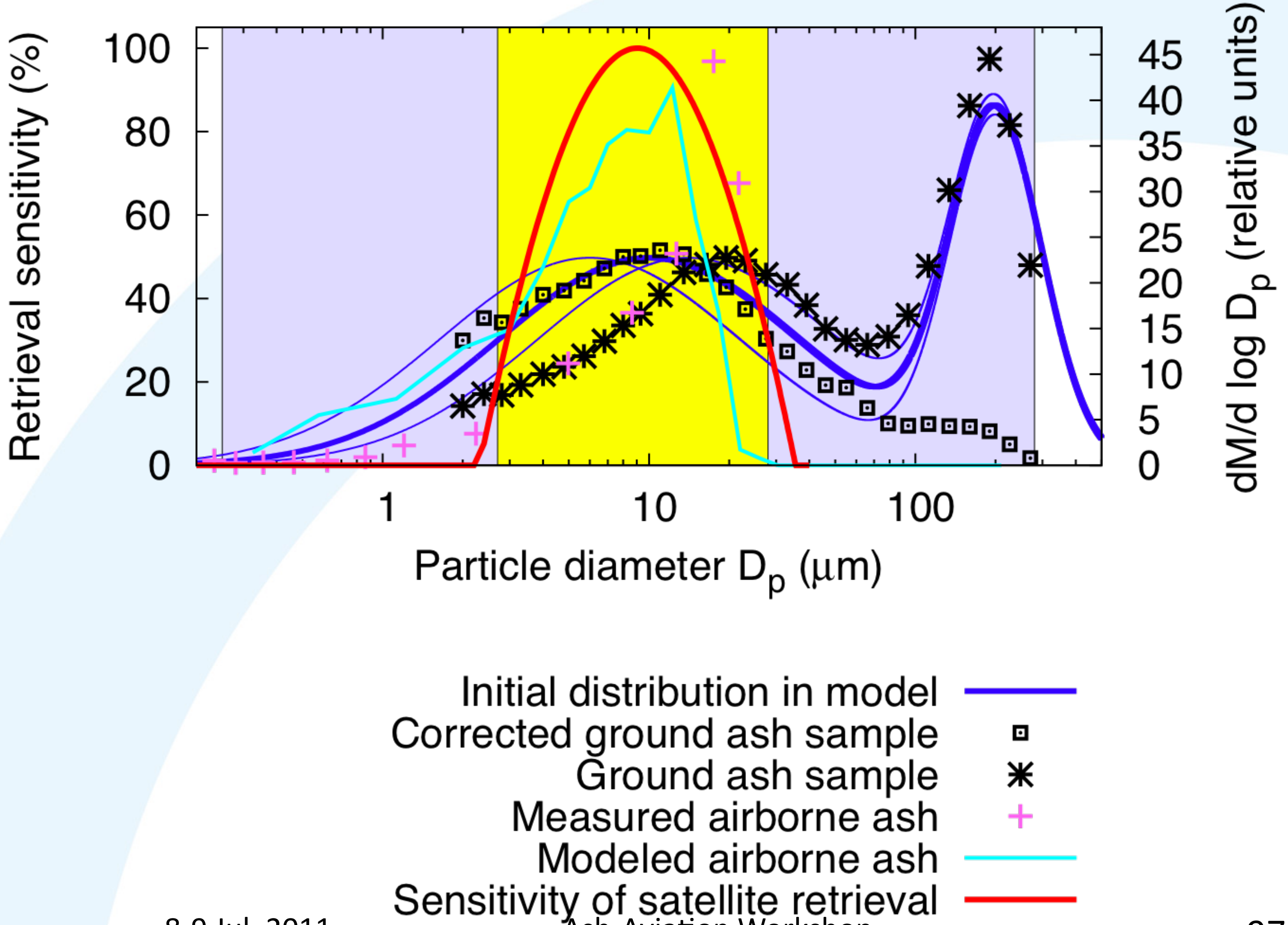

Emission profile

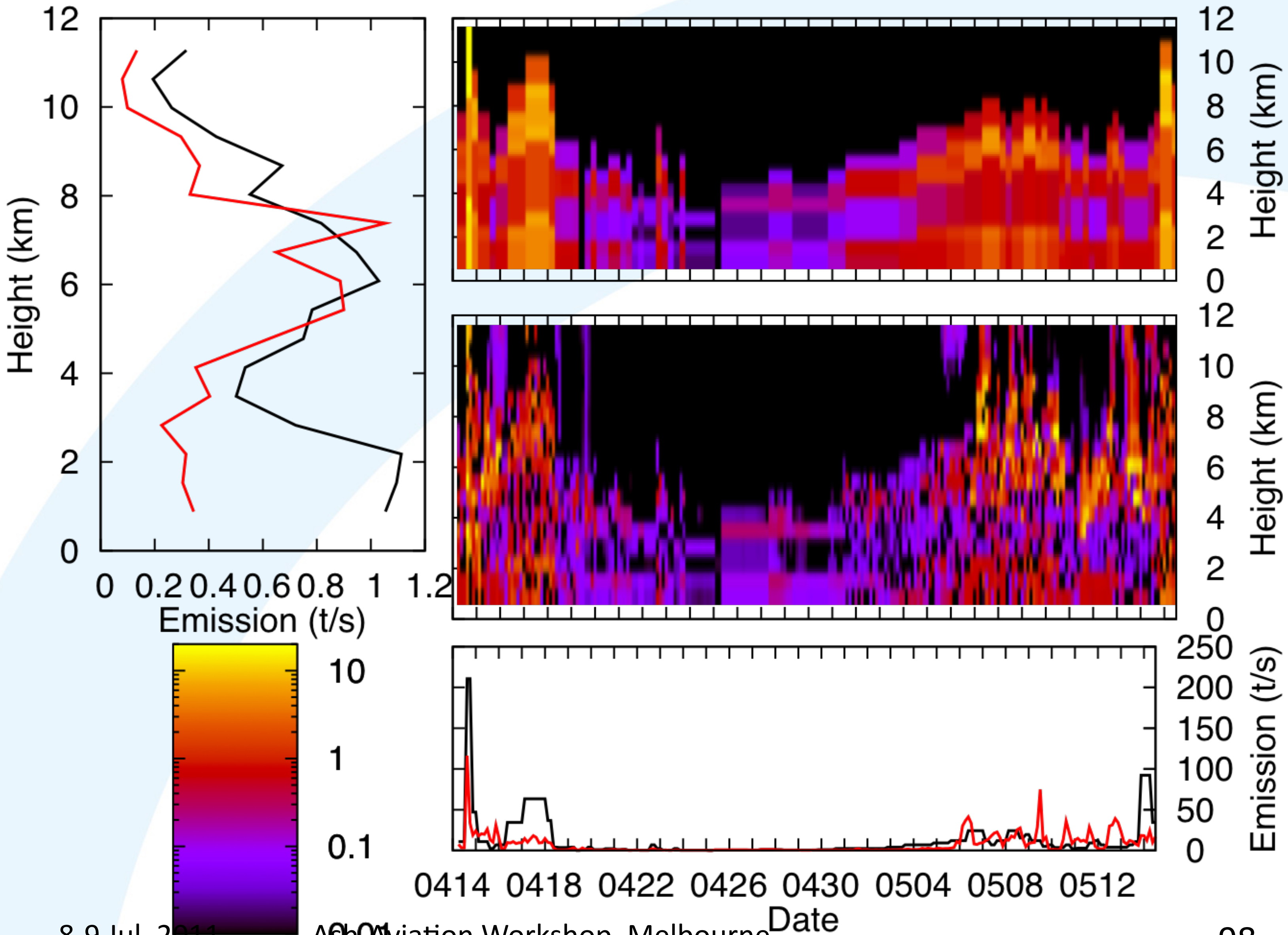

SEVIRI 15th - April 13:30

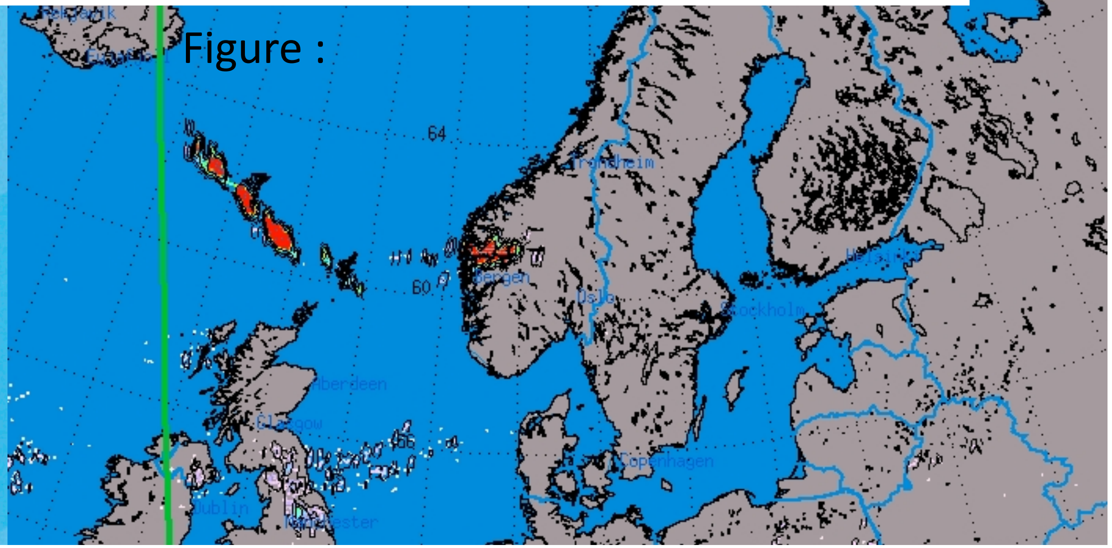

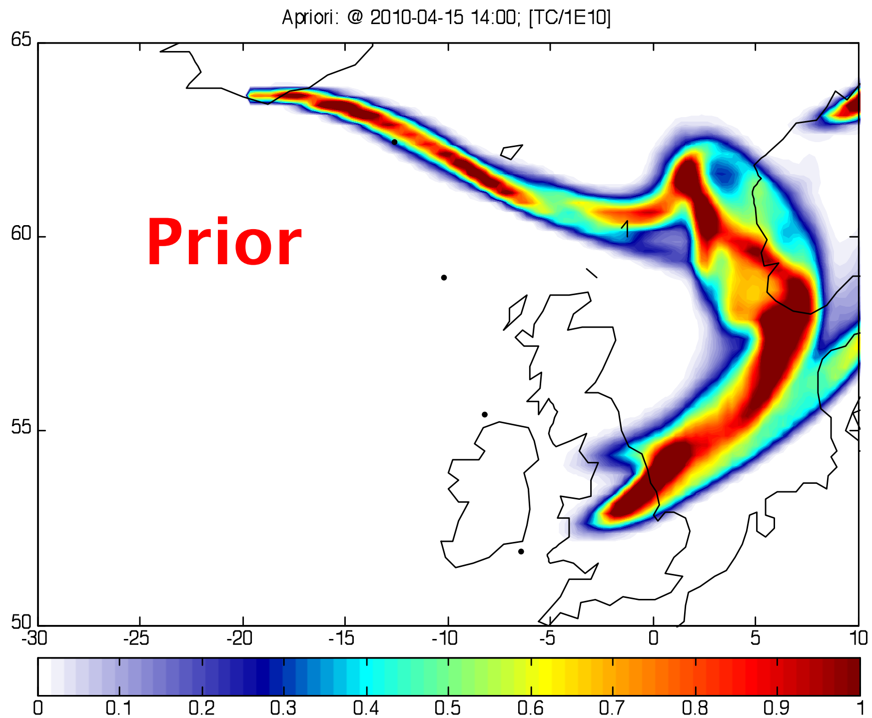

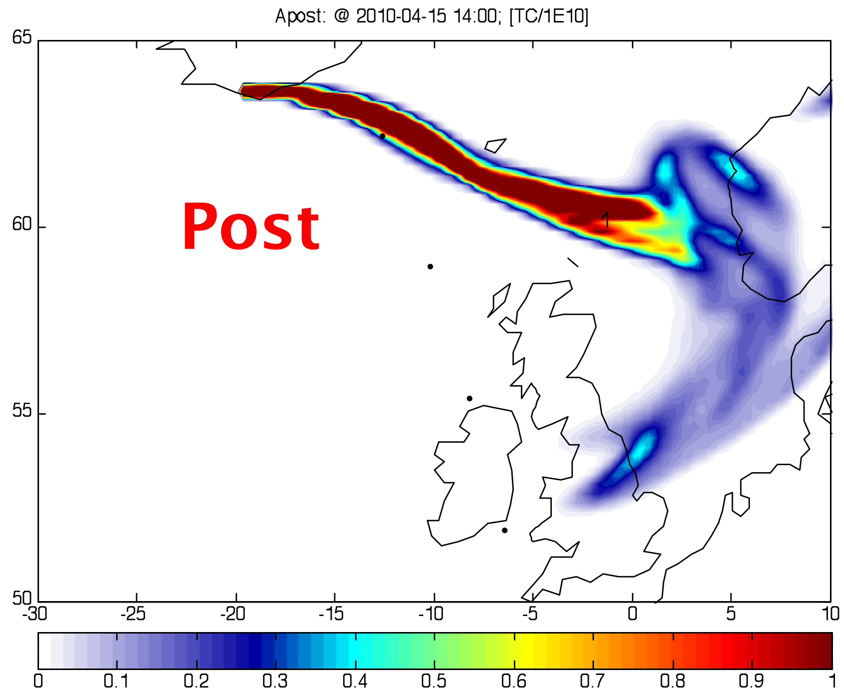

Differences in Source Term

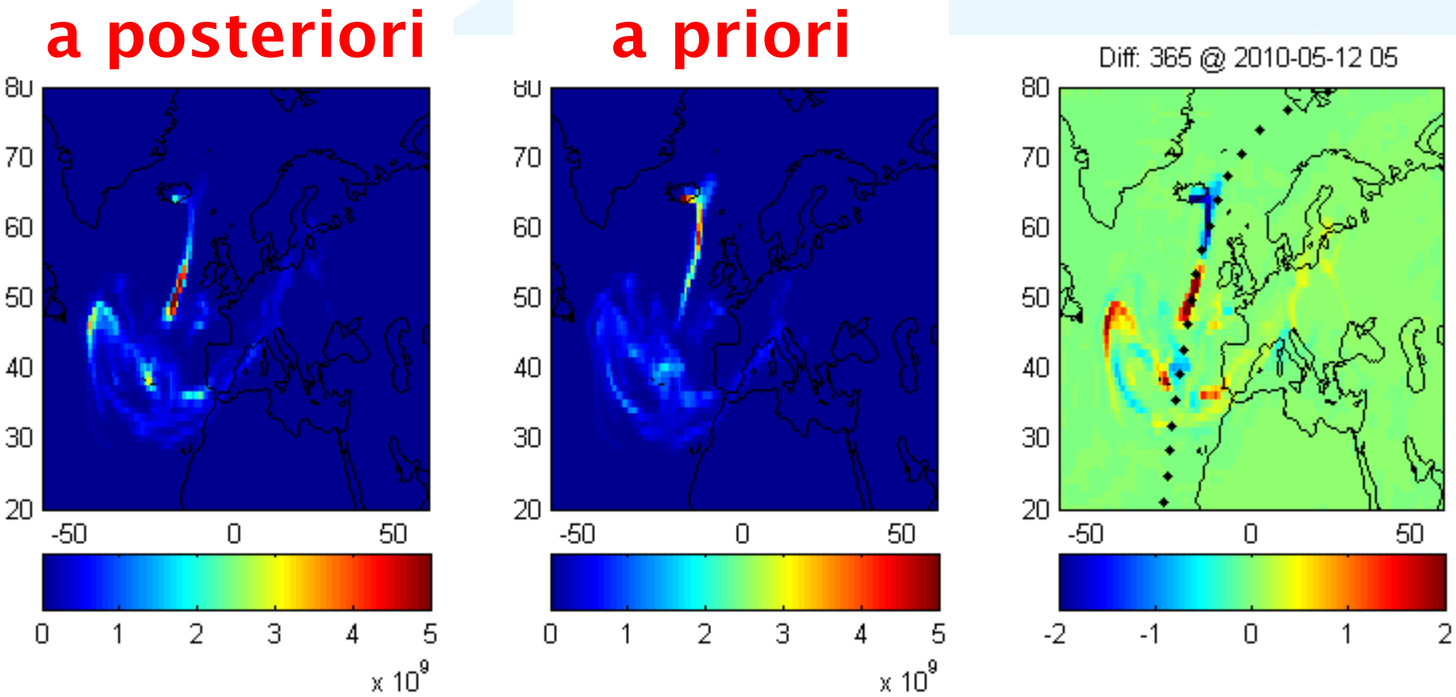

Validation - Calipso, 12th May

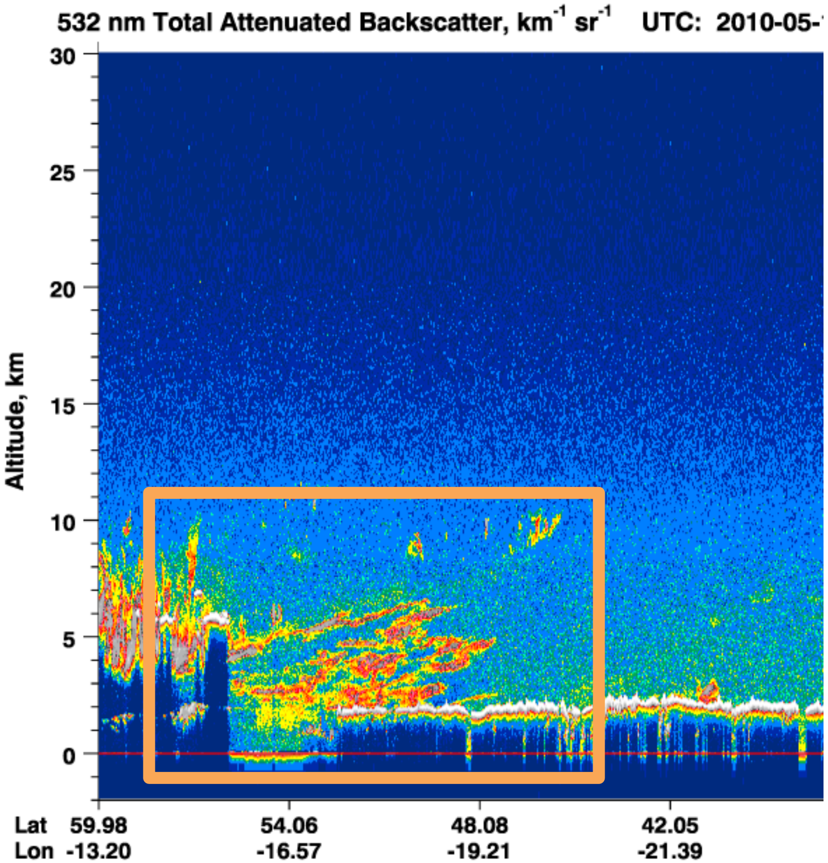

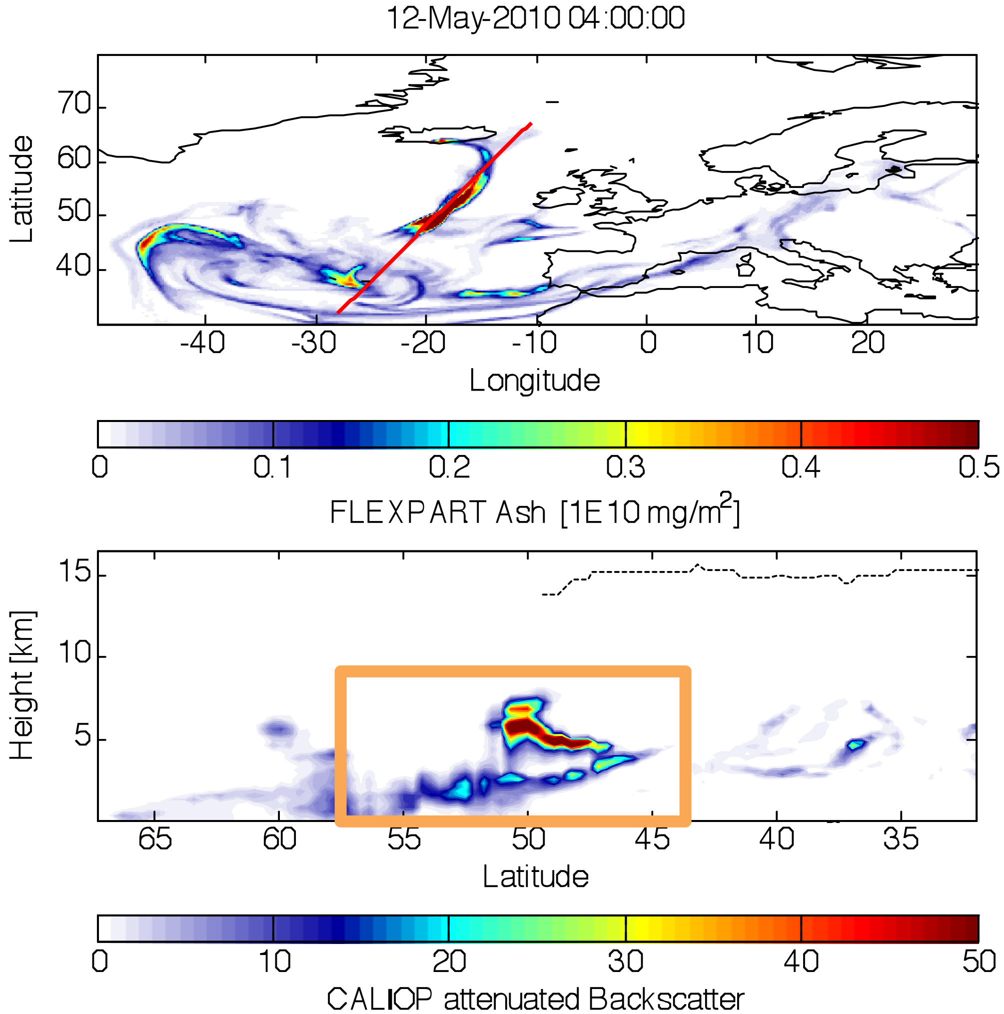

Results

FLEXPART simulation of the ash tracer on 2010/04/14 04:00

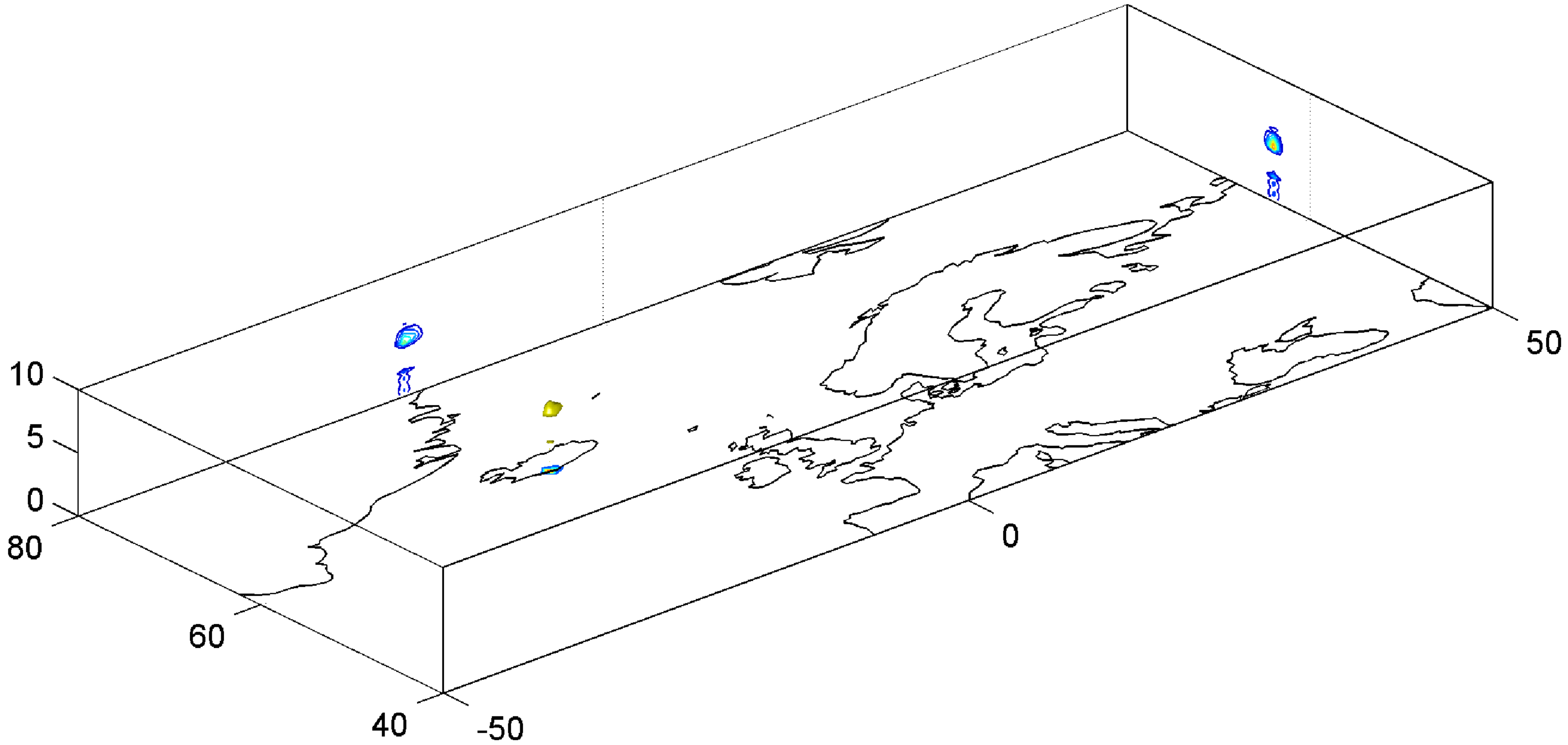

Outputs

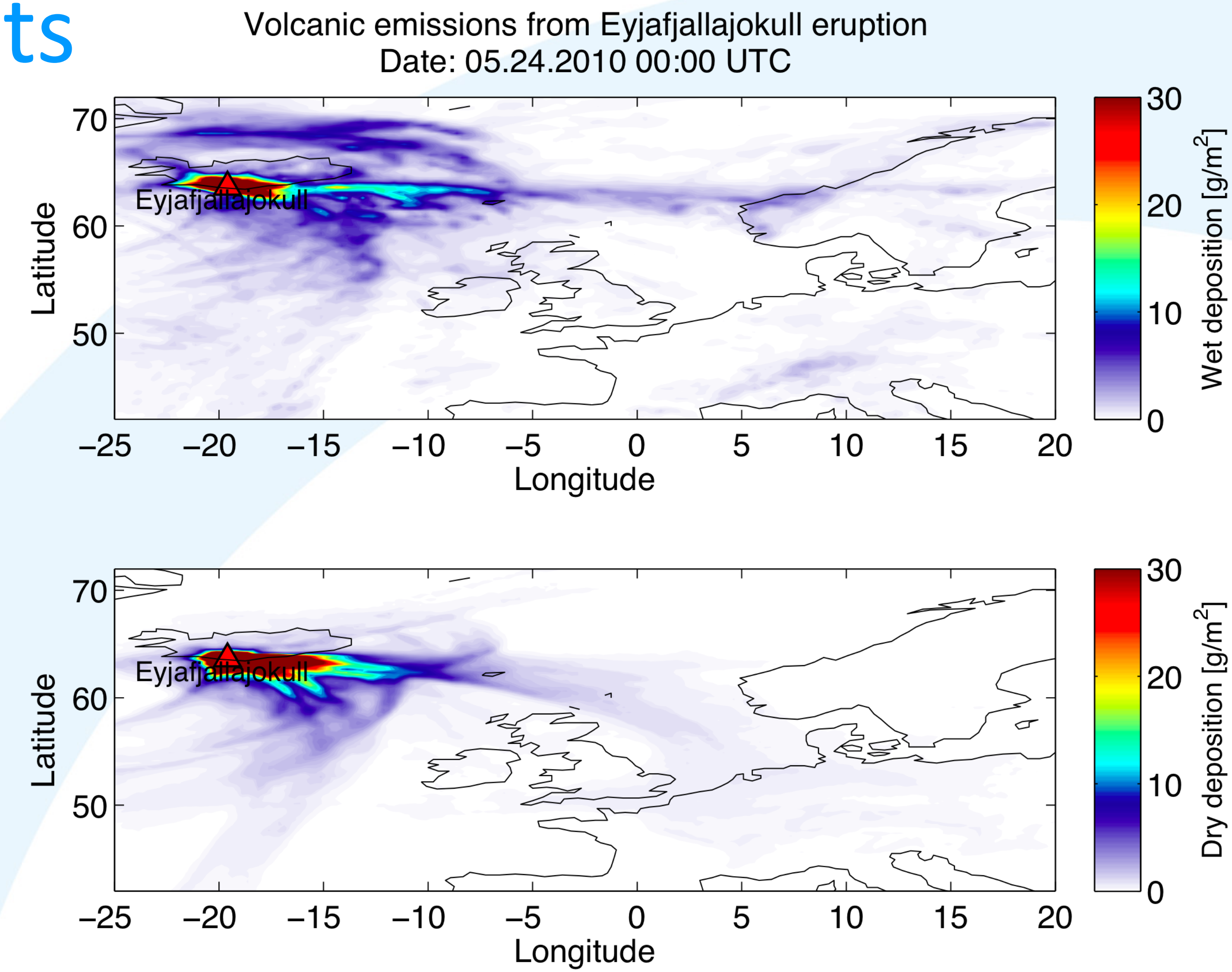

Volcanic emissions from Eyjafjallajokull eruption
Date: 05.24.2010 00:00 UTC
70
60
50
Latitude
Eyjafjallajokull
–25
–20
–15
–10
–5
0
5
10
15
20
Longitude
30
20
10
0
Wet deposition [g/m2]
70
60
50
Latitude
Eyjafjallajokull
–25
–20
–15
–10
–5
0
5
10
15
20
Longitude
30
20
10
0
Dry deposition [g/m2]

Results

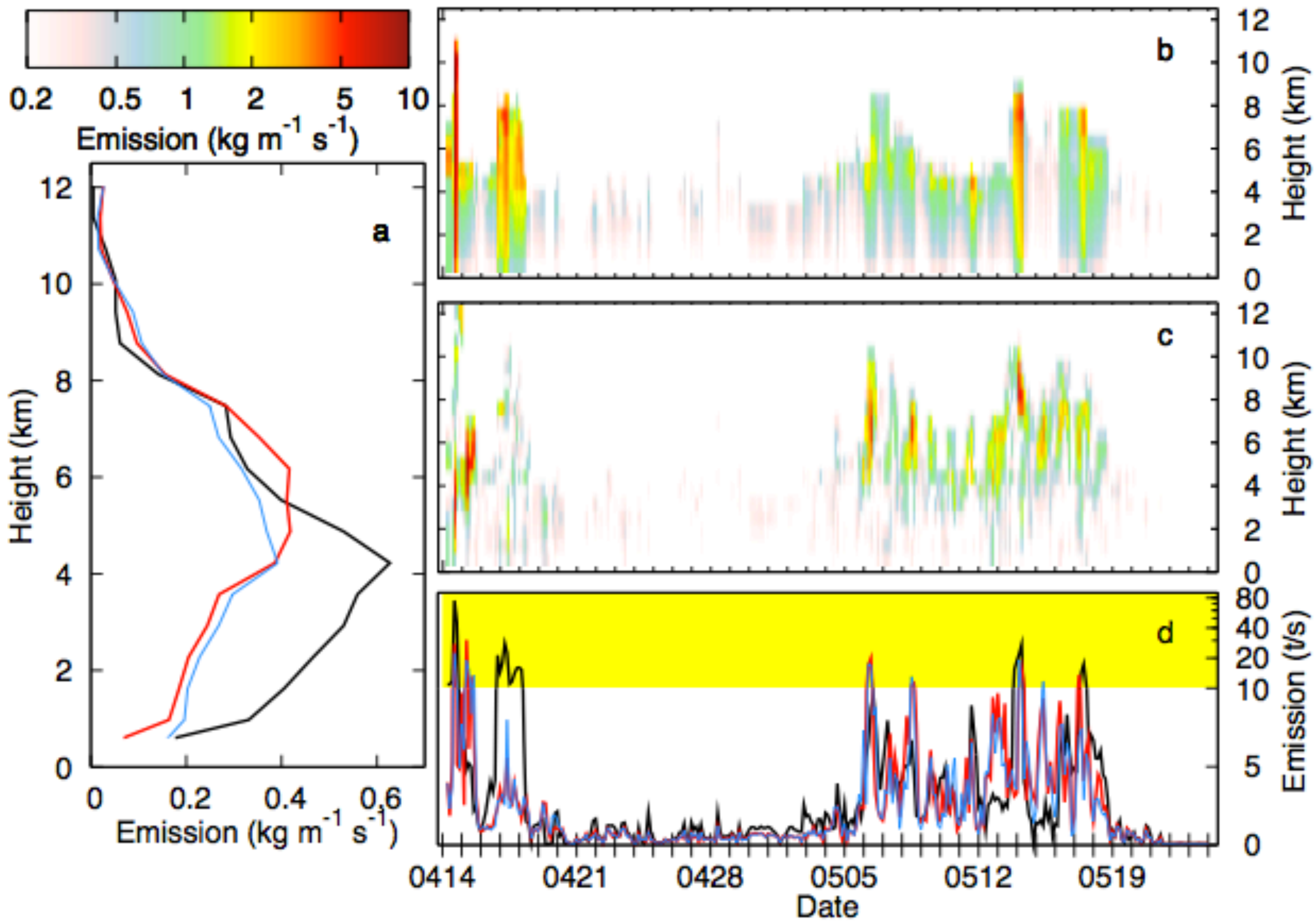

0.2
0.5
1
2
5
10
Emission (kg m^{-1} s^{-1})
a
Height (km)
12
10
8
6
4
2
0
0
0.2
0.4
0.6
Emission (kg m^{-1} s^{-1})
b
c
d
Height (km)
Emission (t/s)
80
40
20
10
5
0414
0421
0428
0505
0512
0519
Date

Results

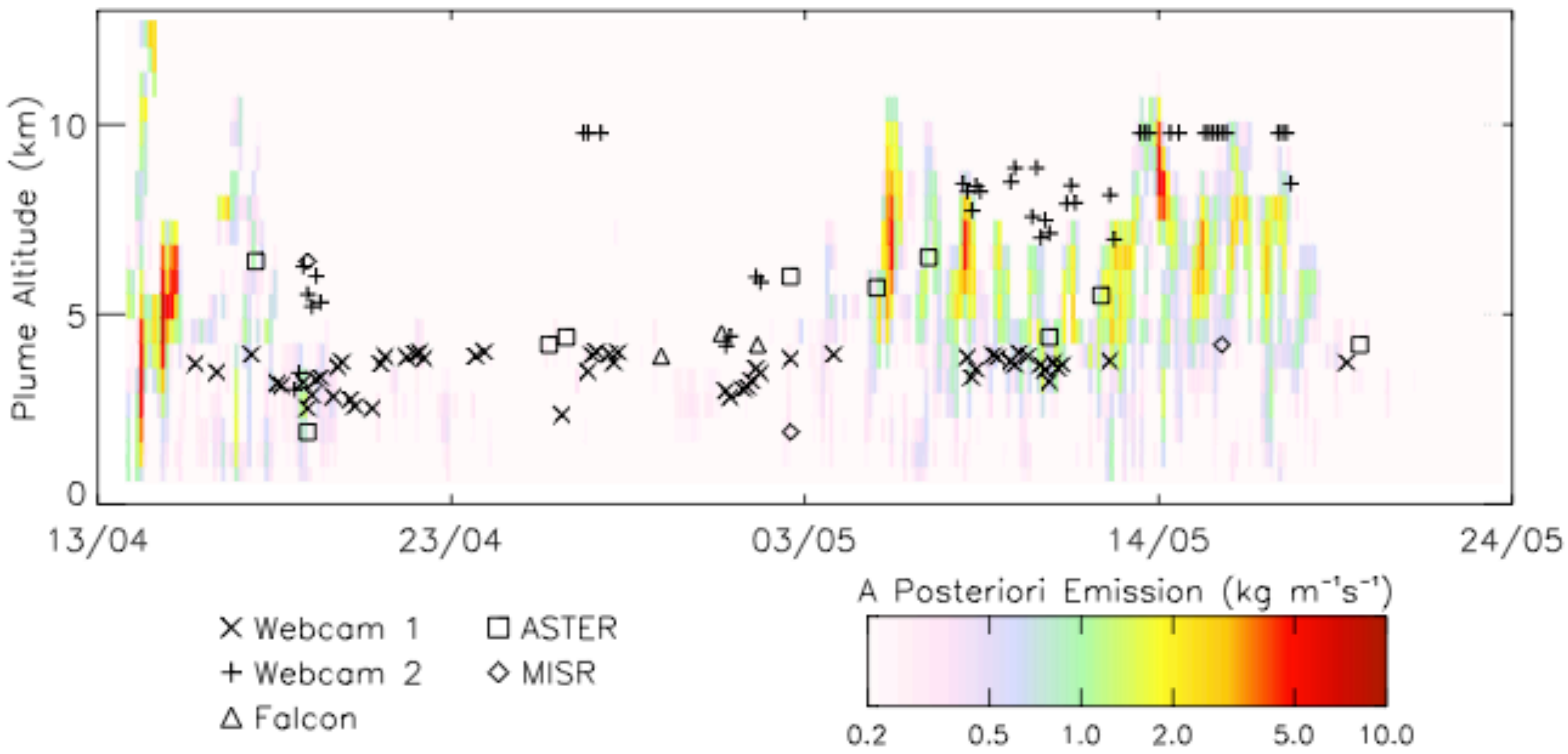

Plume Altitude (km)
10
5
0
13/04
23/04
03/05
14/05
24/05
Webcam 1
Webcam 2
Falcon
ASTER
MISR
A Posteriori Emission (kg m⁻¹s⁻¹)
0.2
0.5
1.0
2.0
5.0
10.0

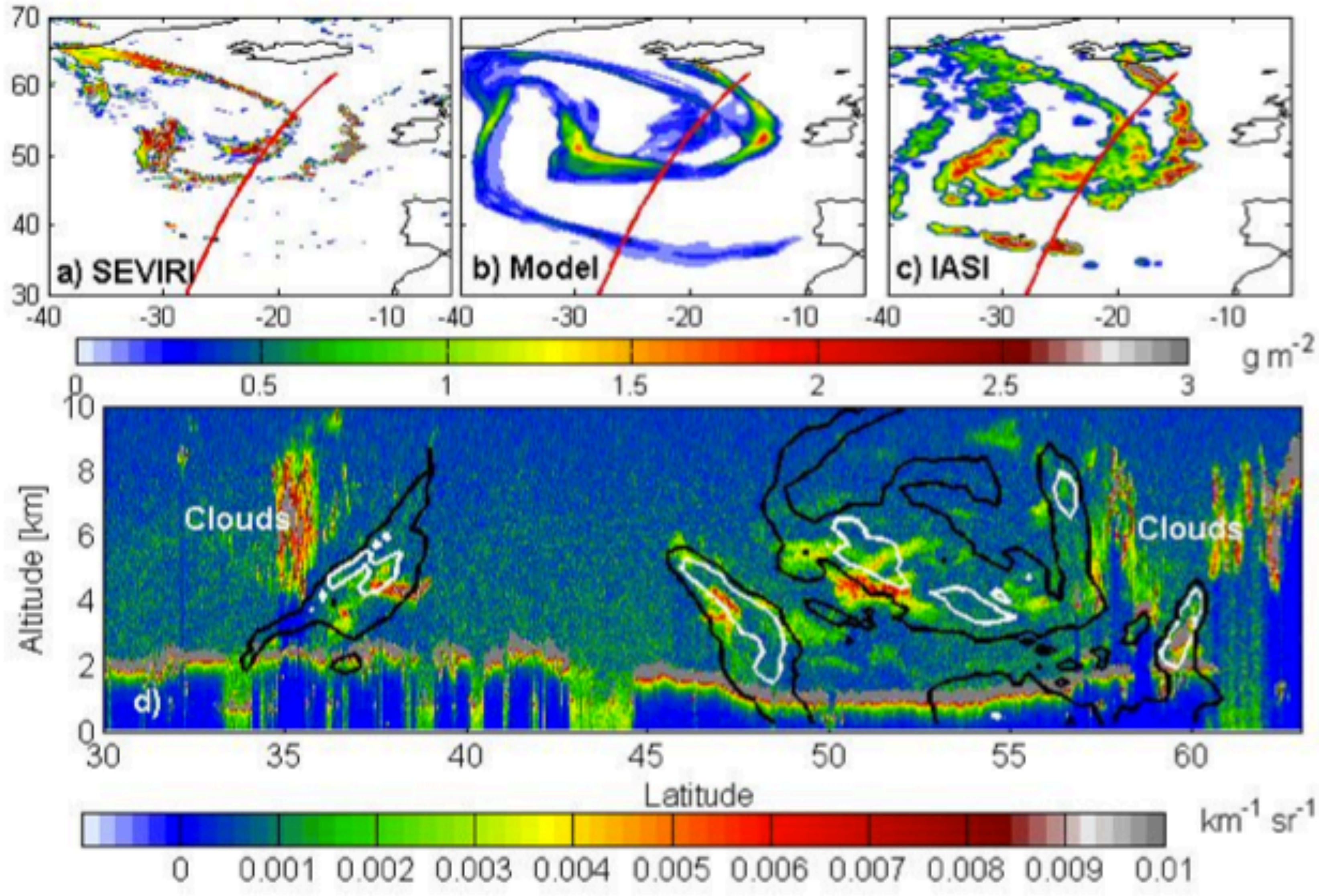

a) SEVIRI
b) Model
c) IASI
g m-2
d)
Clouds
Clouds
Altitude [km]
Latitude
km-1 sr-1

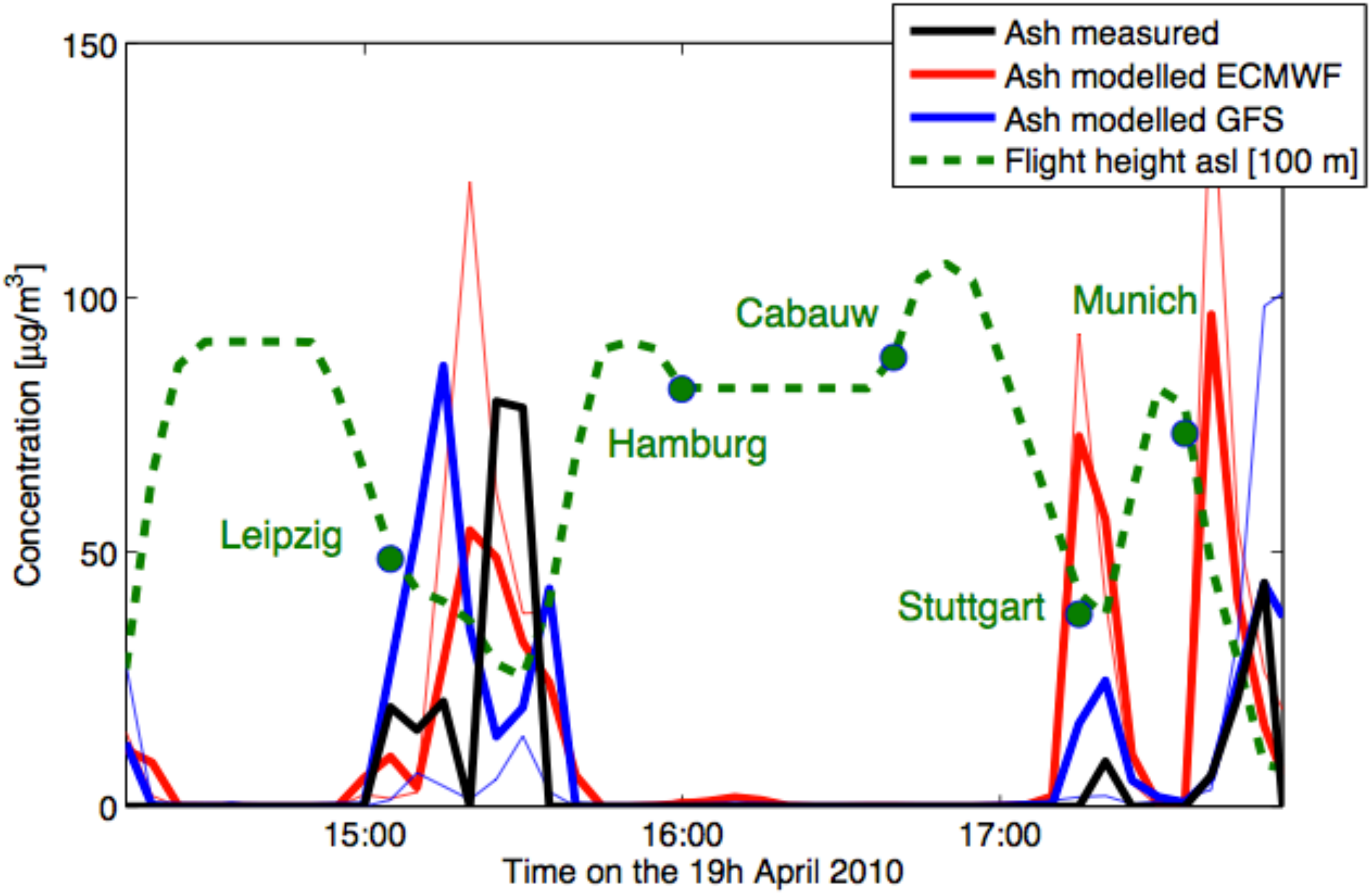
Ash measured
Ash modelled ECMWF
Ash modelled GFS
Flight height asl [100 m]
150
100
50
0
Concentration [µg/m^3]
15:00
16:00
17:00
Time on the 19h April 2010
Leipzig
Hamburg
Cabauw
Munich
Stuttgart

Further Possibilities

- Ash fall-out maps
- Dosage calculations
- Ocean productivity
- Ash-albedo feedback
- Air quality
- Local climate effects

Visualisation

Courtesy: Vince Realmuto, JPL

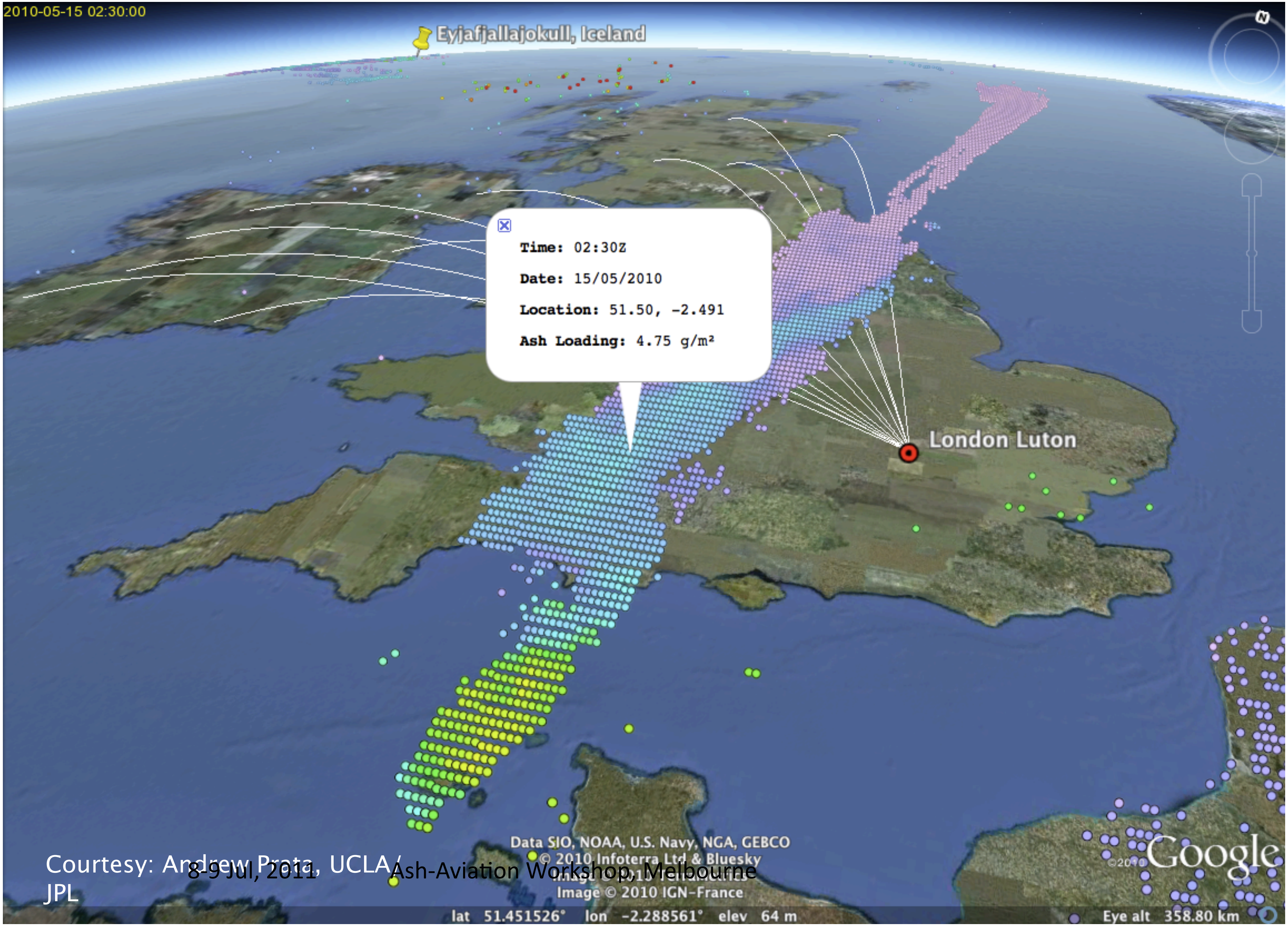

Courtesy: Andrew Prata, UCLA/JPL

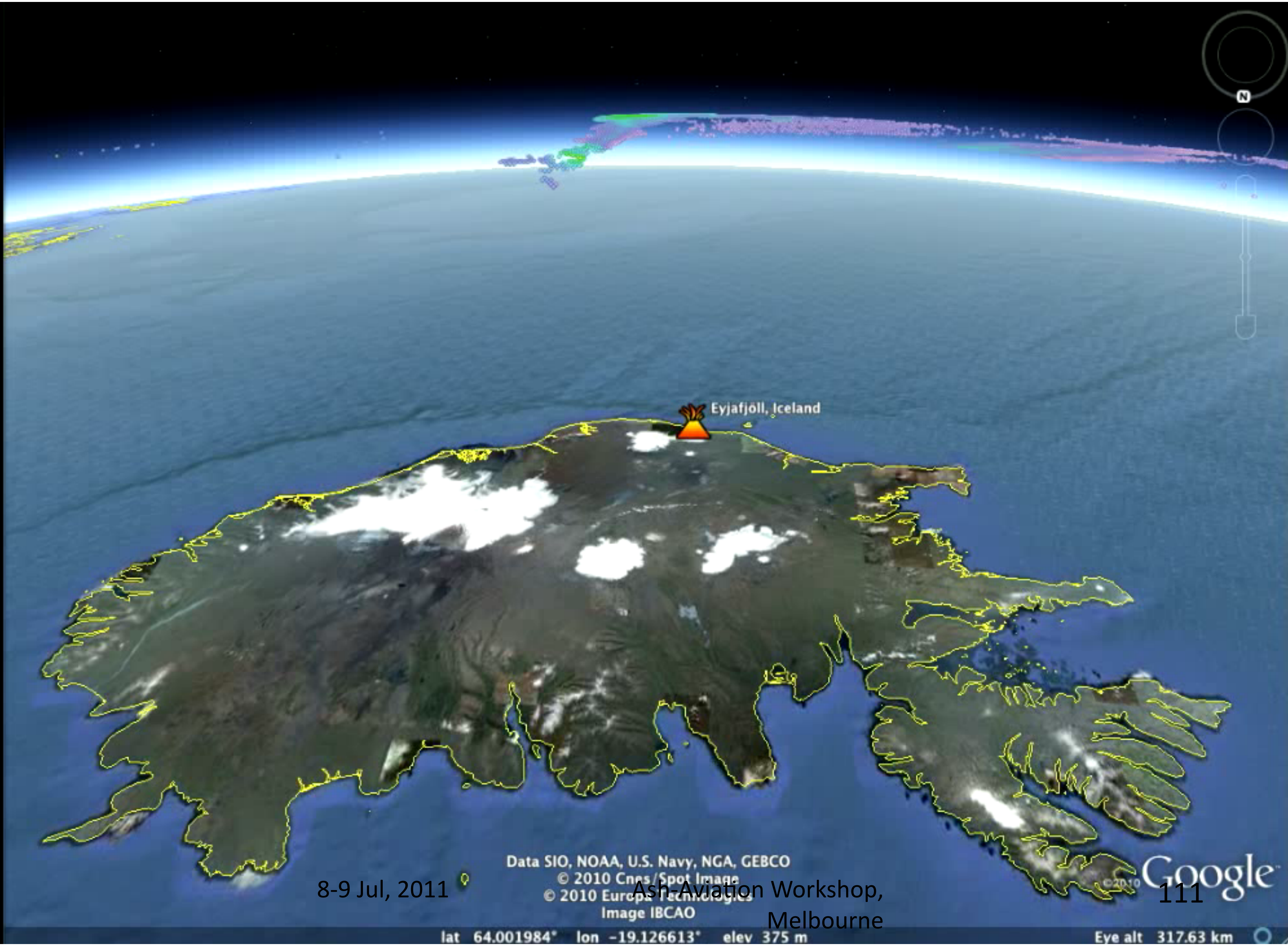
Eyjafjöll, Iceland
Data SIO, NOAA, U.S. Navy, NGA, GEBCO
© 2010 Cnes/Spot Image
© 2010 Europa Technologies
Image IBCAO
lat 64.001984° lon -19.126613° elev 375 m
Eye alt 317.63 km
Google

AVOID can also measure SO_2 with a 3[rd] camera

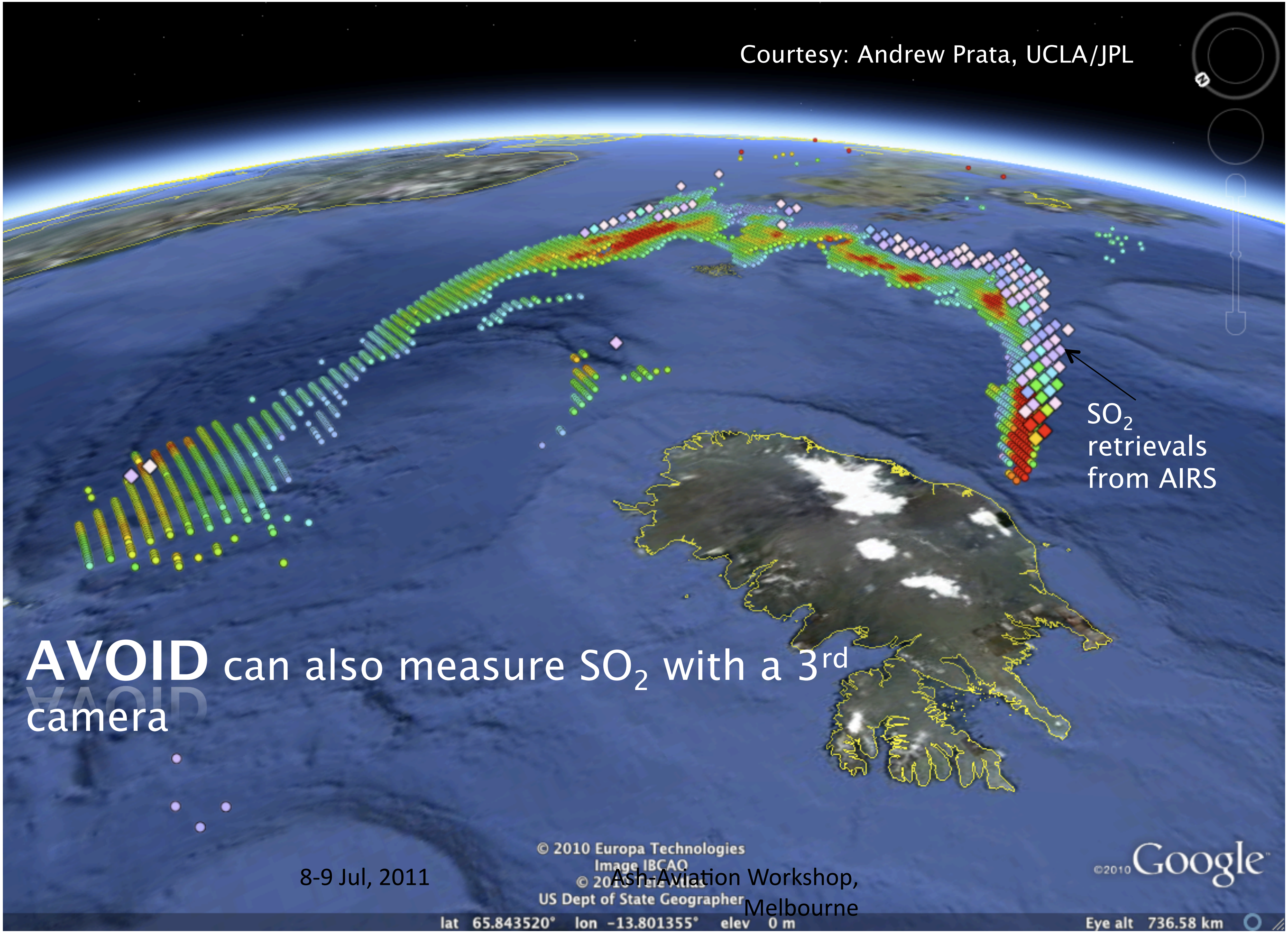

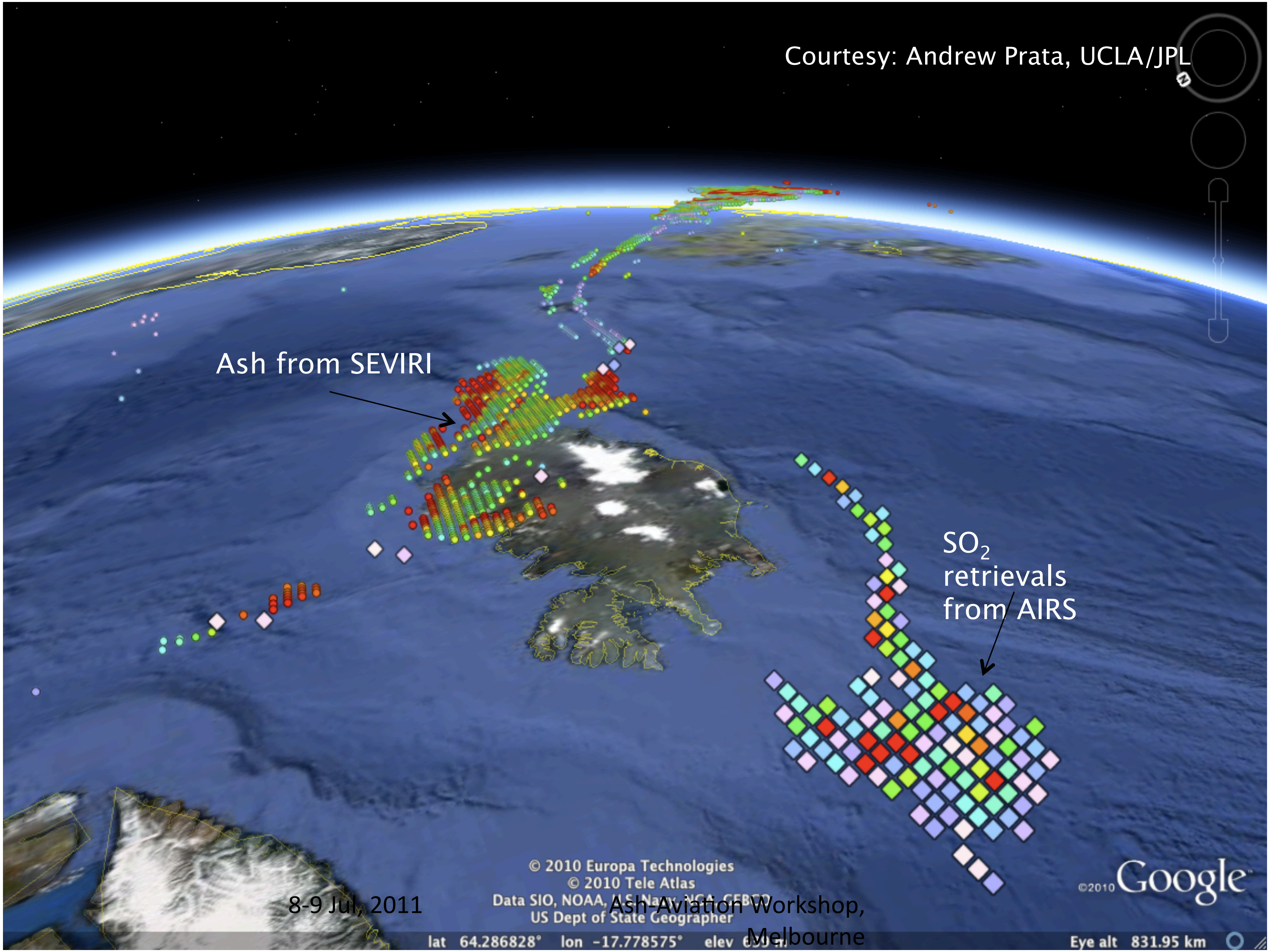
Courtesy: Andrew Prata, UCLA/JPL
Ash from SEVIRI
SO2 retrievals from AIRS
© 2010 Europa Technologies
© 2010 Tele Atlas
US Dept of State Geographer
©2010 Google
lat 64.286828° lon -17.778575°
Eye alt 831.95 km

Remote sensing of volcanic clouds

OMI – SO_2, aerosols, BrO

TES – SO_2, HCl

– strat. SO_2, HCl

MODIS – SO_2, ash, sulfate

AIRS – UTLS SO_2, aerosols, SO_2 profile?

CALIPSO – cloud height, aerosol type

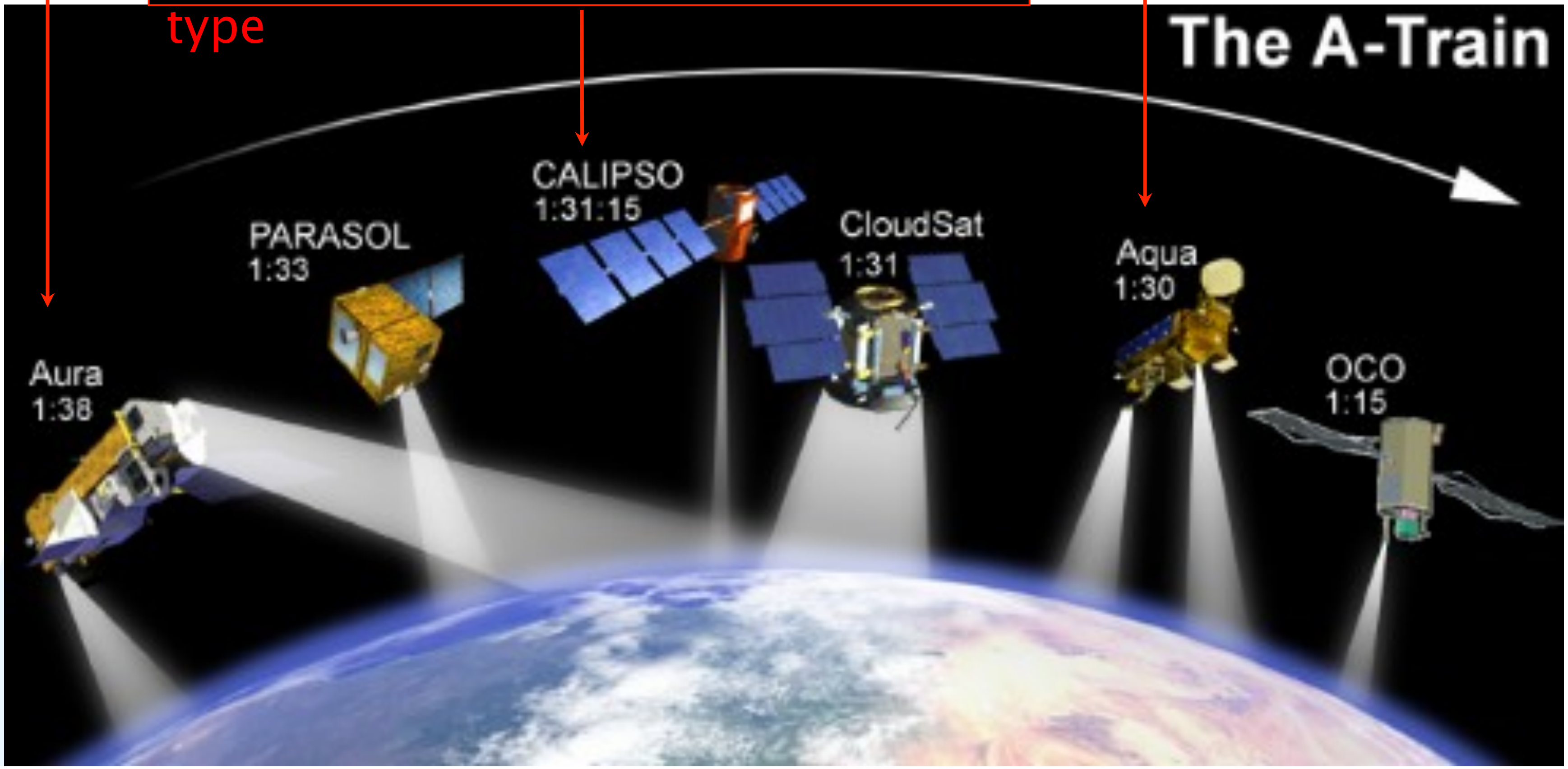

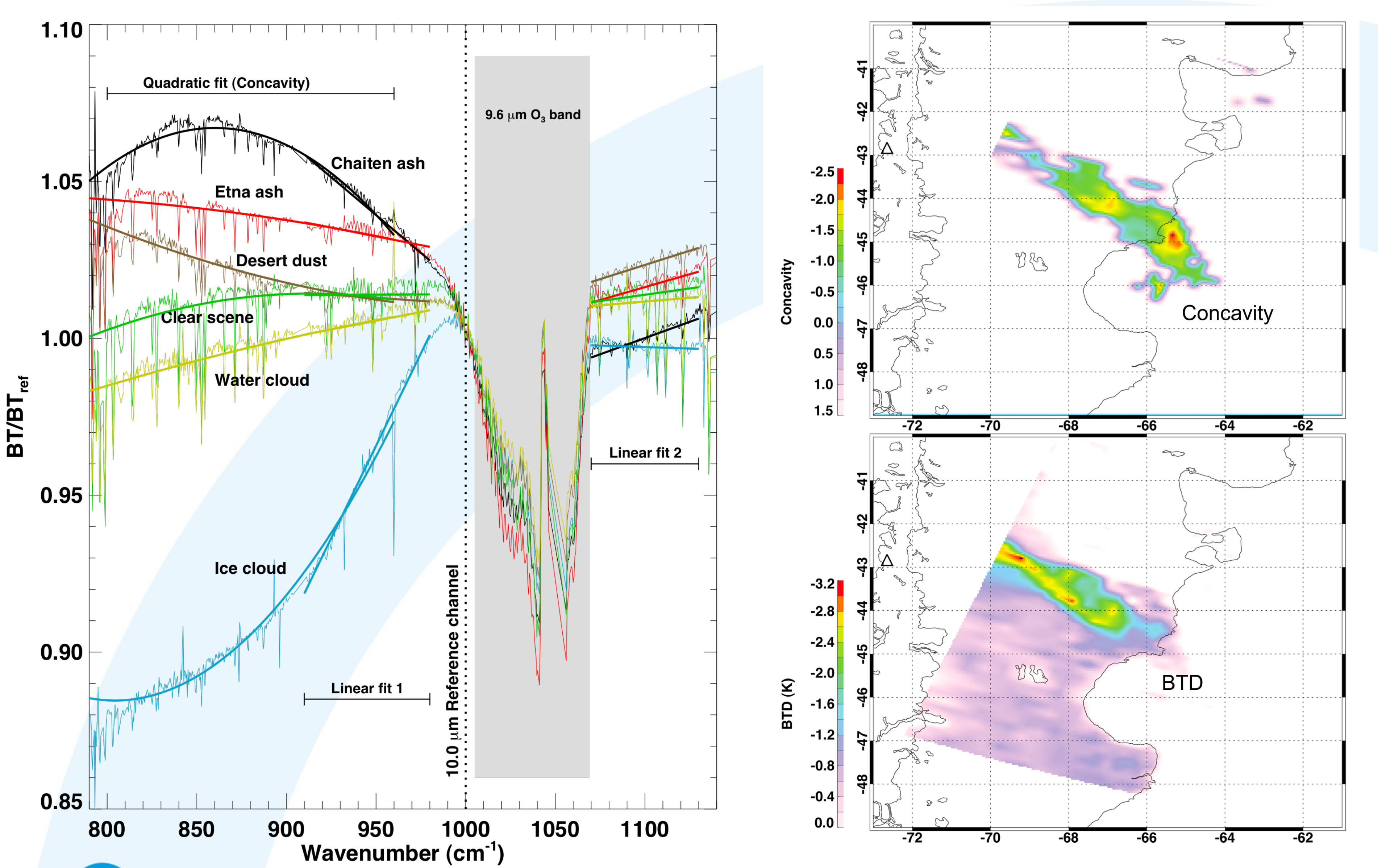
Quadratic fit (Concavity)
9.6 μm O3 band
Chaiten ash
Etna ash
Desert dust
Clear scene
Water cloud
Ice cloud
Linear fit 1
Linear fit 2
10.0 μm Reference channel
BT/BTref
Wavenumber (cm-1)
Concavity
BTD
BTD (K)

Chaitén, Chile

First rhyolitic ash eruption in the satellite era (~30 years)

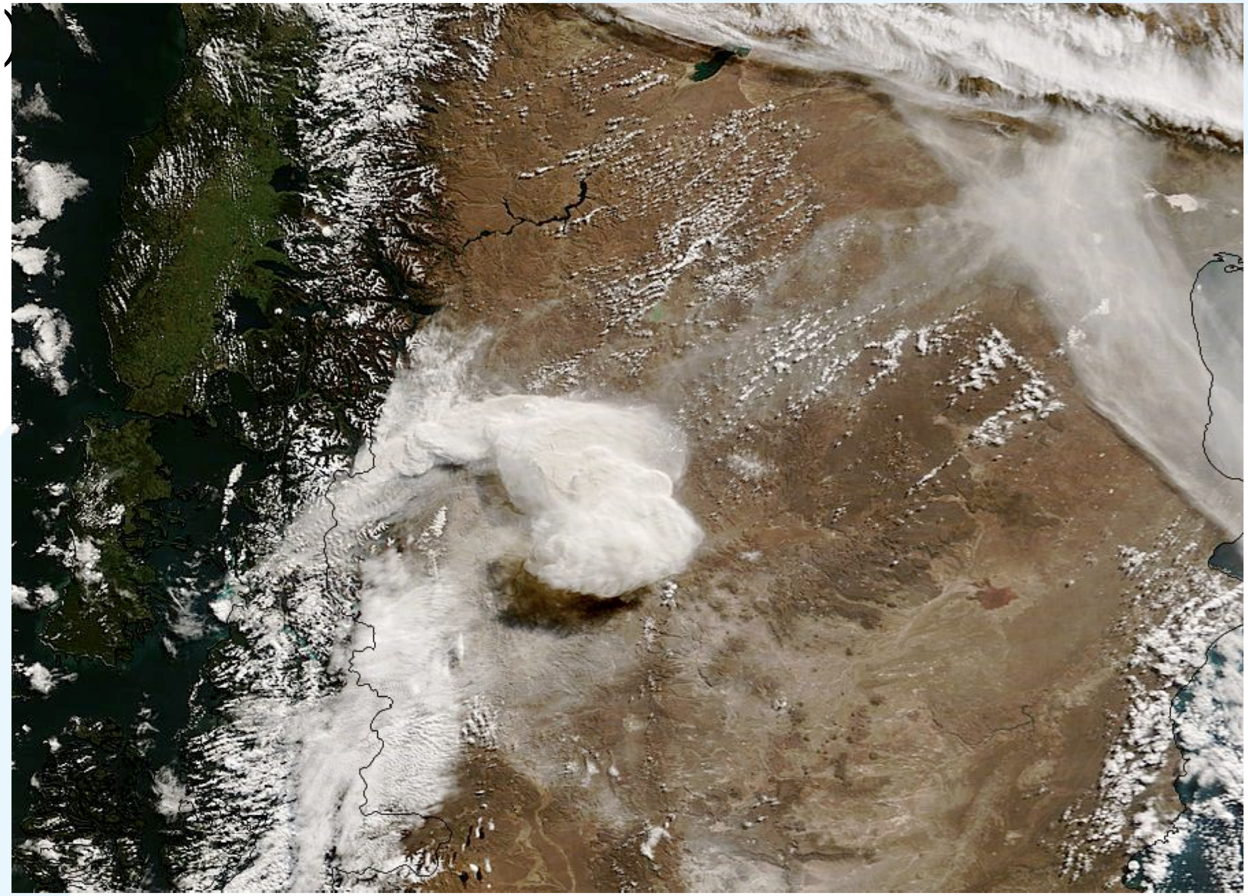

S.A. Carn, J.S. Pallister, L. Lara, J. Ewert, G. Villarosa, M. Fromm, S. Watt, A.J. Prata, D.M. Pyle, T.A. Mather, N. Matthews, R.S. Martin, A. Pavez, R. Aguilera, R. Thomas, W. Rison, P. Krehbiel, J. Johnson, A. Folch, D. Basualto, T.J. Casadevall, M. Guffanti, C. Benitez, J.G. Viramonte, 2008, The awakening of Chaitén volcano, Chile, ***EOS Trans.*** ***(to appear).***

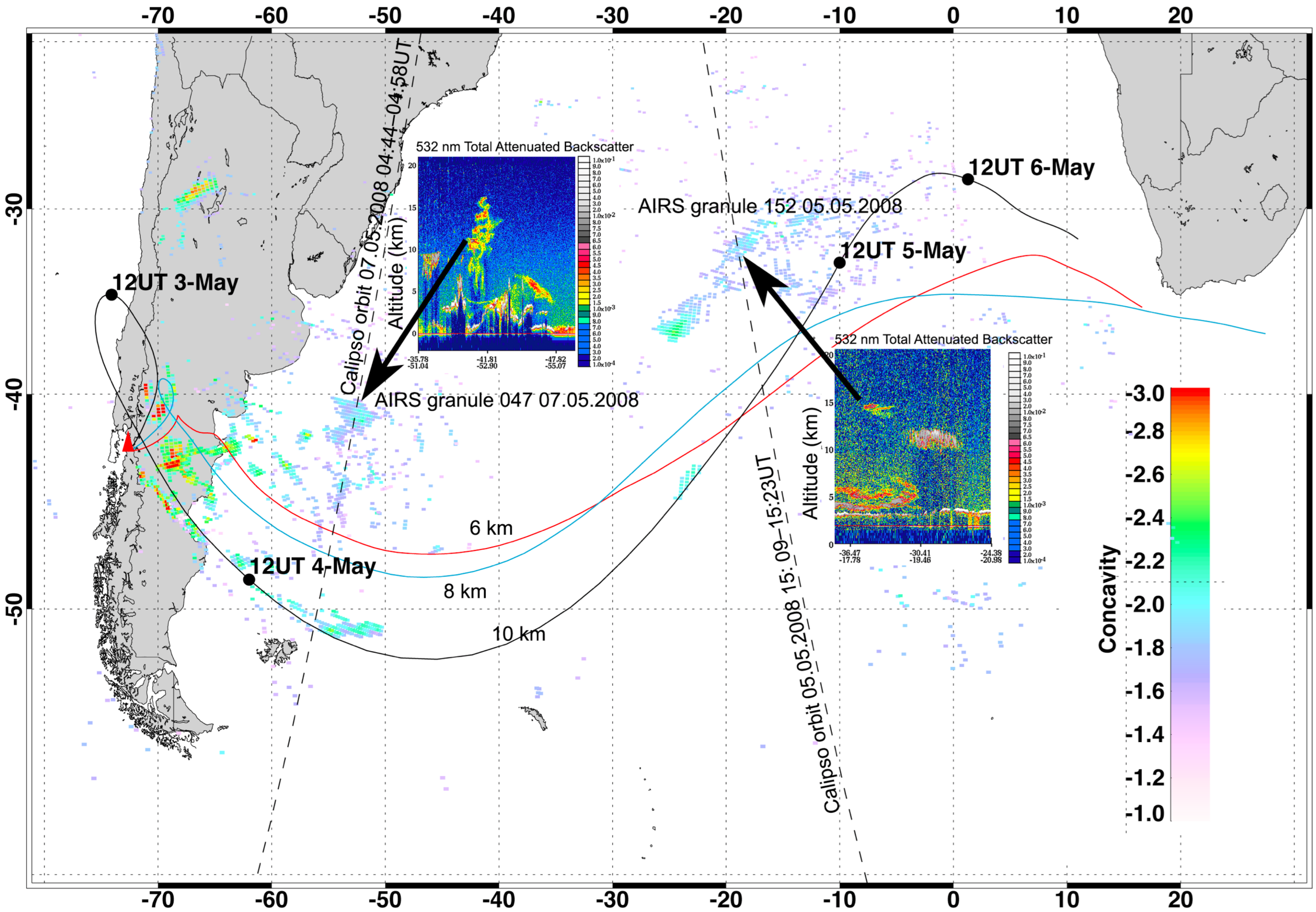

12UT 3-May
12UT 4-May
12UT 5-May
12UT 6-May
6 km
8 km
10 km
AIRS granule 047 07.05.2008
AIRS granule 152 05.05.2008
Calipso orbit 07.05.2008 04:44–04:58UT
Calipso orbit 05.05.2008 15: 09–15:23UT
532 nm Total Attenuated Backscatter
Altitude (km)
Concavity

Collocation of ash and SO_2

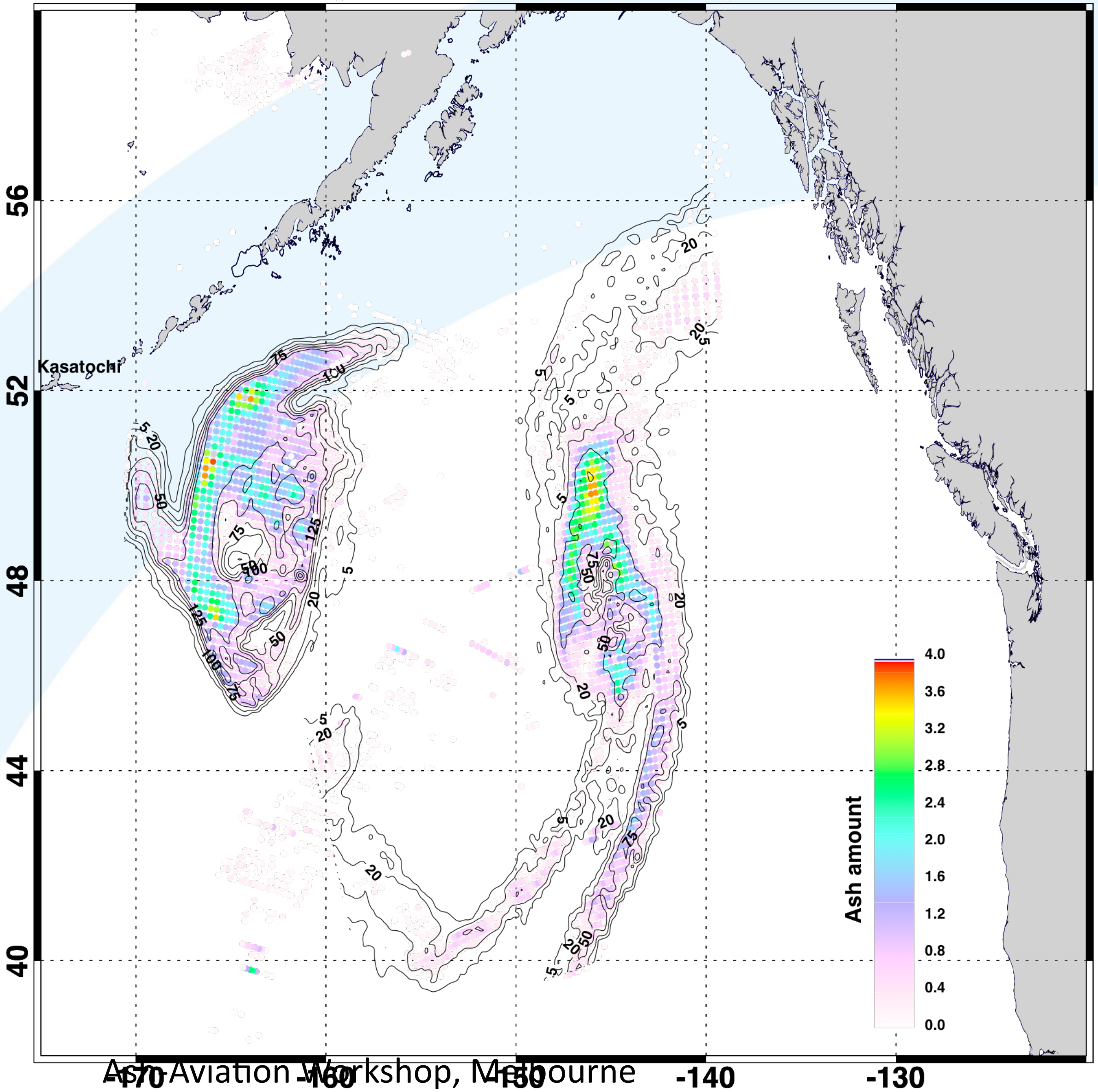

AVOID

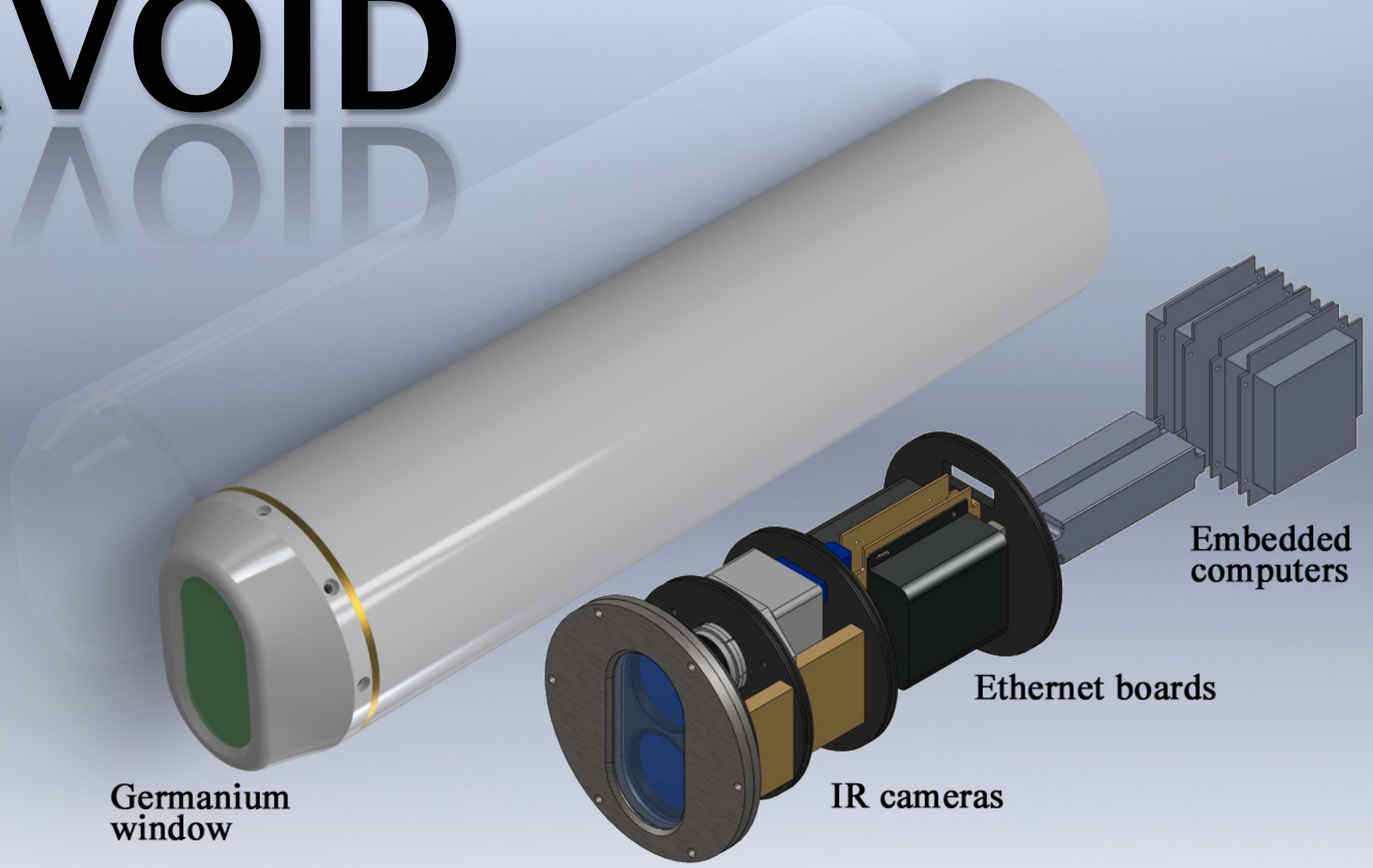
Embedded computers
Ethernet boards
IR cameras
Germanium window


0 30μ
FAAM

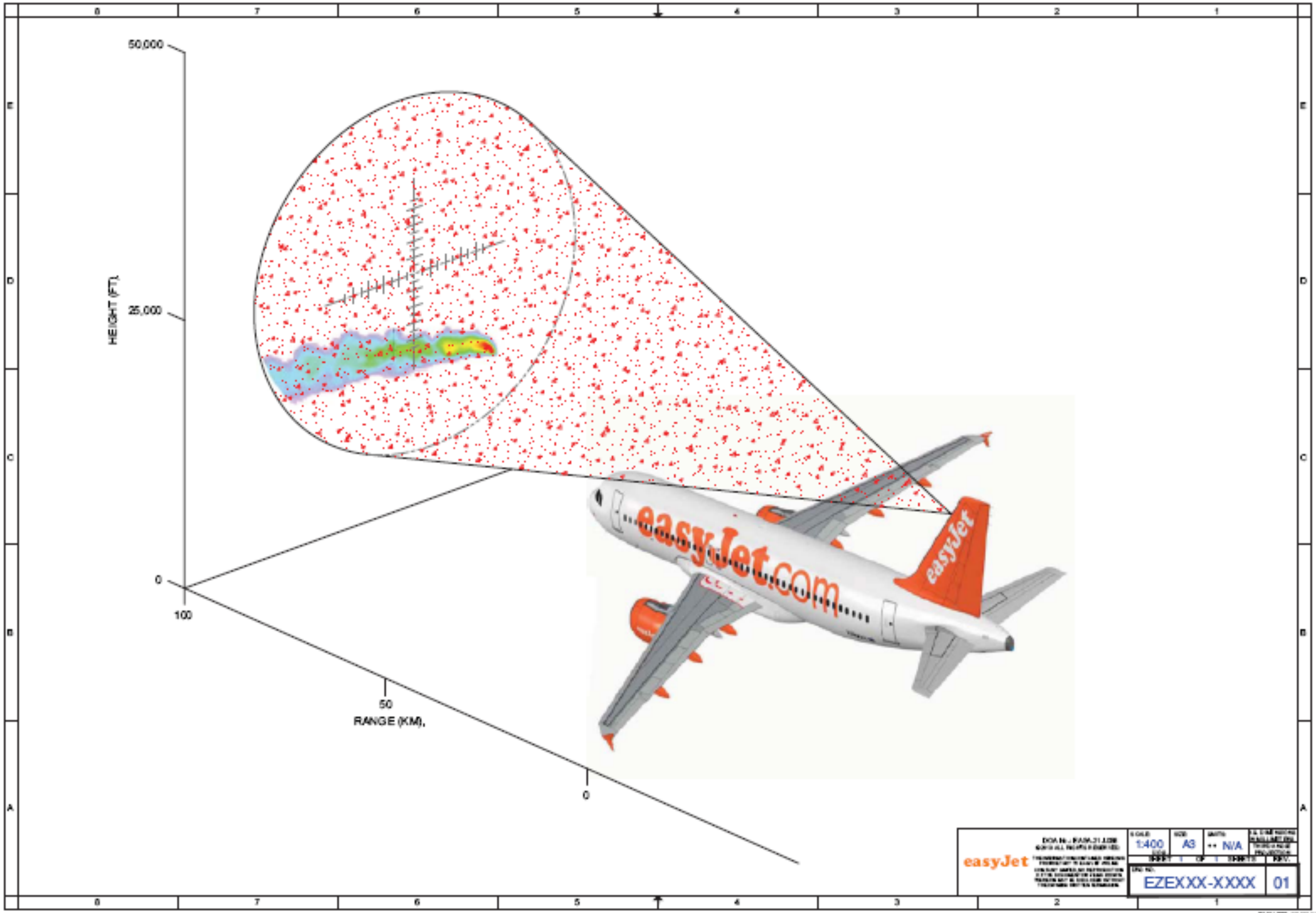
50,000
25,000
0
HEIGHT (FT)
100
50
0
RANGE (KM)
easyJet.com
easyJet
EZEXX-XXXX
01
1:400
A3
N/A

Simulated view of ash cloud viewed from **AVOID**

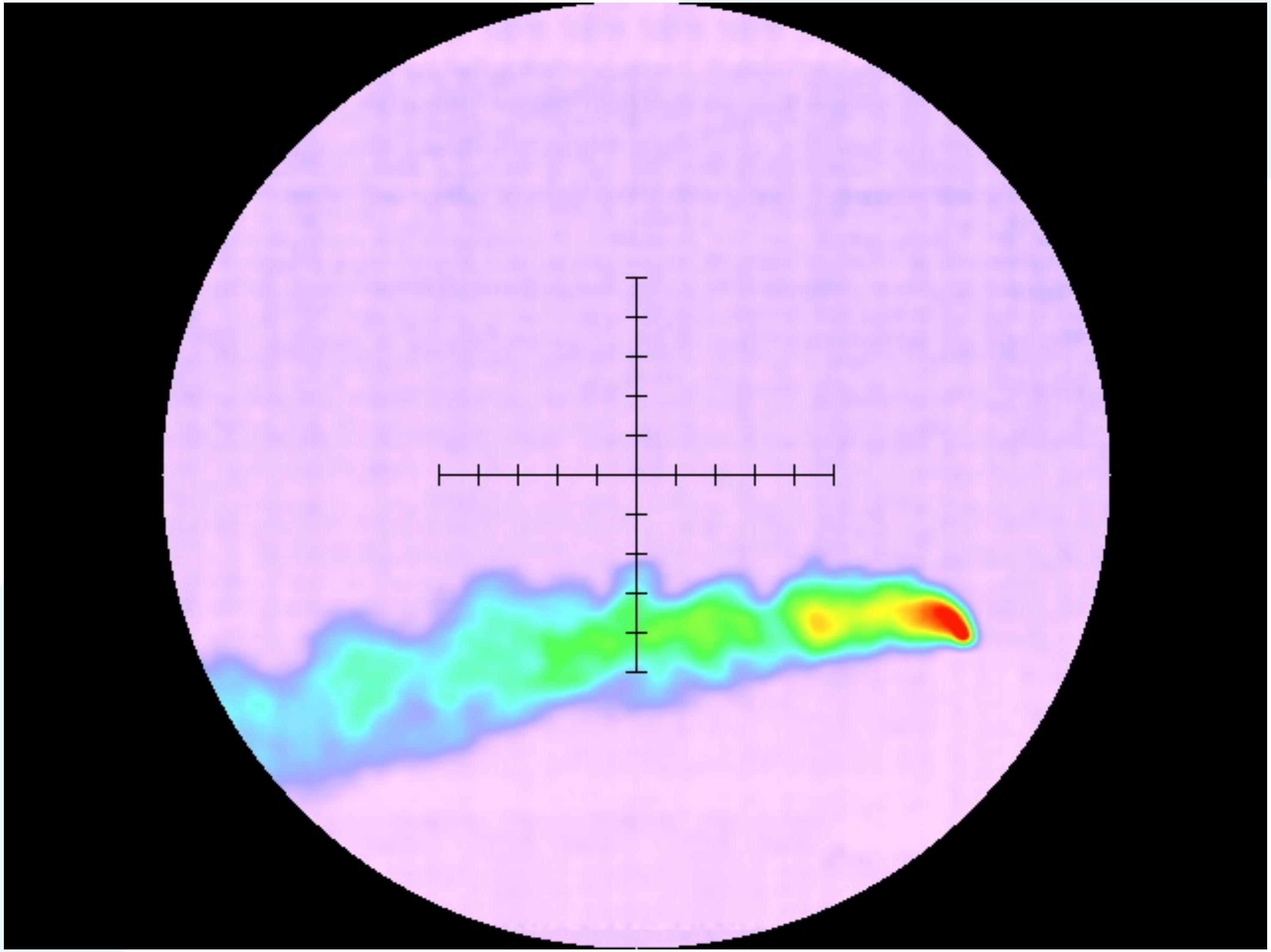

Ground-based measurements

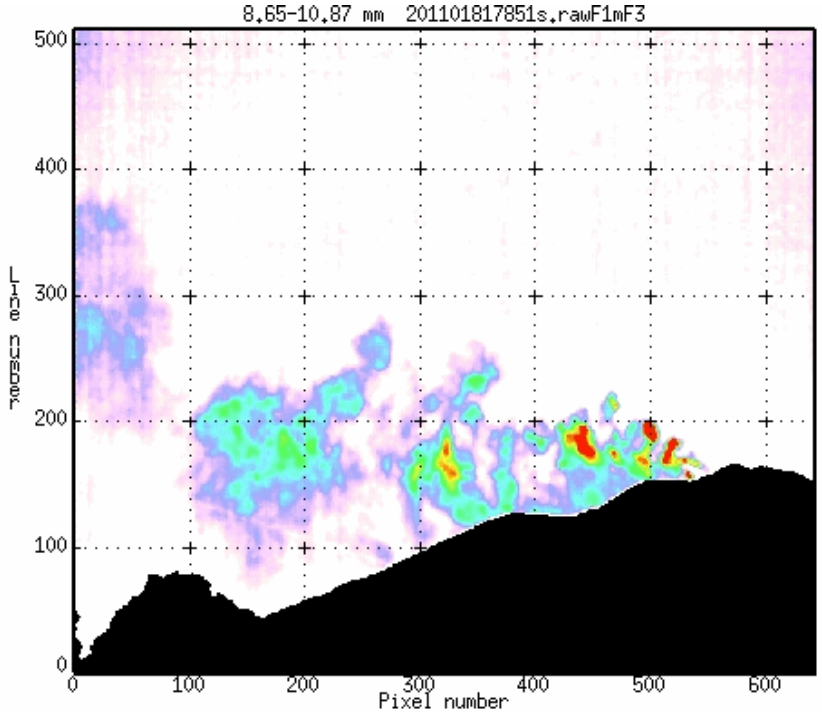

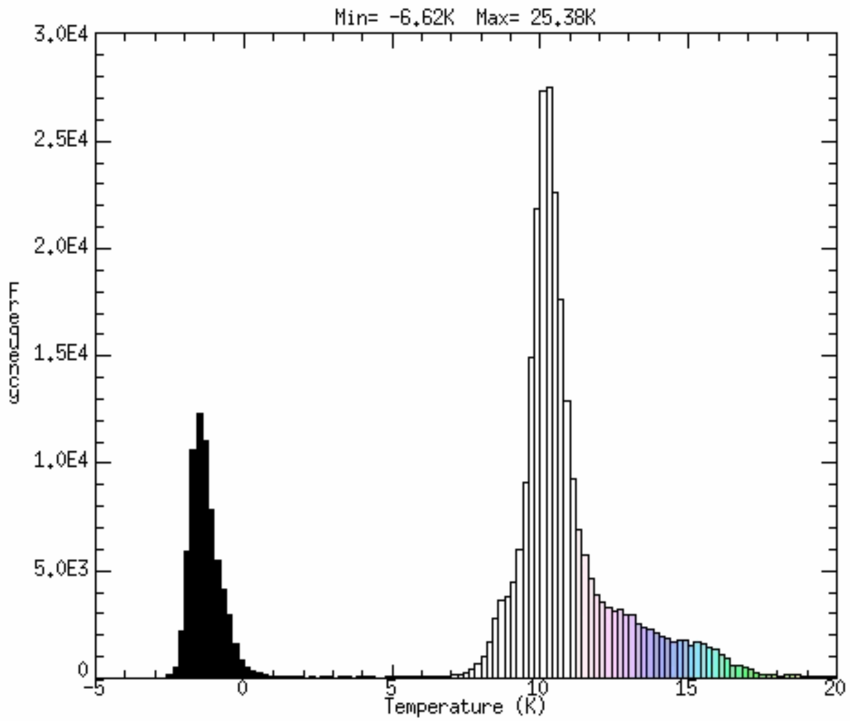

Turrialba, Costa Rica

22 January, 2011

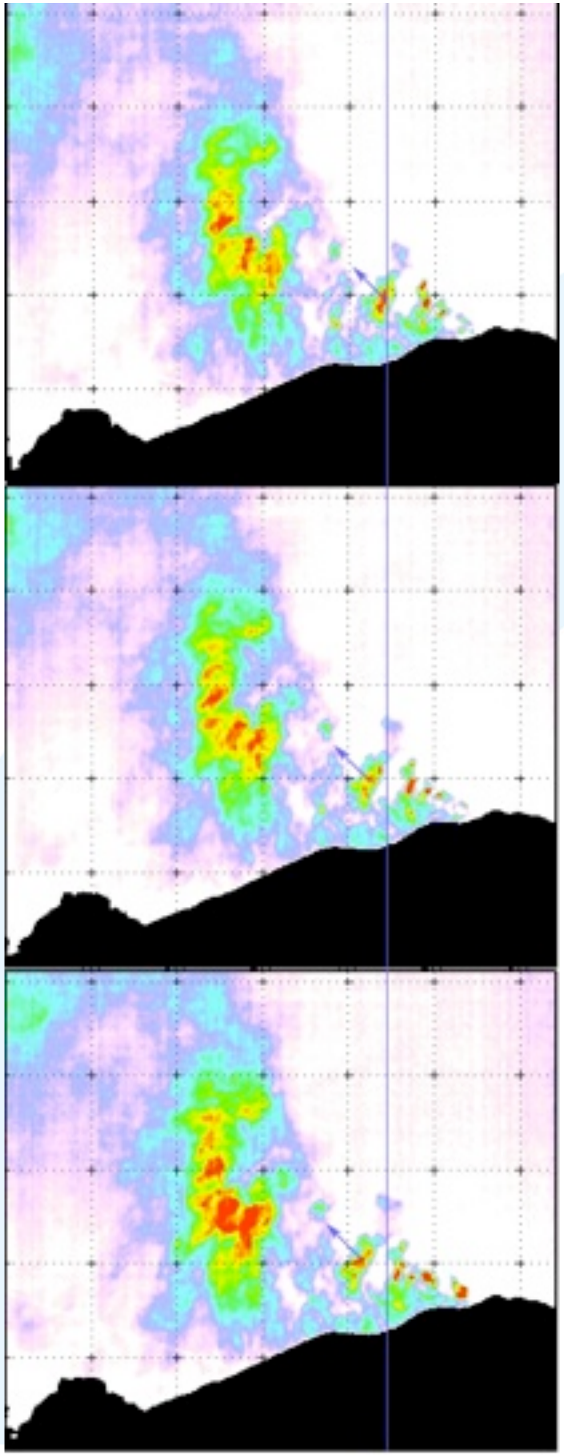

Tracking movement of individual features allows plume speed and direction (plume velocity) to be determined. Thus, fluxes can be inferred.

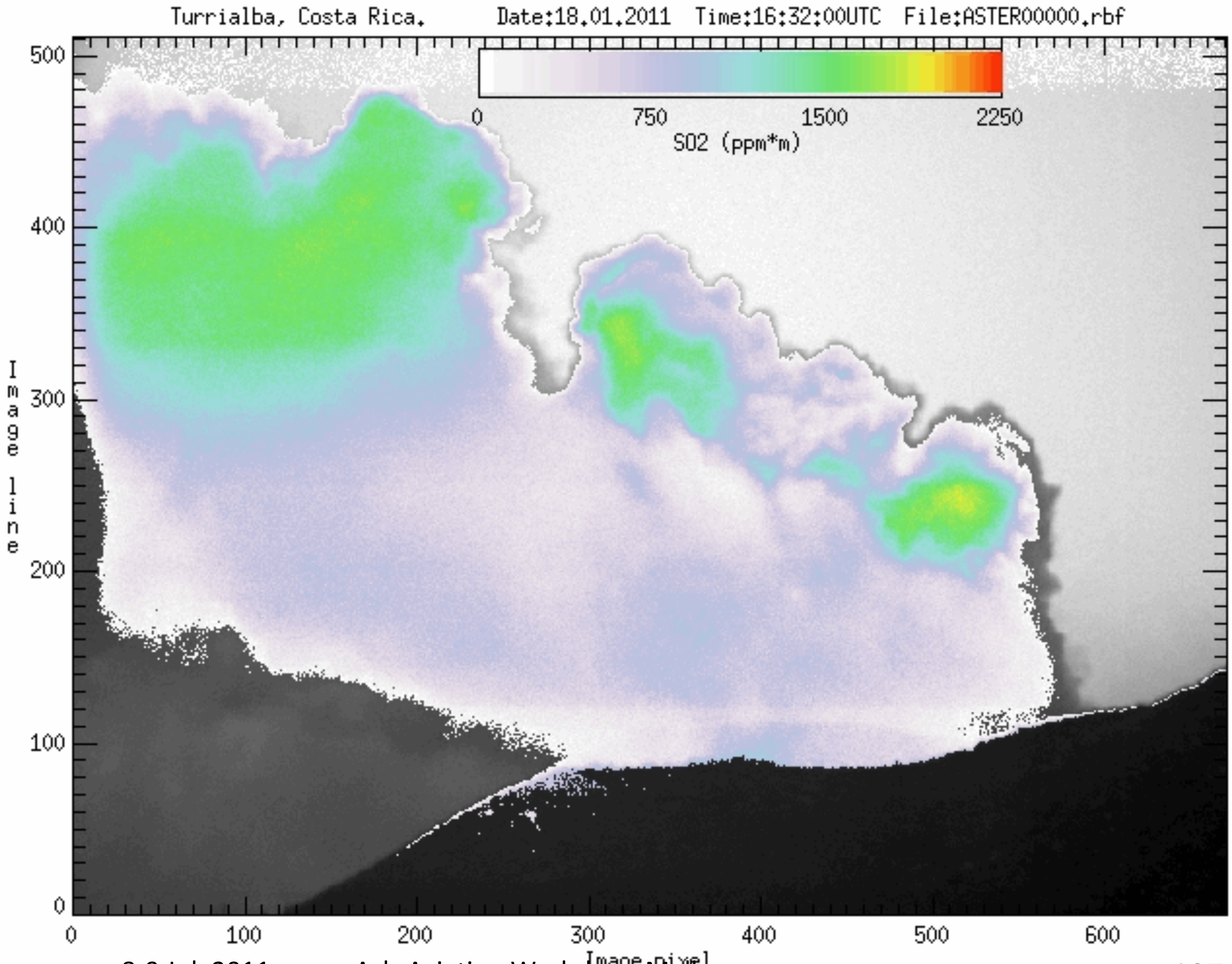
Turrialba, Costa Rica.
Date:18.01.2011
Time:16:32:00UTC
File:ASTER00000.rbf
0
750
1500
2250
SO2 (ppm*m)
Image line
Image pixel
0
100
200
300
400
500
600

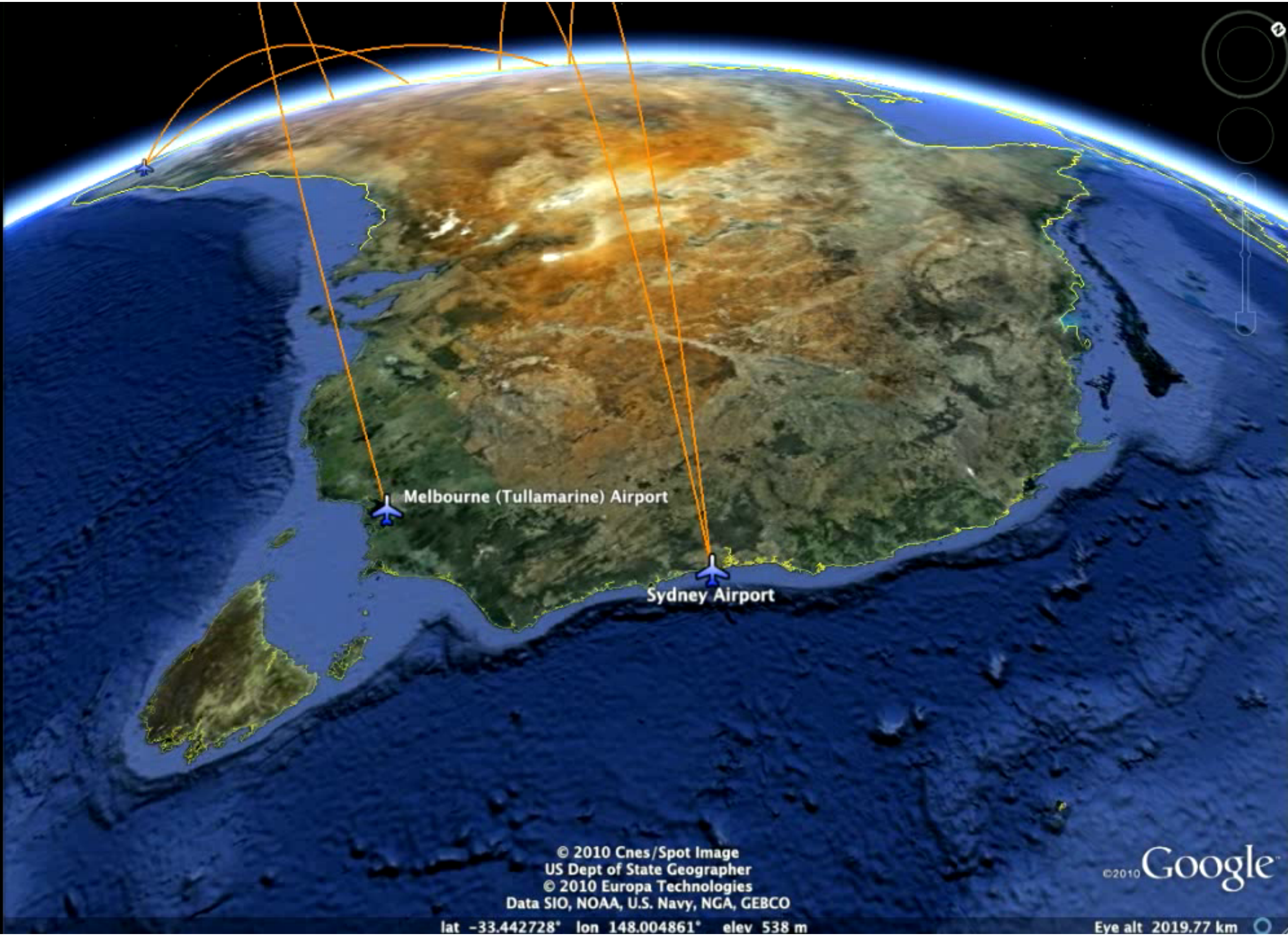
Melbourne (Tullamarine) Airport
Sydney Airport
© 2010 Cnes/Spot Image
US Dept of State Geographer
© 2010 Europa Technologies
Data SIO, NOAA, U.S. Navy, NGA, GEBCO
lat -33.442728° lon 148.004861° elev 538 m
Eye alt 2019.77 km
©2010 Google

Further information

AIRS

- **Prata, A. J**., and C. Bernardo, 2007, Retrieval of volcanic SO_2 column abundance from Atmospheric Infrared Sounder data, ***J. Geophys. Res***., 112, D20204, doi: 10.1029/2006JD007955.

Transport

- **Prata, A. J.,** S. A. Carn, A. Stohl, and J. Kerkmann, 2007, Long range transport and fate of a stratospheric volcanic cloud from Soufri`ere Hills volcano, Montserrat, ***Atmos. Chem. Phys.,*** 7, 5093–5103.

OMI

- Carn, S. A., Krotkov, N. A., Yang, K., Hoff, R. M., **Prata, A. J**., Krueger, A. J., Loughlin, S. C., and P. F. Levelt, 2007, Extended observations of volcanic SO_2 and sulphate aerosol in the stratosphere, ***Atmos. Chem. Phys. Discuss***., 7, 2857–2871.

SEVIRI

- **Prata, A. J**., and J. Kerkmann, 2007, Simultaneous retrieval of volcanic ash and SO_2 using MSG-SEVIRI measurements, ***Geophys. Res. Lett***. 34, L05813, doi:10.1029/2006GL028691.

Aviation

- **Prata, A. J.**, 2008, Satellite detection of hazardous volcanic clouds and the risk to global air traffic, ***Nat. Hazards***, DOI 10.1007/s11069-008-9273-z.
- Tupper, A., I. Itikarai, M. S. Richards, **A. J. Prata**, S. Carn, and D. Rosenfeld, 2007: Facing the challenges of the International Airways Volcano Watch: the 2004/05 eruptions of Manam, Papua New Guinea. ***Weather and Forecasting***, Vol. 22, No. 1,175-191.

UV imager

- Bluth, G. J. S., J.M. Shannon, I.M. Watson, **A.J. Prata** and V.J. Realmuto, 2007, Development of an ultra-violet digital camera for volcanic SO_2 imaging, ***J. Volcanol. Geothermal Res.,*** 161, 47–56.

SO_2 Pinatubo

- Guo, S., Bluth, G. J. S., Rose, W. I., Watson, I. M., and **Prata, A. J.,** 2004, Re-evaluation of SO_2 release of the 15 June 1991 Pinatubo eruption using ultraviolet and infrared satellite sensors, ***Geochem, Geophys, Geosys***, 5(4), Q04001, doi:10.1029/2003GC000654.

TOVS

- **Prata, A. J.,** Rose, W. I., Self, S., and D. M. O'Brien, Global, long-term sulphur dioxide measurements from TOVS data: A new tool for studying explosive volcanism and climate, In *Volcanism and the Earth's Atmosphere* (ed. Robock and Oppenheimer), ***Geophysical Monograph***. 139, 75-92, 2003.